University of Bradford eThesis

The production of a lyotropic liquid crystal coated powder precursor through twin screw extrusion

Lokesh Likhar

Abstract

The twin screw extrusion technique has been explored to produce lyotropic liquid crystal coated powder precursor by exploiting Pluronic F127 thermoreversible gelation property to get powder precursor without granular aggregates or with less compacted granular aggregates. The highly soluble chlorpheniramine maleate loaded in Pluronic F127 solution coated MCC particles prepared through twin screw extrusion was examined to produce the cubic phase (gel) for the development of controlled release formulation and for coating of very fine particles which cannot be achieved by traditional bead coaters. Controlled release formulations are beneficial in reducing the frequency of administration of highly soluble drugs having short half life and also to address the problem of polypharmacy in old age patients by reduction of dosage frequency. An unusual refrigerated temperature (5 ℃) profile for twin screw extrusion was selected based on the complex viscoelastic flow behaviour of Pluronic F127 solution which was found to be highly temperature sensitive. The Pluronic F127 solution was found to be

I

Newtonian in flow and less viscoelastic at low temperature, such that low temperature (5˚C) conditions were found to be suitable for mixing and coating the MCC particles to avoid compacted aggregates. At higher temperatures (35-40˚C) Pluronic F127 solution exhibited shear thinning and prominent viscoelasticity, properties which were exploited to force CPM containing Pluronic F127 solution to stick over the MCC surface. This was achieved by elevating the temperature of the last zone of the extrusion barrel. It was found that to avoid compacted aggregates the MCC must be five times the weight of the Pluronic F127 solution and processed at a screw speed of 400 RPM or above at refrigerated temperature. Processing was not found to be smooth at ambient temperature with frictional heat and high torque generation due to significant compaction of coated particles which can be attributed to the elastic behaviour of Pluronic F127 solution at temperatures between ambient to typical body temperature. PLM images confirmed the cubic phase formation (gel) by Pluronic F127 coating which was found to be thick with maximum Pluronic F127 concentration (25%). SEM images showed smoothing of surface topography, and stretching and elongation of MCC fibres after extrusion which is indicative of coating through extrusion processing. Plastic deformation was observed for the lower Pluronic F127 concentration and higher MCC proportions. There was a significant decrease in work done for cohesion by the powder flow analyser observed in the batches with more aggregates compared with batches with least aggregates. A regression analysis study on factorial design batches was conducted to investigate the significant independent variables and their impact on dependent variables for example % torque, geometric mean diameter and work done for cohesion, and to quantitatively evaluate them. From the regression analysis data it was found that the coefficient of determination for all three dependent variables was in the range of 55-

62%. The pharmaceutical performance of the prepared coated LLC precursor through twin screw extrusion in terms of controlled release was found to be very disappointing. Almost 100% chlorpheniramine maleate was released within 10-15mins, defined as providing burst release. The MDSC method was developed within this work to detect Pluronic F127 solution cubic phase formation. The MDSC method was developed to consider sample size, effect of heating and cooling, sample heat capacity, and the parameters for highest sensitivity which can be followed by sample accurately without the phase lag to produce accurate repeatable results.

PUBLICATIONS ARISING FROM THIS THESIS

Some sections of work from this thesis have previously been presented in the following form.

1. L.Likhar, T. Gough, and A. Paradkar. Visco-elastic characterisation of lyotropic mesophases for process design to manufacture precursors. Presented as poster at APSGB Pharmsci Conference Nottingham, August 2012.

2. L.Likhar, T. Gough, and A. Paradkar. MDSC as a tool for detecting the cubic phase formation in lyotropic liquid crystals precursor. Presented as poster at APSGB Pharmsci Conference Edinburgh, September 2013.

Acknowledgement

"I am always doing that which I cannot do, in order that I may learn how to do it." *Pablo Picasso*

Leaving home and your beloved family to earn a research degree is not always easy. Initially when I arrived in this country I felt homesick and nostalgic about the time which reminds me about my college days, my home town (Bhopal), friends and my parents. Suddenly my ambition took over and I again went into book worm phase of my life. At the first meeting with my supervisors Dr. Tim Gough and Prof. Anant Paradkar, we decided to work on Lyotropic liquid crystals for transdermal drug delivery. But after having done a lot of reading I found that similar kind of work have already been attempted. This is the time when I felt extremely privileged to have such understanding and supportive supervisors, as they allowed me to choose a novel research project. Now here's the biggest challenge to find out a novel research project which has not been explored using lyotropic liquid crystal, this was really frustrating period for me because the time was running down and still the project was not finalised. One day Prof. Anant called me in and said; let's explore the low temperature Twin screw extrusion to produce lyotropic liquid crystal precursor and since then I haven't looked back. At this meeting I was blown away by Prof. Anant's creative mind and out of the box thinking which helped me lend such a novel interesting research project. Dr. Tim's ideas about selecting the specific rhelogical tests have been an asset to me. He's been simply genius in fixing problems and connecting dots. Both my supervisors gave me courage, kept me motivated during difficult times. Especially Prof. Anant has stimulated and broadened my thinking due to which I can see myself now as a well rounded researcher. I am grateful to the

List of Figures

List of Tables

Abbreviations

CMC: Critical micelle concentration

CPM: Chlorpheniramine maleate

Cryo-TEM: Cryo transmission emission microscopy

CSD: Controlled shear deformation

CSR: Controlled shear rate

d_g: Geometric mean diameter

DMTA: Dynamic mechanical thermo-analysis

DSC: Differential scanning calorimetry

GMO: Glyceryl monooleate

G'': Loss modulus

G': Storage modulus

H_1: Hexagonal phase

H_2: Reverse hexagonal phase

I_1: Micellar cubic phase

I_2: Reversed micelle

LLC: Lyotropic liquid crystal

L_α: Lamellar phase

MCC: Microcrystalline cellulose

MDSC: Modulated differential scanning calorimetry

PAT: Process analytical tool

PEO: Poly-ethylene oxide

PLM: Polarized light microscopy

PPO: Poly-propylene oxide

SAXS: Small angle X-ray scattering

SEM: Scanning electron microscopy

TGA: Thermo gravimetric analysis

Tg: Glass transition temperature

TSE: Twin screw extrusion

WDC: Work done for cohesion

Chapter 1: Introduction

===

Lyotropic liquid crystal (LLC) systems commonly consist of amphiphilic molecules in conjunction with a solvent (usually water) which may exhibit different types of lyotropic liquid crystalline phases classified mainly into hexagonal, lamellar, and cubic forms. Formation of these LLC phases is dependent on the quantity of solvent present in the solution for the specific arrangement of the solute molecules, however temperature induced phase transitions are also observable at given concentrations. These structures or phases exhibit different lattice arrangements of the molecules or the micelles within the solvent. All these phases illustrate some distinct individual properties and can offer advantages such as: stabilization and protection of sensitive drug molecules, proteins (Shah et al., 2001) and enzymes (Nylander et al., 1996), they may provide a viscous barrier for improved stability (Jain *et al,* 2011) of formulations and post-surgical adhesion formation (Steinleitner et al., 1991), and they can offer a mechanism for the controlled release of drugs (Kumar et al., 2004) as well as solubility enhancement (Engström et al., 1999). This can be exploited according to design and can enhance the performance and efficacy of the formulation to improve patient compliance.

These LLC phases react very distinctly under the application of shear and the in-situ delivery site conditions which both aids and imposes challenges for processing, drug delivery to specific sites and the robustness of the dosage forms. For instance, low viscosity lamellar phases are very shear sensitive (Paasch et al., 1989) which can help in high shear drug delivery such as in intravenous injection (Maheshwari et al., 2006), whereas cubic and

hexagonal phases tend to be highly viscous, mechanically tough and thermodynamically resistant and can survive with excess of water however are less mucoadhesive than the lamellar phase (Nielsen et al., 1998). LLC phases have proved their versatility in drug delivery from parenterals to ophthalmic formulations, improving the stability of bioactives from proteins to nucleic acids and exhibiting a high solubilisation capacity from hydrophilic to hydrophobic APIs as well as further applications such as bio adhesion and controlled release. Despite all of these advantages these LLC phases also impose various challenges such as processing of these highly viscous LLC phases, transformation to a relatively low viscosity phase with shear during delivery or processing which can potentially deteriorate the performance of the dosage form and the handling or delivery of these highly viscous bulk LLC phases to a specific delivery site.

The answer to all the above challenges like shear induced phase transformation during drug delivery, difficulty in delivering highly viscous LLC and handling bulk LLC is the formation of an LLC powder precursor. The LLC powder precursor will ultimately acquire the special interest properties of the LLC phases by forming the same. However this transformation from the precursor to actual LLC phase requires specific type of stimulus mostly in the form of the temperature or the availability of the solvent or sometimes both. Manufacturing of the precursor is itself not an easy task because it sometimes requires high energy input in terms of shear, and also heat generation while processing which can potentially deteriorate or transform LLC phase. The LLC's complex or highly viscous flow behaviour also have to dealt with which might slow down the process and actives to be incorporated also pose changes to LLC flow behaviour and the LLC phase shown by the system. Therefore, the processing equipment variables, the economic aspects of the process and its speed also have to be considered accordingly so that the ultimate goal of achieving the

desired result in terms of specific LLC phase, performance, efficacy, robustness of the dosage form, affordability within timeline can be achieved.

This area of drug delivery involving the precursor has not been much explored; only a few reports explaining the precursor development, processabilty and the performance of the dosage form are available and these are all from within the last ten years. Recently, Shah et al (2006) developed a spray dried methodology to produce cubic phase (I_1) powder precursor using a quaternary (glyceryl monooleate, magnesium trisilicate, diclofenac sodium and isopropyl alcohol) system. In this study they tried to address the 'stickiness' of the glyceryl monooleate (GMO) and the quick transformation of the shear sensitive lamellar phase precursor into a cubic phase acting as cubic phase precursor. It was shown that with the increase in the amount of magnesium trisilicate (MTS), the percentage yield also increased which was attributed to increase in adsorption of the GMO on MTS. The increased amount of MTS ultimately reduced the particle size and ensured the complete adsorption of the GMO over the MTS which aided a rapid transformation of the lamellar phase into the cubic phase which was confirmed by polarised light microscopy. The functional relationship between the quantity of MTS and the viscosity of the precursor was found. The spray dried dispersion with the highest MTS was found to have highest viscosity which is due to the complete adsorption of GMO over MTS. Therefore, this strongly supports the transformation to highly viscous cubic phase and its ultimate effect is seen on the controlled drug release profile. Another study on powder precursors was published by Maheshwari et al (2006) addressing the different issue of higher polymer concentration needed to achieve the desired high viscosity which ensures the pharmaceutical performance of the controlled release dosage form. A spray dryer was used for the ternary (Pluronic F127, Aerosil and Isopropyl alcohol) system. In this study the authors tried to address the relationship between the Aerosil concentrations and the

transformation of cubic phase to hexagonal phase which was tracked using rotational rheometry. They reported that the hexagonal phase is obtained at very high polymer concentration because it requires highly dense packing of the molecules. Aerosil does this by adsorbing the majority of water due to its larger surface area with relatively low polymer concentration. This change from cubic phase to hexagonal phase was achieved by adding very small amount of gelling agent (Aerosil) which was investigated by comparing the gelation and the gel melting temperature with the rheological parameters. Addition of the Aerosil increased the linear viscoelastic range (LVR) which was attributed to strong physical entanglement, a higher extent of hydrogen bonding and more closely packed micelles. The domination of the elastic modulus (G') over the loss modulus (G'') shown with the Aerosil during dynamic frequency tests was attributed to the stability of the system which again indicates a more closely packed system. Increasing temperature also added to the stability by inducing more entanglements and its effect was clearly seen on the increased value of both elastic (G') and the viscous modulus (G''). The increase in G' was found to be a function of frequency with all Aerosil concentrations. With the increase in Aerosil concentration at specific frequencies in a dynamic oscillation frequency sweeps performed under LVR a decrease in tan δ was observed, similar observation was also found in vice-versa case. There was slow decreasing rate of tan δ shown by system at a particular Aerosil concentration at 30°C than at 20°C with the increasing frequency. Therefore, on the basis of the above observations of the dynamic frequency sweeps author interpreted that with increasing Aerosil concentration, frequency and temperature the gel has developed more resistance towards structural changes acquiring high viscosity strong gel network. Thus the problem of desired high viscosity with lower polymer concentration was solved by the authors. (Carvalho et al., 2013) explore the nasal drug delivery route to protect the antiretroviral drug Zidovudine from the pre-systemic metabolism and degradation from the gastro-intestinal environment. PPG-5-

CETETH-20, oleic acid and water (55, 30, 15% w/w) ternary systems was used as a LLC precursor solution which was also helpful in eradication of some of the limitations of the nasal route of administration such as low permeability of nasal epithelium, drug removal by mucociliary mechanism of nasal cavity and the enzymatic degradation in the mucus layer. It was shown that the ternary system was Newtonian in flow behaviour and isotropic in appearance under polarised light microscopy but after its dilution with the artificial nasal mucus it was transformed into the anisotropic lamellar phase. At the nasal temperature the lamellar phase transformed solution shows a high G' as revealed by oscillatory frequency tests. Three times increase in work force of adhesion for detaching the transformed lamellar phase formulation by the nasal mucosal model was observed which was done by texture analyser demonstrating the bio adhesion ability of the lamellar phase. This transformation to the lamellar phase demonstrated an eighteen fold increase in the permeability of Zidovudine observed in ex-vivo permeation studies, this being due to increased bio adhesion. The in-vivo study revealed the faster absorption of the drug from the nasal route than via intravenous delivery. Thus this study demonstrated the advantages of using the LLC precursor by enhancing the performance of the formulation and the ease of delivery to the specific site. Spicer et al. (2002) developed spray dried cubic phase powder precursor nanoparticles (cubosomes) which are very difficult to produce and stabilize. To produce the cubosomes from the bulk cubic phase systems requires high shear dispersion which has various limitations. Spicer et al. formulated ternary (starch–monoolein–water) and quaternary (dextran–monoolein–ethanol–water) systems which were used to encapsulate the monoolein to decrease the 'sticking' of the powder cubosome precursor. While spraying drying the two systems, they found that it was relatively easy to spray dry the quaternary emulsion system then the ternary dispersion of cubic liquid crystalline particles which is obvious due to viscous cubic phase. Broad range of particle size distribution was found while spray drying cubic

liquid crystalline dispersion which was bit problematic due to high viscosity. The encapsulants also helped in stabilization of the cubosomes in a colloidal state. The production of the cubosomes and their size distribution were confirmed by cryo-TEM, small angle X-ray scattering (SAXS) and laser diffraction respectively. Both the systems produced colloidally stable cubosomes $0.6\mu m$ in size in dispersions with water. The above reports provide insights into the advantages, limitations and the processability to some extent. In this project the main focus will be on processing and its effect on the drug release profiles.

The aim of the present work is to produce the cubic phase lyotropic liquid crystalline coated free flowing powder precursor through twin screw extrusion (TSE) for the controlled release and to gain further insights into the effect of process variables on product consistency and drug release in the light of co-polymer solution flow behaviour containing dispersed API. The thought behind optimising free flowing consistency is that with this type of consistency one can produce capsules, compact tablets and can also be used as talcum powder containing suitable anti-bacterial. Pluronic F127 is used for coating over microcrystalline cellulose (MCC) which is tri-block (PEO-PPO-PEO) non-ionic co-polymer (see fig. 1.1) having average molecular weight of 12600 (BASF Technical Bulletin, 2012). The Pluronic F127 exhibits unique property of thermoreversible gelation within the concentration range of 20-30% w/w by weight (BASF Technical Bulletin, 2006). At lower temperature within thermoreversible concentration range the system remains in sol state (acts as Newtonian fluid) but as the temperature is increased the system gets transformed to cubic phase gel. This gelation is the consequence of cubic lattice arrangement of the micelles at specific concentration and temperature (BASF Product Brochure, 1997). Thus here I are tried to exploit thermoreversible gelation property of Pluronic F127 solution containing chlorpheniramine maleate (CPM) for coating over MCC through twin screw extrusion (TSE).

CPM is used as model drug here which is histamine H1antagonist used in allergic reactions. It is highly soluble drug (5.5 gm/lit) which is used here to check its controlled release by solubilising CPM in co-polymer Pluronic F127 solution.

$$H \; (O - CH_2 - CH_2)a \; (O - CH - CH_2)b \; (O - CH_2 - CH_2)a \; OH$$
$$|$$
$$CH_3$$
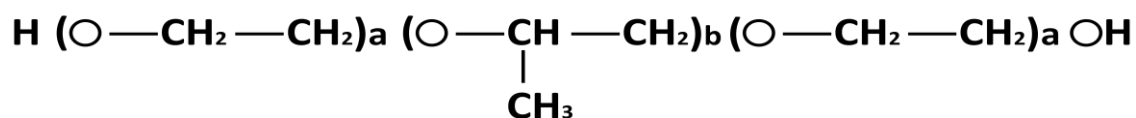
[Fig. 1.1 Chemical structures of Pluronic F127 (Poloxamer 407)]

> **Specific objectives of the work includes**

1. To understand the twin screw extrusion process.

2. To study the effect of co-polymer (Pluronic F 127/Poloxamer 407) solution concentration on processing.

3. To acquire an indepth understanding of the effect of co-polymer solution concentration, screw speed, and the amount of adsorbent MCC on the particle size distribution of the processed powder precursor and the drug release through this system.

4. To understand the twin screw extrusion process by optimization of the process variables to obtain the desired free flowing powder precursor.

5. To study the effect of an API (Chlorpheniramine maleate) on the co-polymer gelation temperature.

❖ **Scope of the work**

Chapter 2 deals with the general background information of LLC and their precursors, the challenges in the development and handling of LLC precursors and its advantages in pharmaceutical drug delivery to a specific site.

Chapter 3 provides information on the twin screw extrusion process, its mechanism, screw geometry and configuration and also its advantages over single screw extrusion for the present work.

The materials methods and instrumentations used for their characterisation both for preliminary studies and the processed product are provided in chapter 4.

Chapter 5 is composed of results and discussion in which sections 5.2 and 5.3 deals with preliminary batches and factorial design batches respectively. Regression analysis is discussed in sections 5.3.5 while section 5.4 deals with the modulated differential scanning calorimetry (MDSC) method development.

The final conclusions are presented in chapters 6 while chapter 7 is composed of suggestions for future work.

Chapter 2: Background

===

2.1 Lyotropic liquid crystals

Both water and oil is the representative of the two major classes. When the class belonging to water was probed, it was found that molecules belonging to this class are polar. This polarity was simply due to the uneven distribution of electrical charge on the atoms when came together for bonding. One part of the molecule is slightly positively charged and the other is slightly negatively charged. On the contrary the atoms of molecules belonging to the class containing oil have uniform distribution of the electrical charge. Therefore molecules belonging to this class are non-polar.

Interestingly some molecules are composed of two groups, one would eventually mix with water and the other would not. The part that mixes readily with water is called the hydrophilic group while the hydrophobic group which doesn't. These types of molecules that contain both the groups are called amphiphilic molecules. The amphiphilic molecules mainly used in daily life are surfactants. Phospholipids, which constitute part of our skin, mitochondria and other cell organelles are also amphiphilic. Due to the amphiphilic nature of the molecules they tend to move towards the surface of the liquid. More specifically if the liquid is of the class of water then the hydrophilic group tends remain in contact with water but the hydrophobic part tries to avoid the liquid and this can only be facilitated at the surface; and this is also true in case of nonpolar liquids having amphiphilic molecule.
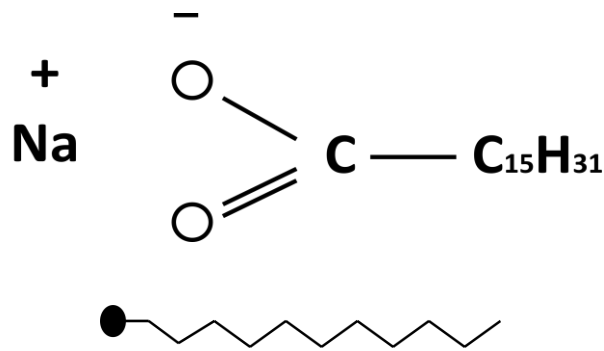
[Fig. 2.1 Typical soap molecule, sodium laurate.]
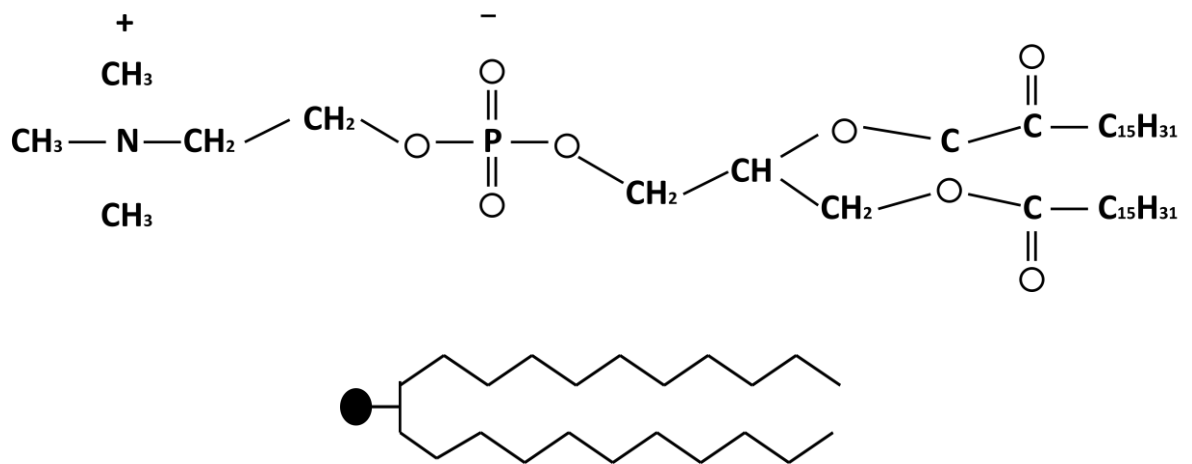
[Fig. 2.2 Typical phospholipid molecule, diapalmitoylphosphatidylcholine.]

Figure 2.1 represents a typical surfactant molecule consisting of polar head formed by bonding of a sodium atom with a carboxyl group, and a non polar hydrocarbon chain. A common symbol is also shown representing the polar head by a small solid circle and non-polar chain by zigzag lines. There are a variety of soaps that can be made using many other polar head groups and hydrocarbon chain groups of various lengths connected together. A typical phospholipid molecule is shown by figure 2.2 consisting of large polar head group containing a phosphorus atom and two non polar hydrocarbon chains. Its representative simplified symbol is also shown. There are also many different types of phospholipids due to

the large number of possible combinations of various head group and hydrocarbon chains of various lengths.
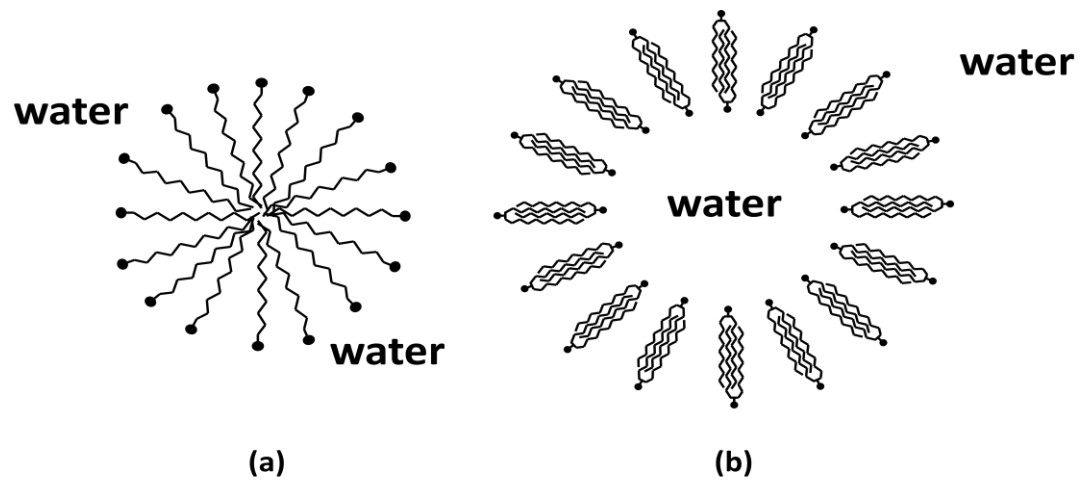
[Fig. 2.3 Cross sectional diagram of (a) micelle and (b) vesicle formed in water.]

If a very small amount of amphiphilic material is mixed with water, it is very likely that the molecules will dissolve. As the concentration of the amphiphilic material increases, eventually, there is the formation of two possible structures. The formation of these two structures is dependent on the strength of polarity of the head group as compare to the non-polar part of the molecule. If the head group molecule is strongly polar then the amphiphilic molecules begin to arrange themselves into a sphere, with the polar head group on the circumference of the sphere and the non-polar hydrocarbon chain towards the centre. This structure is known as a micelle (Fig 2.3a). Micelles are stable as long as the concentration of the amphiphilic material is above a certain limit known as the Critical Micelle Concentration (CMC). If the head group polarity is not strong enough relative to the hydrophobic part of the amphiphilic molecule then the molecules begins to form spherical vesicles which are double layered in terms of having polar head both inside and outside the spherical structure and form shell with water on the inside and outside (Fig. 2.3b). This double layered structure is the

consequence of the arrangement of the amphiphiles exactly opposite as in case of micelle which is because of the less polarity of amphile head group. In the case of vesicles the hydrophilic head groups are on the outside of the structure in contact with water molecules, while the hydrophobic end chains are in contact with each other and shielded from water both from inside and outside. As the concentration of the amphiphilic material is increased further more micelles or vesicles form. In the majority of cases the micelle or vesicle shapes and sizes remain constant as their number increases. In some instances vesicles with several bilayers are formed containing water in between each bilayer. The cross sections of both these structures are shown in figure 2.3.
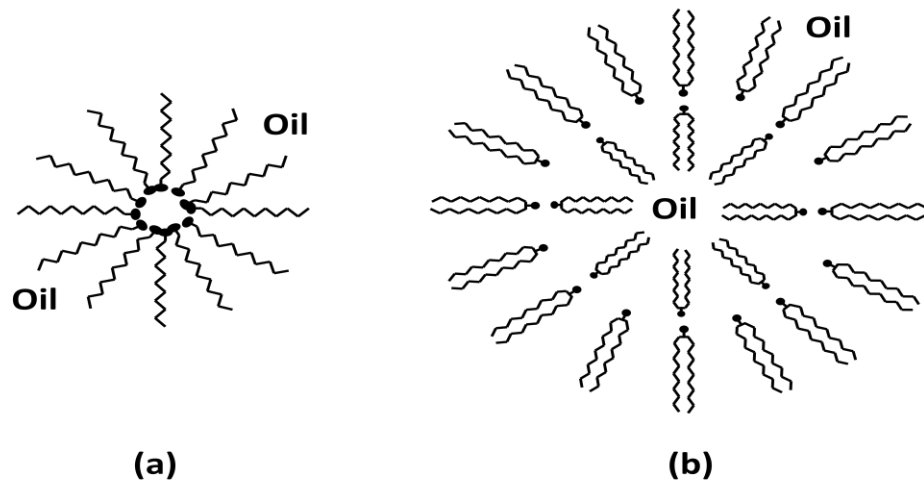
[Fig. 2.4 Cross sectional diagram of (a) micelle and (b) vesicle formed in oil.]

In the case of non-polar liquids similar structures are formed with the addition of amphiphilic material but with exactly the opposite arrangement of amphiphiles in water. The cross sections of the both these structures are shown in figure 2.4.

If the concentration of the amphiphilic material is increased further from here, a point is reached where the micelle and vesicles combine to form larger structures. These large structures are called as Lyotropic Liquid Crystals (LLCs). These LLCs exhibit various

structures which are capable of being transformed into each other in a definite sequence under very special circumstances, known as mesophases (Friberg et al., 1976, Benton et al., 1982). The amphiphilic materials responsible for producing these mesophases are known as mesogens. The amphiphilic molecules play a very important role in the structuring of the LLC as they orient themselves according to these structures by diffusion throughout these structures. The density of the amphiphilic molecules in these structures varies dramatically from one region to another. The amphiphilic molecules form these structures and the water present between these structures also contains a relatively small number of single amphiphilic molecules. The amphiphilic molecules are free to diffuse throughout both the structures and the water trapped inside them but they do so by maintaining the structural orders. A good deal of research has been performed on which polar head groups are responsible for the formation of these structures and which are not. It is not necessarily essential that the polar head group needs to be ionic for these structural formations or that only the polar non-ionic head groups forms these structures. It is only the result of a delicate balance of hydrophilic and hydrophobic tendencies of the amphiphilic molecule.

Temperature also plays a very significant role in the formation and the stability of these LLC structures. If the temperature is not high enough none of these structures can be formed. For the formation of these structures there has to be free relative movement of the amphiphilic molecules but if the temperature is too low, these molecules tends to form crystalline structures. The temperature at which these crystalline structures do not form and LLC structures come into existence is known as the Krafft temperature.

2.1.1 Classification of Lyotropic Liquid Crystals

Lyotropic liquid crystals are classified on the basis of X-ray diffraction studies into three different types of lyotropic liquid crystal phases as follows:
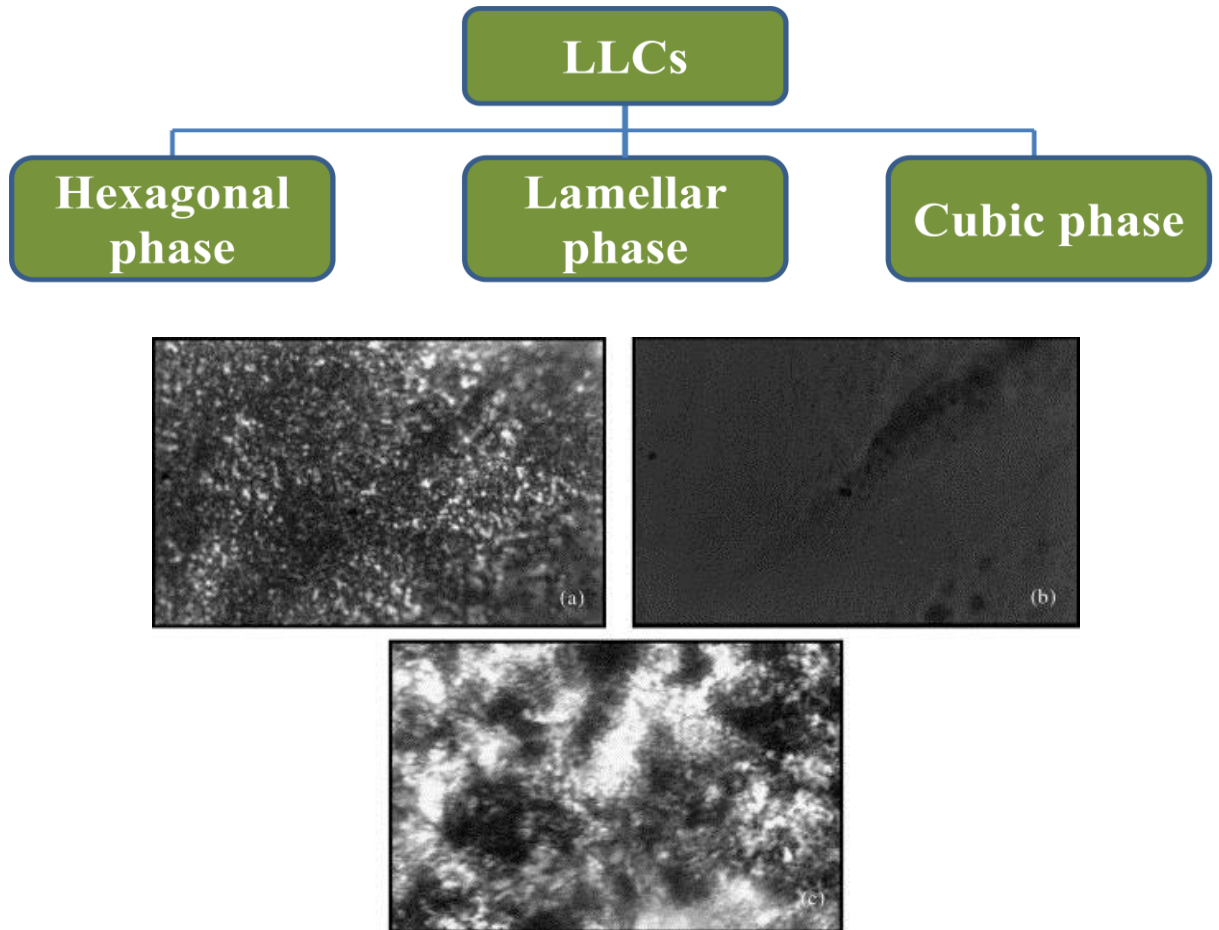
[Fig. 2.5 Polarized light microscopy images of GMO matrices showing (a) lamellar, (b) cubic and (c) hexagonal phases; (From (Shah and Paradkar, 2005)]
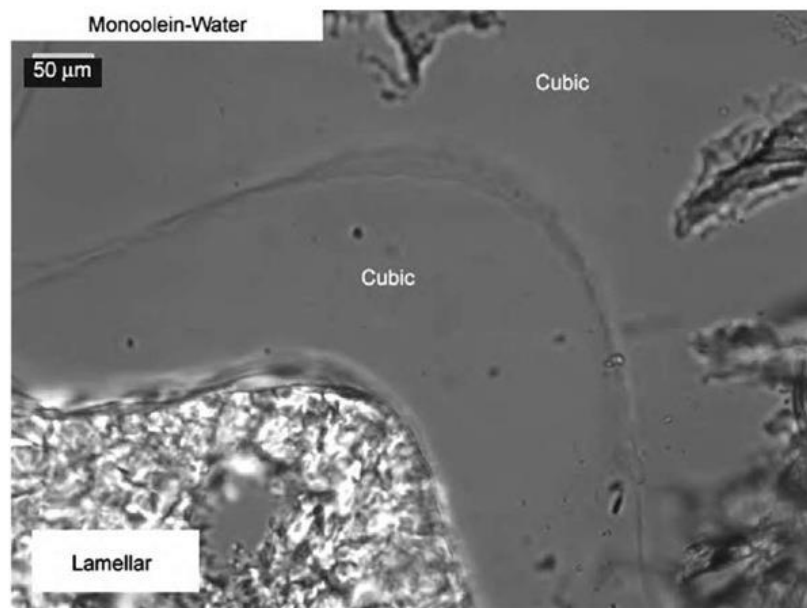
[Fig. 2.6 Polarized light microscopy images of aqueous phase progression exhibited by

monoolein in excess of water showing lamellar and cubic phases; From Spicer 2003]

➤ **Lamellar phase (L_α)**

The neat or lamellar phase (L_α) has amphiphillic molecules arranged in a flat bilayer structure

which are separated from each other by water layers (Fig. 2.7). These layers can extend over a

range of the order of microns or more. The water content governs the thickness of the water

layer which can vary from approximately 10Å to 100Å or more. Mostly, lamellar mesophases

exists down to a 50% concentration of amphiphillic material. Below this 50% concentration,

transition from lamellar to hexagonal phase (H_1) or an isotropic micellar solution may occur.

The lamellar phase consists of parallel layers of amphiphilles separated by water which can

easily slide over each other during the application of shear. This is the reason why lamellar

phases are less viscous and more shear sensitive than the hexagonal and cubic phases. These

phases are also identified by equally spaced peaks within SAXS results which correspond to α, 2α, 3α, etc where α stands for the spacing between adjacent bilayers (Hyde ST., 2001).

Non-polar chains

Polar head group

Bilayer unit

Water layer
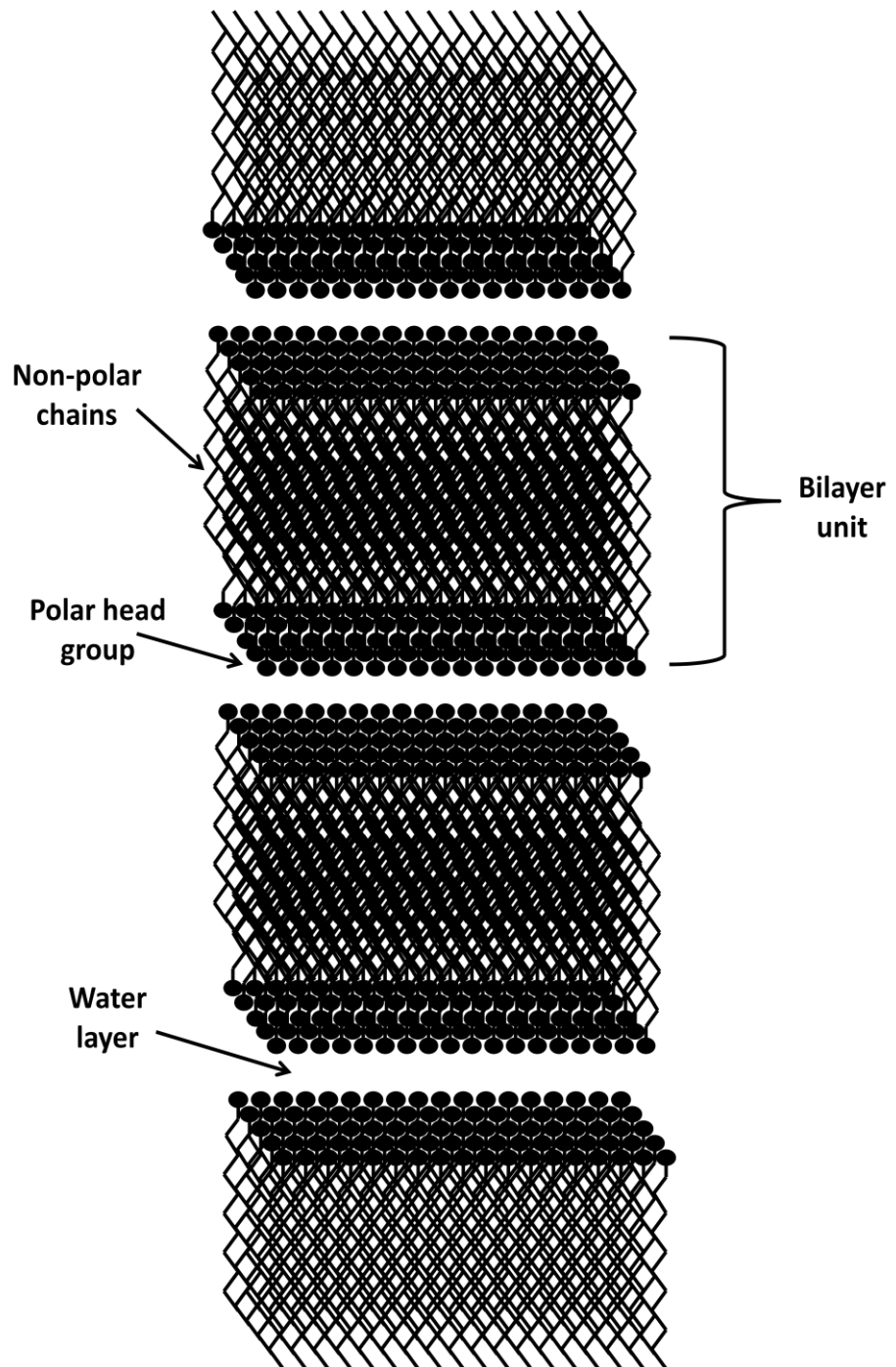
[Fig. 2.7 Schematic arrangement view of amphiphilic molecules in lamellar phase.]

➤ Hexagonal phase

As the name suggests, there can exist a hexagonal ordering of the micellar aggregates. In this phase two types of structure are found, the hexagonal phase (H_1) (Fig. 2.8a) and the reverse hexagonal phase (H_2) (Fig. 2.8b). In the hexagonal phase (H_1), the rod shaped (calamitic) micelles of indefinite length are packed together in hexagonal arrangements which are separated by continuous regions of solvent. The spacing between the micellar cylinders is dependent on the amount of the solvent and the amphiphillic material and is in between 10 to 50Å. The hexagonal phase has high water content but remains very viscous due to the calamitic micelles and the hexagonal arrangement which poses the rigidity of the structure. In the case of the reversed hexagonal phase (H_2), the hydrophobic hydrocarbon chains occupy the spaces between the hexagonally packed water cylinders of infinite length in comparison to the length of amphiphile which is the result of the inverted micellar arrangement as compared to the hexagonal phase (H_1). The reversed hexagonal micellar cylinders containing water have a typical diameter of 10 to 20Å. The non-polar chains overlap to bring the cylinders much closer to each other than the hexagonal phase (H_1).
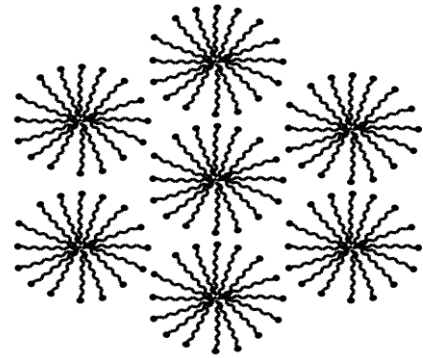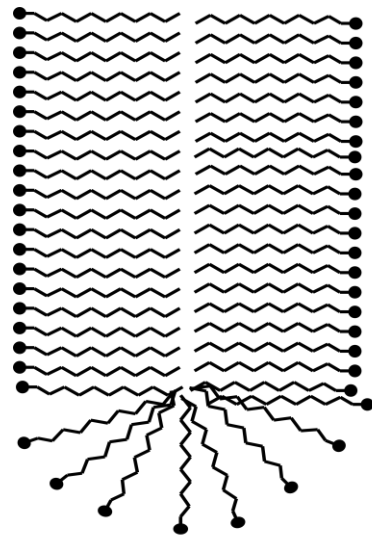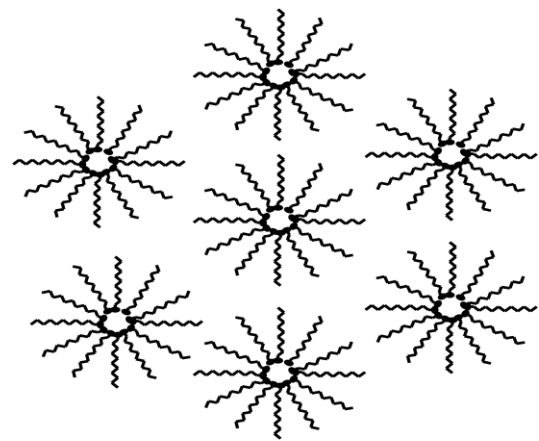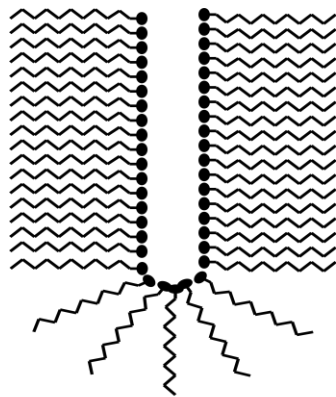
[Fig. 2.8 Structures of (a) hexagonal phase and (b) reversed hexagonal phase.]

> **Cubic phase**

Cubic phase is also known as the viscous isotropic phase because of its highly viscous nature and isotropic appearance under polarized light microscopy. There is a cubic molecular arrangement of aggregates within this phase. These aggregates are similar to normal micelles (I_1 phase) or reversed micelles (I_2 phase). The cubic phases are even more viscous than the hexagonal phases. The micelles or the spherical unit are arranged in a specific lattice to form cubic phase. To date only seven cubic structures have been discovered (Q^{212}, Q^{223}, Q^{224}, Q^{225}, Q^{227}, Q^{229} and Q^{230}) (Gruner et al., 1988) and they can be either micellar or bicontinuous. Out of the above seven, only three exhibit an inverse bicontinuous structure: the primitive (P) type (body-centred lattice (*Im3m*, denoted by Q^{224})) (Fig. 2.9a), the diamond (D) type (primitive lattice *Pn3m*, denoted by Q^{229}) (Fig. 2.9b) and the most frequent gyroid (G) type (*Ia3d*, denoted by Q^{230}) (Fig. 2.9c) (Gruner et al., 1988). The structure P contains two aqueous channels which are separated by an amphiphillic bilayer. The P type unit cell contains three mutually perpendicular aqueous channels which are connected in continuation with unit cells. Structure D contains two interpenetrating aqueous channels separated by a bilayer. Four aqueous channels of the D surface meet at a tetrahedral angle of 109.5˚. In the case of the G structure, the two fold axis and mirror plane symmetry shown by D and P is absent. There are two separate aqueous helical channels, left and right handed. These channels can extend throughout the matrix but they never intersect each other unlike in the P structure; however they are connected to form a helical arrangement.
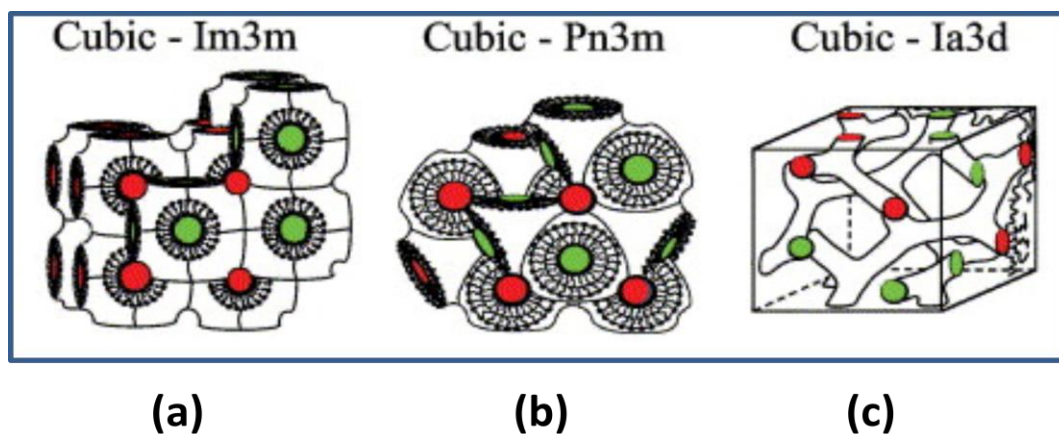
[Fig. 2.9 Schematic representation of cubic structures; (a) P-type (body-centred lattice (*Im3m*, denoted by Q^{224}), (b) D-type (primitive lattice *Pn3m*, Q^{229}), (c) G-type (*Ia3d*, denoted Q^{230}); From (Caffrey, 2003)]

2.1.2   What are Lyotropic Liquid Crystal Precursors?

Lyotropic liquid crystal precursors are the solutions (Czarnecki &Williams, 1993; Spicer et al., 2001) of amphiphiles which upon favourable conditions like specific temperature and concentrations form LLC. Sometimes these solutions are dried to produce powdered LLC precursor which will in future form the LLC with the help of proper stimulus like temperature or upon reaching the favourable conditions like presence of solvent for the LLC formation. This stimulus mostly comes in the form of temperature, pH or both (He et al., 2008) and with favourable condition such as 'the correct' concentration. LLCs forms only at certain temperatures and concentrations, although the effect of shear cannot be neglected which has proved its importance in dissolving LLC phases (Paasch et al., 1989). However these stimuli and conditions will be very specific for the different kind of amphiphilic material.

2.2 Applications of Lyotropic Liquid Crystals

One of the most commercial and primitive application of the LLCs is as detergents, in fact the 'goo' present in our soap dishes is also an LLC phase. Amphiphilic compounds have been used as soap and detergents for more than three thousand years, however our knowledge of their working is only very recent but many questions are still to be answered. These amphiphilic materials or surfactants have been explored extensively in the crude oil industry for the recovery of oil trapped in porous rocks of 'dry' wells. LLCs are extensively used by the food industry as emulsifiers to provide the texture, colour, flavour and, most importantly, the viscosity which can help in both maintaining the consistency of the product and in chewing. These emulsifiers are used in beers, ice creams, whipped creams, mayonnaise, cheese, and jellies. Some of these LLC producing compounds are found in the variety of wheat which produces a good quality of bread since efficient mixing of ingredients is required to rise and bake the bread properly and these naturally found LLC emulsifiers ensure good mixing.

LLCs have also been frequently used in the area of drug delivery owing to their excellent solubilisation capacity for both water and oil soluble APIs, their ability to stabilize bio-actives from enzymes to nucleic acids and their use in the formation of controlled release drug delivery systems. Apart from these common applications they show potential for artificial skin production (DiBiase and Rhodes, 1996), post surgical adhesion formation and for increasing drug penetration or diffusion through membranes.

2.3 Characterisation of Lyotropic Liquid Crystals

The characterisation of the LLCs is still very much confined to X-ray diffraction, mostly small angle X-ray scattering (SAXS), Polarized light microscopy (PLM) and rheological measurements. The structure elucidation of LLCs is constrained to X-ray diffraction which has also been the basis of classifying the LLC phases but cryo-transmission emission microscopy (cryo-TEM) has also been employed to study the sub-micron sized cubic phase particles (Spicer et al., 2001). However PLM has proved its calibre in characterizing the LLC phases. PLM is relatively easy to use, effective, straight forward in interpretation and versatile enough to accommodate a hot plate or with some media which is very helpful in getting insights to the factors responsible for particular phase formation with specific physico-chemical requirements. With PLM, lamellar (Fig. 2.5a), cubic (Fig. 2.5b) and hexagonal (Fig. 2.5c) phase detection has been simply achieved using the classification established by Rosevear (1954). Specific LLC phases exhibit distinct flow behaviour and also react very distinctly under shear. This specificity of the flow behaviour of each phase is the outcome of the rheological measurements (Wang et al., 2005). Rheometry has proved its importance in quantifying LLC phase sensitivity towards shear and the system rigidity through dynamic oscillation rheological measurements (Maheshwari et al., 2006). Although SAXS is a very reliable technique for the microscopic structural determination of the LLC mesophases the scattering patterns are of vary low intensity and can possess non-uniform LLC structures. Hence the above techniques are generally used in combination for confirmation of LLC phase formation (Spicer et al., 2002, Carvalho et al., 2013).

2.4 Why Lyotropic liquid crystal precursor formulations?

In this era of drug discovery where majority of potential new chemical entities discovered to have therapeutic activity suffer from poor pharmacokinetics and where patient compliance, especially in the case of elderly patients going through polypharmacy, are both major issues which can be addressed by developing new controlled drug delivery systems. These LLC systems can enhance solubility, provide a controlled drug release profile and simultaneously improve patient compliance by reducing dosage frequency. Controlled release drug delivery systems have already proved their potential in dealing with these types of problems as they disseminate a limited amount of API per unit time into the given amount of dissolution media both in-vitro or in-vivo which helps in solubilisation by restricting saturation. This provides very dilute API concentration within dissolution media for a long time period which also help in reducing dosage frequency. Most of the present highly soluble drugs like chlorpheniramine maleate have a short half life therefore, to maintain the desired effective peak plasma concentration over a long time period; the dosing frequency needs to be high. This can be very effectively achieved by controlled release drug delivery systems with reduced dosing frequency and thereby increasing patient compliance. Controlled drug delivery systems also improve the benefit: risk ratio in case of particular drugs where the level of drug after a certain maximum plasma concentration is responsible for side effects. This is done by maintaining relatively low and controlled plasma concentration of API. Thus the above advantages have provoked many researchers to develop controlled drug delivery systems through various approaches. In this study we are trying to explore the cubic phase lyotropic liquid crystalline coated powder precursor developed through twin screw extrusion for controlled release.

2.5   Approaches for Lyotropic liquid crystal precursor formation

To date there have been few approaches explored for precursor production from which dilution and temperature dependent restriction approaches seem the simplest methods, where a lower or higher amount of solvent is added to LLC producing material to restrict the arrangement of molecules into LLC. However sometimes unsuitable temperature is maintained which will oppose LLC production. Apart from these conventional approaches research into alternative methods has been very limited. Some of them are from last decade such as Hydrotrope method (Spicer et al., 2001) but in case of powder precursor production which is also a very exclusively explored area and that to only with the help of spray drying (Shah et al., 2006) (Maheshwari et al., 2006) and freeze drying technique (Kim et al., 2000) both of which are based on drying phenomenon as their name suggests.

➤ Dilution and temperature induced method

This particular approach has been well explored by many researchers (Carvalho et al., 2013), (Pisal et al., 2004) because its principle is based on the LLC production principle in which they have experimented with solvent quantities to provide the space in terms of volume for the specific arrangement molecules at specific temperature. There exist many disadvantages associated with this approach such as difficulty in handling these bulk precursors, complex flow behaviour and in drug delivery associated with shear application such as intravenous injections. In this approach the LLC forming ingredients are initially formulated with limited or excess amount of solvent at a specific temperature which both restricts LLC phase formation. In some studies only temperature restriction is applied but this differs from material to material showing specific LLC phase formation at specific concentration and

temperature such as GMO exhibits cubic phase only with 20% w/w water but Pluronic F127 exhibits cubic phase throughout from 20-30% w/w from ambient to body temperature. These formulated precursors, in the presence of favourable conditions for LLC phase formation (dilution, temperature) are transformed to the LLC phase. These conditions are mostly provided by the in-situ environment in the case of most drug delivery routes.

> **Spray drying approach**

In this technique spray dryers are used as processing equipment. This technique has already proved its calibre in the food and pharmaceutical industries during 150 years of evolution and research. The first recognition of this technique came in 1860. And spray drying first found application in the food industry. Spray dryers are still extensively used for milk powder production and post world war they became utilised in the pharmaceutical industry. The first pharmaceutical setting of spray drying was to obtain the dry extracts of active raw material from plants. The basic principle of the technique is the removal of liquid content from the feed with the help of a gaseous drying medium. This process involves various parameters which are helpful in obtaining distinct powder properties of the dried substance for the various forms of drugs (Vehring, 2008) (Xu et al., 2009). This technique has been studied by a few researchers (Maheshwari et al., 2006) (Spicer et al., 2002) for LLC powder precursor formation. By spray drying one can achieve complete coating of LLC producing polymers with the desired thickness but it is very difficult to control the particle size of the spray dried precursor. It becomes even hard to optimize the process because of the complex visco-elastic flow behaviour of LLC and avoiding the agglomeration of particles was even a greater challenge with this process due to highly viscous nature of the LLC (Spicer et al., 2002).

The spraying drying process comprises of three major phases. First one is atomization where the liquids are broken down to produce very small droplets of specific particle size and high surface area to facilitate quick drying. The next step is the interaction of the fine droplets with the drying gas subjected to a suitable temperature. During this process the liquid content present in the dispersion droplets is evaporated which results in the formation of the solid particles. The final phase is the separation of the solid particles from the gaseous media and their collection in an appropriate tank. All the phases and the process conditions can have a huge impact on both efficiency and final product properties.

> **Freeze drying approach**

Freeze drying or lyophilisation has been extensively investigated in various fields from processing flood affected books, documents and museum artefacts to non-living bio-products, pharmaceutical products, tissues and foodstuffs whose desired organoleptic properties have to be maintained. This technique has also proved advantageous for micro-organism conservation, dehydration of thermolabile chemical products and production of various inorganic products but, up to now, this technique has only been explored by Kim et al., 2000 for LLC precursor production where they tried to produce the dried cubosomes (nano-sized discrete cubic phase particles). This technique has major advantage in terms of not having shear which might deteriorate LLC formation or shear induced mesophase transformation but simultaneously in this technique temperature needs to be changed to get the process going. Thus it posses risk of temperature induced changes in LLC.

Freeze drying comprises three stages. The first stage involves freezing of the product to produce a solid matrix for drying. The second step, known as primary drying, removes the ice (unbound water) through sublimation with the help of reduced pressure of the product environment while maintaining the product below the glass transition temperature (Tg). The final step is known as secondary drying in which bound water is removed until the desired moisture level is acquired. A general industrial application may involve cooling the vials containing the material down to 5˚C and then cooling further to -10˚C, this temperature was kept for 30 minutes to ensure uniform super cooling. To help crystallize the bulking agent (mostly water) sometimes an additional annealing step is involved in which the shelf temperature is raised up to or above the Tg of the formulation. After freezing, primary drying is performed by employing a vacuum in the chamber. The chamber pressure is forced below the saturated vapour pressure of ice at freezing temperature. This difference in vapour pressure of ice and the chamber pressure causes the sublimation process. The chamber pressure is maintained below saturated vapour pressure and sublimation continues. After the complete removal of the bulk frozen ice by primary drying there is still some bound unfrozen water left in the sample, for which the secondary drying step is applied which involves dehydration at higher temperature. For this, the shelf temperature is raised to ambient or higher temperature and held until the desired residual moisture is achieved. This completes the secondary drying; the chamber can be equipped to apply stoppers to the vials. After ensuring complete closure of the vials inside the chamber the vacuum is completely released and then vials are unloaded from the chamber. This completes the freeze drying technique.

2.6   Challenges with Lyotropic Liquid Crystal precursor formation

The major challenges to the precursor formation are very much same as in case of the drug delivery involving LLC phases as briefly discussed in chapter 1. It is very difficult to handle these LLC phases in the bulk because of their complex flow behaviour, shear induced transformation and the physico-chemical environment. Careful attention to maintain particular phase or the consistency while handling, transferring or delivering must be paid.

As discussed in section 2.1.2 LLC precursors require a particular physico-chemical stimulus for its transformation from the sol state to LLC phase or from a particular LLC phase to another. Hence it is very important to maintain specified temperature, amount of solvent and chemical conditions. Maintaining an individual condition may be an easy task for the storage, but in drug delivery or processing, may present a far more daunting issue. In the case of processing to produce the precursor, the raw materials also have to be considered very seriously in terms of their interactions and their stability to restrict or produce the desired product before or after processing and then delivering the system to a specific site which will then eventually acquire the desired LLC phase after suitable stimulus. During processing shear is inevitable. Hence the selection of process equipment and operating variables must be considered accordingly to keep shear within limits to restrict undesirable shear induced LLC phase transformation or dissolution at any specific point in the downstream processing. LLC has been explored as the drug delivery vehicle for almost all common delivery routes with each specific delivery route posing its own challenge for LLC phase formation or transformation at the specific delivery site owing to their physico-chemical environment in terms of the pH, fluids being discharged and prevailing temperature. All these factors will effectively induce transformation of precursors to LLC phases and must be controlled. All the above discussed factors have to be contemplated in combination; from processing, raw

material compatibility up to drug delivery at a specific site to restrict or to acquire the specific

LLC phase from the precursor.

Chapter 3: Twin screw extrusion

==

Twin screw extrusion is one the most extensively used techniques within the polymer industry for product manufacture. The extrusion process was first utilized for bulk manufacturing in 1940's. Due to the versatility of this process, more than half of plastic products are manufactured by hot melt extrusion. In pharmaceutical uses, hot melt extrusion is the technique in which drug and excipient are processed by melting under controlled conditions prior to them being forced through a die to accomplish the desired shape. This extrusion technique has consequently attracted much interest as evidenced by a number of publications in the last decade (Crowley et al., 2007). Crowley et al. (2007) has also reported the steady increase in the number of patents issued on the extrusion technique from the early 1980's. The extrusion technique is a single step continuous process which can provide desired formulations with high yield. The single step operation can also eliminate batch to batch variation making it an economic and efficient process.

3.1 Introduction

The extrusion technique is an emerging and viable technique for pharmaceutical systems and various research groups have developed many drug delivery systems such as implants (Rothen-Weinhold et al., 2000), pellets (Follonier *et al.,* 1994), granules, sustained release tablets (Crowley et al., 2004), trans-dermal drug delivery systems (AitkenNichol et al., 1996) and trans-mucosal patches using the technique.
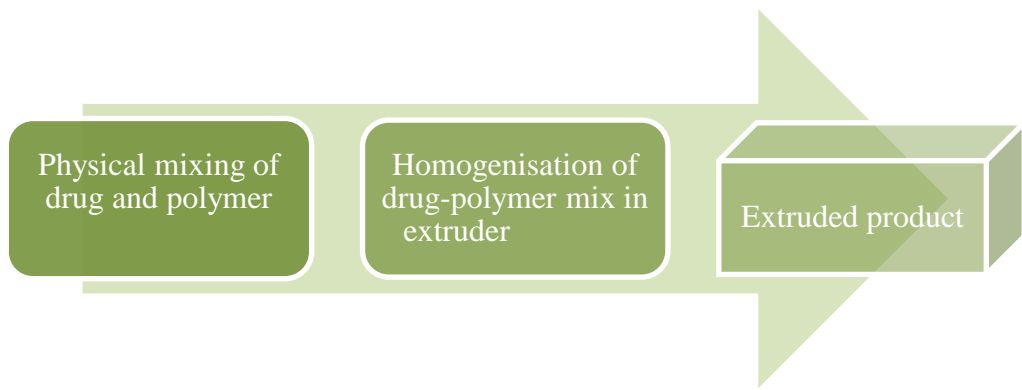
[Fig. 3.1 Flow diagram demonstrating extrusion process]

As shown in figure 3.1, during the extrusion the thermoplastic polymer gets converted into its molten state which then acts as binder for the drug prior to being forced out of the die in the desired shape prior to solidification. Below given column chart fig. 3.2 and the pie diagram fig. 3.3 (Crowley *et al.,* 2007) shows the number of patents issued on extrusion increased from 1984 to 2002.
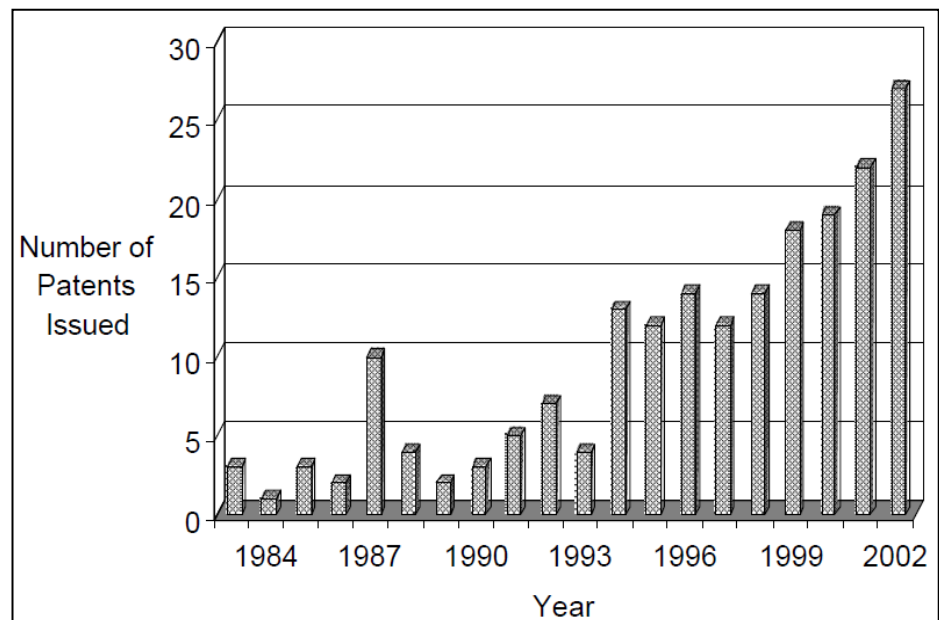
[Fig. 3.2 Increase in melt extrusion patents from 1984-2002 from Crowley *et al.,* 2007]
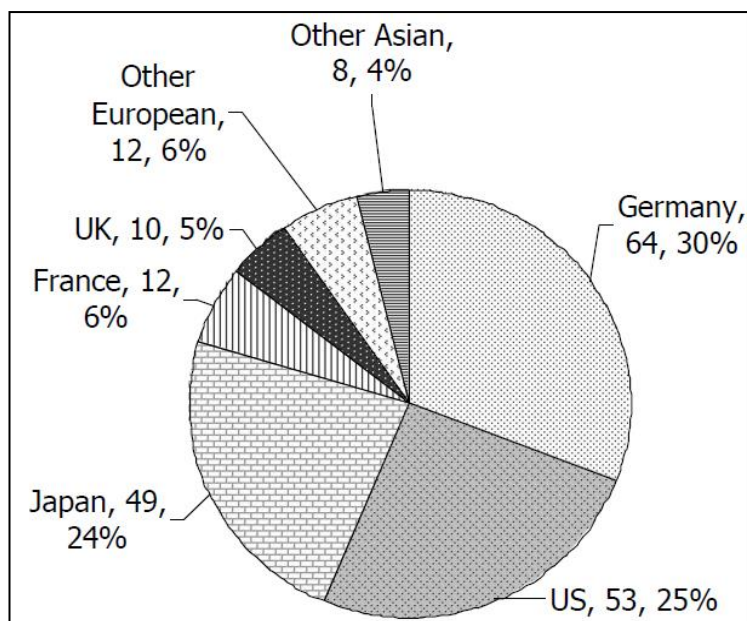
[Fig. 3.3 Percentage of patents issued from different countries since 1984 from Crowley *et al.,* 2007]

Extrusion's continuous processing has the well known advantages over batch processing such as limited variation, high efficiency and improved economy which has been addressed in many scientific publications in the pharmaceutical industry. Extrusion processing has proved its efficiency along with several benefits over other conventional batch processes with reference to its continuous and solvent-free nature and simplicity in operation. It can also eliminate the drying step thus reducing production time. In this continuous technique polymers can easily shaped into films unlike in the solvent cast technique. Intense mixing and deep agitation causes de-aggregation which helps the drug to disperse uniformly into the molten polymer. The bioavailability of the API is found to be improved in the extruded system because the drug gets dispersed at the molecular level. The blend of the polymer and API is carried forward by the rotating screw at elevated temperature thus producing a solid dispersion. Gamlen's (1986) research revealed that extrusion requires low costs in terms of labour and capital investment which proved its superiority over other techniques.

3.2 Underlying mechanism of extrusion process

As discussed above, the extrusion the technique involves the transfer of the reacting components in the presence of elevated temperatures with the help of rotating screw(s) to force the material out of the die into desired shape (Crowley *et al.,* 2007).
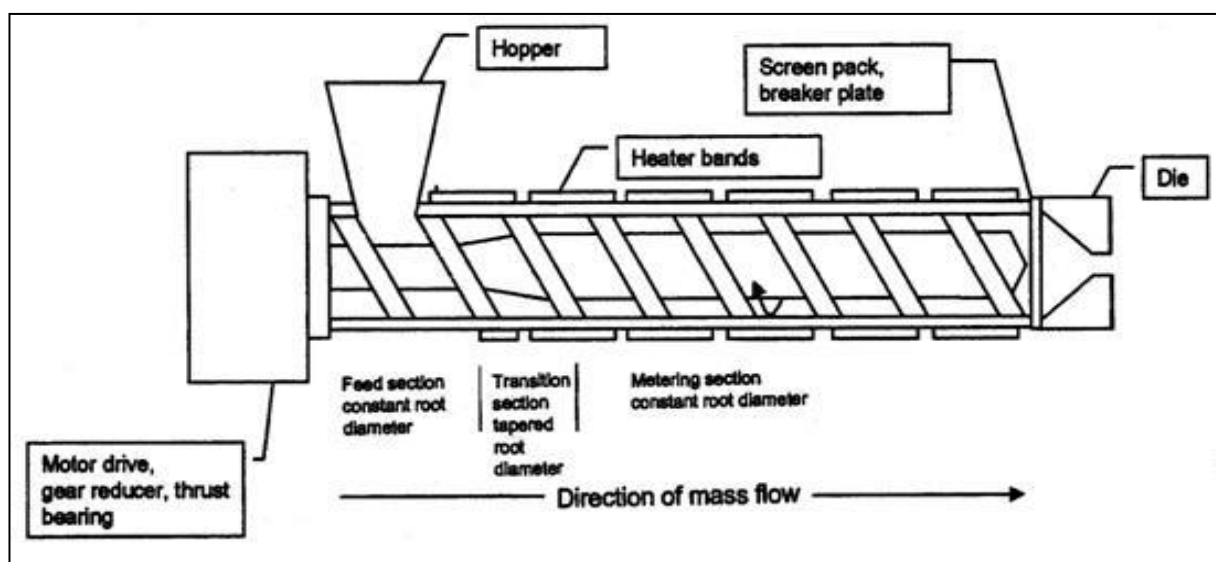
[Fig. 3.4 Diagrammatic representation of an extruder from Crowley *et al.,* 2007]

Figure 3.4 shows a schematic of a single screw extruder. The hopper contains starting material which is taken away by the rotating screws along the extrusion barrel. The barrel is the hollow part of the extruder which accommodates the single or twin screws. The extruder is equipped with heating and cooling zones which help in maintaining the desired processing temperature. As the feed stock from the hopper starts travelling along the barrel at elevated temperature additional heat generation also occurs due to friction (Crowley *et al.,* 2007). There are two types of frictional forces being generated within the barrel; one between the feeding material and the barrel surface and the second one between the screw interface and the material which plays a significant role in dispersive mixing of the materials. The forward moving force for the material within the barrel is the consequence of resultant frictional

differences between the screw interface and the entire barrel (Crowley., 2003). Crowley et al (2007) also reported that the feeding efficiency of raw material is affected by the coefficient of friction between the starting material and the barrel surface. Crowley (2003) has made another important point that the feeding efficiency depends on the bulk properties of the material. For example, if the angle of hopper is less than the angle of repose of the bulk material having poor flow properties, this may result in the formation of a 'solid bridge' at the throat of the hopper which leads to inconsistent feeding. Friction within the barrel can also be optimised by adjusting the temperature of the barrel.

It is essential to maintain efficient consistent feeding for elevated pressure in the compression and conveying zones (Crowley., 2003). Changes in screw configurations impose changes in shear rate, the melting process and the mass flow of material. Melting is one of the most critical steps leading to mixing and dispersion of the components. If the material inside the barrel remains solid there is a possibility of blockage in the barrel and inside the channels which carry the material towards the die. Another important issue to look after is the shear produced by the dispersing or mixing zones which can cause degradation. Therefore, it is very important to have very selective processing conditions which play pivotal role in the optimization of the process parameters. These process parameters are dependent on the physico-chemical properties of the material such as melting point(s), onset of degradation, effects of shear and stability of the material at the process temperature.

3.3 Classification of Extruders

On the basis of the basic principle of operation the extrusion technique is divided into two main classes Ram extrusion and Screw extrusion. The figure 3.5 below shows the outline of classification.
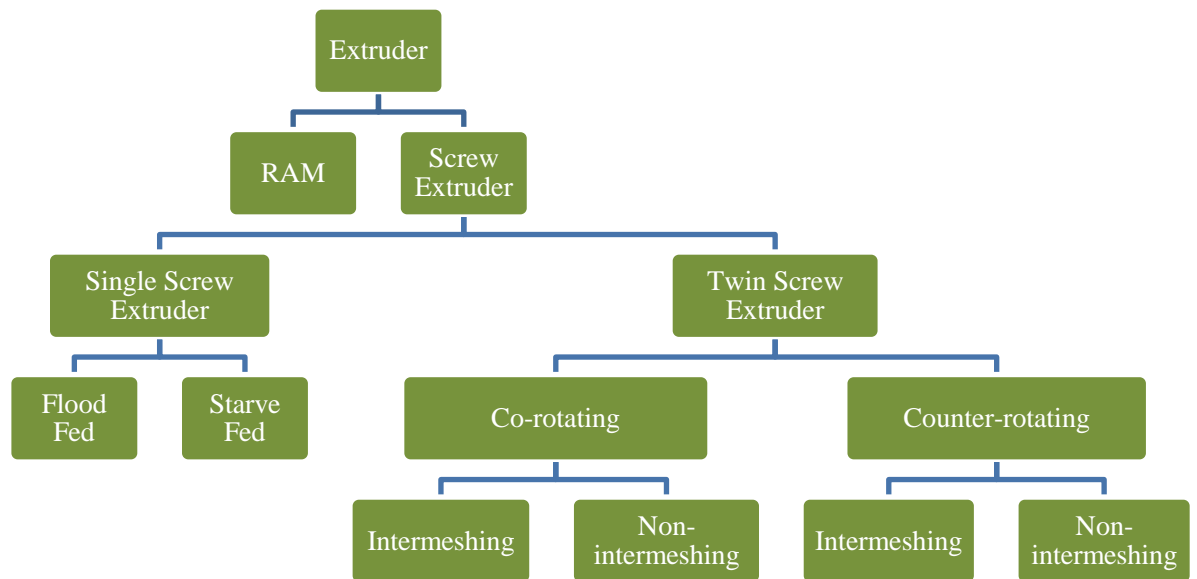
[Fig. 3.5 Classification of extruders]

3.3.1 Ram Extrusion

Ram extrusion based on the positive displacement of the component matrix through the die with the help of piston generating high pressure. When the material is introduced into the barrel it gets softened by elevated temperature and then pressurised through the die into the desired shape. The extrudates obtained from this techinque can be poor in homogeneity. Another disadvantage is that the technique has limited melting capacity which can be seen in temperature variation within extrudates. Thus Ram extrusion will not be suitable for LLC

powder precursor because it requires good homogeneity at low temperature in case of Pluronic F127.

3.3.2 Screw extrusion

In screw extrusion, the barrel is equipped with rotating screws which provide shear, intense mixing and conveying of the material. Screw extruders consist of three main parts: the conveying system, the die and auxiliary down-stream equipment. Apart from the above major components, screw extruders are also equipped with additional components such as accurate feeders, process analytical tools (PAT), thermocouples and temperature controllers etc. Process control can be provided through monitoring the zone temperatures, pressures, torque and rotating screw speed. This technique is further divided into single screw extrusion and twin screw extrusion.

❖ **Single screw extrusion**

This is one of the most extensively used techniques utilising only one screw for feeding, melting, pumping and devolatalising (Crowley *et al.,* 2007). Conveying, melting and pumping is achieved by frictional and viscous forces generated inside the conveying zones and then molten material is forced outside through the die (see fig. 3.6). This process is further categorized into flood feed and starve feed depending on the manufacturing process. In the flood feed process, the amount of material taken by the screw depends on the screw speed while in the starve feed mode output is dependent on the mass flow rate. The single screw extruders are found weak when it is reduced to 18mm in diameter which is also one of the

setbacks of this process. To overcome this, vertical screw is used which is being driven from the discharge end.
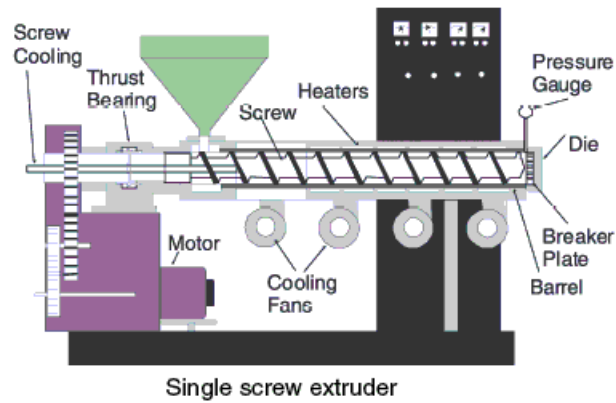
[Fig. 3.6 Diagrammatic representation of single screw extruder]

❖ **Design of single screw extruder**

The design of the extruder screws plays a pivotal role in processing since the specific arrangements provides differentiated shear required for the extrusion process. Several applicable screw designs have been described by Whelan and Dunning (1988). They state that single screw extruders have been designed with division in conveying, mixing, compressing and metering as per the process requirement. Typically, the three major zones are named after their function as per the division of screw mentioned above as conveying (feeding), mixing (compression) and metering.
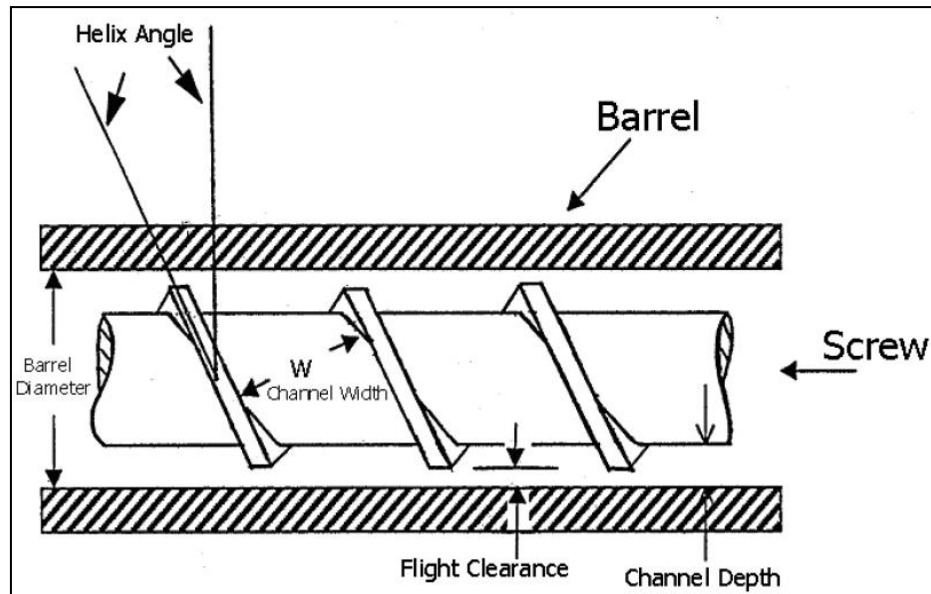
[Fig. 3.7 Design of a single extruder screw from Crowley *et al.,* 2003]

The conveying zone feeds the material from the hopper to the mixing or the compression zone. Therefore, conveying screw flights are designed in a way as to provide wide channel depth so that a large mass transfer at a constant rate can be achieved (see fig. 3.7). For the mixing or the compression zone the channel depth is reduced. Here the components melt because of elevated temperature and due to the reduced depth the material is compressed which reduces the material thickness. This compressed thin layer of material in contact with heated barrel and screws is melted efficiently which is then with the help of mixing screws are dispersed or start reacting with each other. After the mixing zone comes the metering zone which is responsible for forcing the extrudate out though the die. Similar to the conveying zone, the mass flow in the zone relies on the channel depth and the length of the metering zone. The final product can be obtained into the desired shape using specific die geometry.

Within the extrusion industry, screw dimensions are typically described in terms of length/diameter (L/D) ratio. Generally screw dimensions are in the range of 24:1 to 40:1 which is according to the types screw used. To achieve the maximum output rate, there should

be a desired equilibrium between the free volume in the channel depth and the torque. The torque is also affected by channel depth.

❖ Twin screw extrusion

Twin screw extrusion consists of intermeshing of two screws inside the barrel (see fig. 3.8). The first twin screw extruder was designed in late 1930's in Italy. Within twin screw extrusion, modular configurations may allow the bespoke imposition of high shear, low shear, dispersive mixing etc in the desired zones of the barrel.

[Fig. 3.8 Twin screw extruder screws (barrel-parallel_twin_screw03)]

On the basis of direction of rotation, twin screw extruders are divided into two overall designs: co-rotating and counter rotating. If the screws rotate in the same direction they are termed co-rotating and if they rotate in opposite directions to each other they are known as counter-rotating (see fig. 3.9). Counter-rotating screws work on the principle of squeezing the material and can thus be utilised for high shear applications. As these rotate in opposite direction to each other, there is fair chance of air entrapment. Another limitation is that they cannot be operated beyond a certain maximum rotation speed as there is possibility of interlocking and breakdown, therefore results in lesser output.

Intermeshing zones
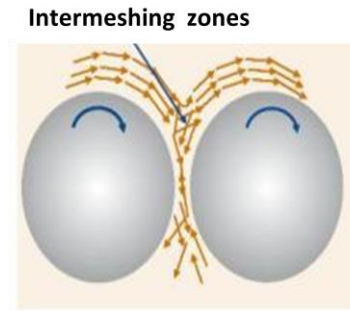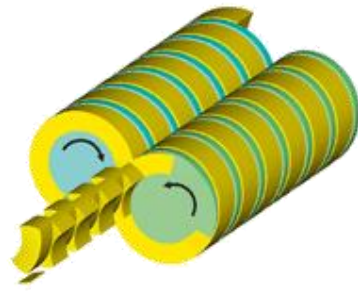
[Fig. 3.9 Counter-rotating screws (from (technology) and co-rotating screws (aquafeed, 2008)]

On the contrary, co-rotating screw extruders possess intermeshing design which is exactly opposite to the counter rotating extruders. As they rotate in the same direction, they are termed as self-wiping (Breitenbach, 2002). Co-rotating screws possess several advantages over counter-rotating screws such as high speed of operation, good mixing and higher output which why they also offer great industrial applicability.

3.3.3 Advantages of twin screw extrusion over single screw extrusion

1) Good mixing capability.

2) Short residence time: - this is due to self-wiping screws ensuring high speeds which results in shorter residence for the material and emptying the barrel.

3) Due to specific type of screw arrangements, twin screw extruders can offer high dispersing and kneading capabilities.

4) Versatility: - different type of specific screw arrangements can be configured accordingly to get the desired high or low shear for operation.

3.4 Processing equipment

Presently the extruders are majorly classified as plastic and pharmaceutical extruders. The extruder shown below in fig. 3.10 is a pharmaceutical class extruder twin screw extruder.

[Fig. 3.10 Pharmaceutical class extruder]

Pharmaceutical extruders have evolved to meet the highly regulated requirements of the pharmaceutical industry in terms of metallurgy of the contact parts (Crowley *et al.*, 2007). The metal of the contact part should be non-reactive and non-additive to the material being processed. These pharmaceutical class extruders have been designed so that they offer ease in validation and cleaning requirements which are necessary for pharmaceutical conditions.

3.5 Twin screw extrusion in lyotropic liquid crystal powder precursor formation

This is the first time exploration of the twin screw extrusion in LLC powder precursor formation. Basically the idea is to coat the Pluronic F-127 tri-block co-polymer on to the Micro-crystalline cellulose (MCC) through twin screw extrusion to form a controlled release LLC powder precursor. For coating different concentrated solutions of Pluronic F-127 with water containing dissolved Chlorpheniramine maleate (CPM) according to its saturation solubility are used. The Pluronic F-127 solution's concentrations are selected in the range where both the flow through the peristaltic pump and also the unique thermoreversible gelation property is maintained. Figure 3.11 demonstrates the experimental conditions used for producing LLC coated powder precursor through twin screw extrusion. The effect of various process parameters and the amount of MCC on the processing and the particle size of the finished LLC powder precursor are explored.
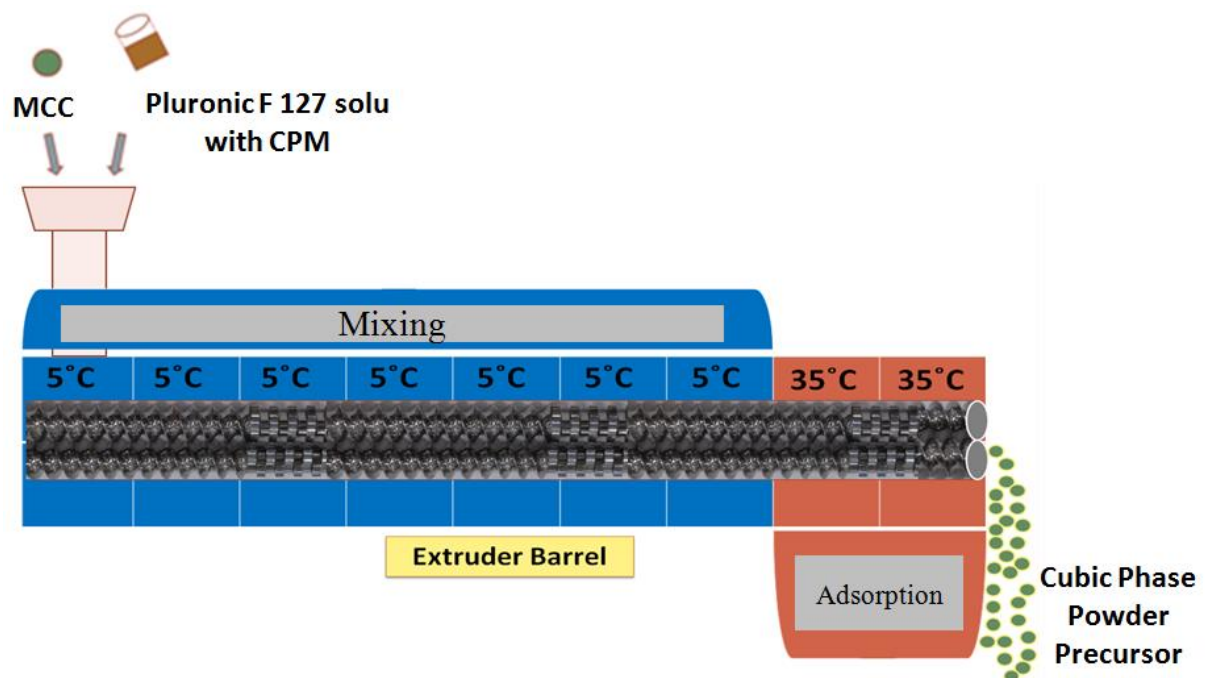
[Fig. 3.11 Diagrammatic representation of twin screw extruder in LLC powder precursor formation]

Chapter 4: Materials, methods & Characterisation

==

4.1 Materials

Specifications of materials used are described in the following table 4.1.

No.	Drug/ Polymer/ Excipients/ Chemicals	Supplier	Grade	Lot Number
1.	Chlorpheniramine Maleate	Alfa Aesar, UK	Analytical Grade	J8840A
2.	Pluronic F127	BASF, Germany	Analytical Grade	WPWG593B
3.	Microcrytalline Cellulose	FMC Biopolymer, Belgium	Analytical Grade	Q1215C
4.	Potassium Dibasic Phosphate	Sigma Aldrich, Germany	Analytical Grade	115K0030
5.	Sodium Hydroxide	Sigma Aldrich, Germany	Analytical Grade	045K003H
6.	Methylene Blue	Sigma Aldrich, Germany	Analytical Grade	10 G 220003

[Table. 4.1 - Specifications of chemicals]

4.2 Methods

4.2.1 Chlorpheniramine maleate containing Pluronic F127 solution preparation method

The saturation solubility at 20˚C of CPM was determined. The excess of CPM was maintained in equilibrium with water at 20˚C for 24hr. The amount of CPM in the supernatant was determined spectrophotometrically at 261nm. The saturation solubility was found to be 76mg/ml. The saturated solution of CPM was added to different proportions of Pluronic F127. Cold method of preparation was used for the Pluronic F127 solution. The weighed amount of Pluronic F127 was added slowly into the constantly stirred CPM solution maintained at refrigerated temperature (5˚C).

4.2.2. Lyotropic liquid crystal coated powder precursor

The following method was used for preparation of LLC coated powder precursor.

➤ **Twin screw extrusion**

For the coating of LLC over MCC a 16 mm co-rotating twin-screw extruder (Pharma lab, Thermo scientific, UK) was used. A screw length to diameter ratio of 40:1 for the standard mixing screw configuration (specified below in this section) was used for all batches. The extruder was operated without a die but with a die adapter attached along with thermocouple for maintaining temperature. The die adapter aids by increasing the flow length which ultimately allows a longer path for transferring more heat to the precursor at the end of the barrel. The MCC was fed into the extruder with the aid of a gravimetric feeder at different quantified feed rates (see table 4.5).

The twin screw extruder used for this study was shown in figure 3.10. The two co-rotating screws provide shear to the material being processed. The amount of shear applied and flow of material depends on the screw geometry and speed of rotation. The details of the screw elements and the screw configuration can be explained as follows:

❖ Screw elements/mixing paddles

The standard mixing configuration was used for extrusion to get the desired mixing and powdery consistency with minimum quantity of compacted granules. The various screw elements were specifically arranged to get standard mixing configuration (specified below in this section) to achieve the desired dispersive and staggered mixing (see fig. 4.2), forward conveying as well as discharge of final product from the extrusion barrel. Different screw elements and arrangements of kneading screws at specific angles are shown in fig. 4.1. The kneading elements arranged at specific angle are responsible for staggered mixing where material is minced and stretched. These give rise to different mixing efficiencies and conveying abilities (see table. 4.2) during twin screw extrusion and the combination of these kneading screws at specific angles with the conveying screws gives rise to specific screw configurations which provide different shear intensities and mixing.
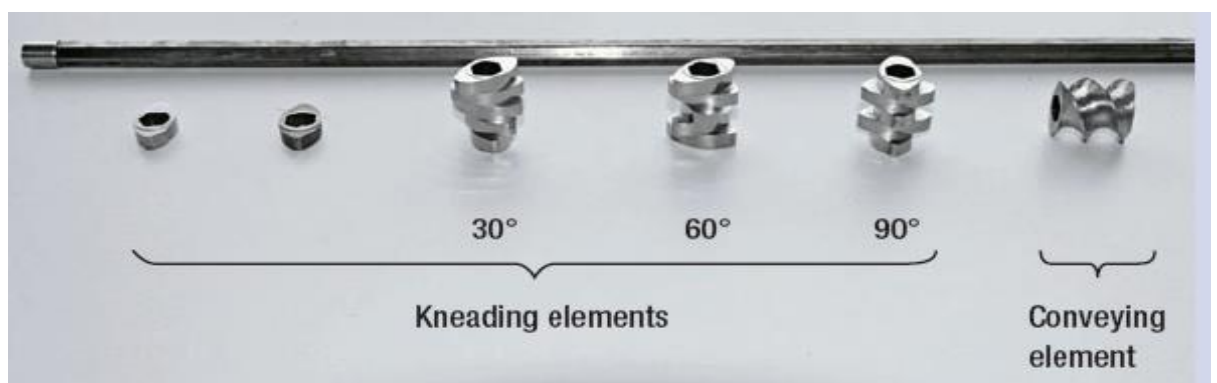
[Fig.4.1 Different angles created by mixing paddles]

The conveying screw element shown above is only applicable for pushing the material in a forward direction. They may provide limited dispersive mixing. Kneading elements offer high mixing and less conveying with the increase in their angle of arrangement. Their arrangement at small angles is responsible for a high compression and vice-versa. Table 4.2 demonstrate the conveying and mixing ability of different screw arrangement to achieve the desired results.

a) Conveying & dispersive mixing   b) Discharge

b) Staggered mixing
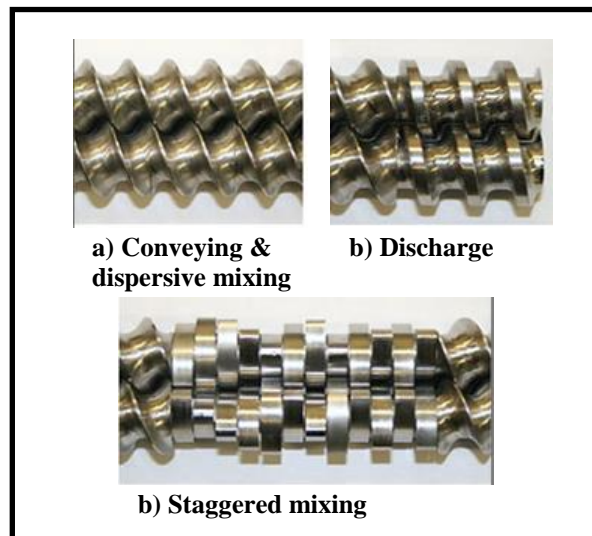
[Fig. 4.2 Application of various types of screws]

	CONVEYING	MIXING
Feed Screws	+++++++	+
30 deg Forward	+++++	++
60 deg Forward	++++	+++++
90 deg Alternate	zero	+++++++
60 deg Reverse	- - - -	++++++

Other elements available for special effects

[Table. 4.2 Screw arrangements and their special effects]

❖ Standard mixing configuration and its geometry

The standard mixing screw configurations was adopted and studied during processing of LLC coated powder precursor to provide a suitable mixing regime and moderate shear.

The screw geometry for the standard mixing configuration is as follows:-

<u>Standard mixing configuration : Geometry</u>

The length of one conveying screw (see fig. 4.1) is equivalent to six kneading elements (see fig. 4.1) and one discharge screw is equivalent to one and half conveying screw.

Length (in terms of conveying screw or element)	No. of screws	Element type
11	11	Forward conveying
2	4	30˚ forward mixing
	4	60˚ forward mixing
	4	90˚ mixing
6	6	Forward conveying
1	6	30˚ forward mixing
8	8	Forward conveying
2	4	60˚ forward mixing
	8	90˚ mixing
6	6	Forwarding
1.5	1	Discharge

[Table: 4.3 Standard mixing configuration]

<u>Description of Standard mixing configuration:-</u>

The standard mixing configuration contains three mixing zones separated by a number of conveying screws. It includes a large number of 90° mixing elements which provide high mixing of the material (see table 4.3).

❖ **Temperature profile**

In this project, an unusual temperature profile was used uncommon in extrusion. To prepare the LLC coated powder precursor via twin screw extrusion using Pluronic F127 solution for coating a refrigerated temperature (5˚C) was used except for in the last zone and the attached die holder where the tempersture was kept at 40˚C. This temperature profile was particularly selected based on the complex viscoelastic behaviour of the Pluronic F127 at specific temperatures which will help in spreading and then sticking the Pluronic F127 solution onto the MCC powder surface. The extrusion barrel is divided into ten different zones. The highest temperature was maintained in the last zone and the die holder attached without the die equipped with the thermocouple to maintain the temperature (see fig. 4.3 and table 4.4).
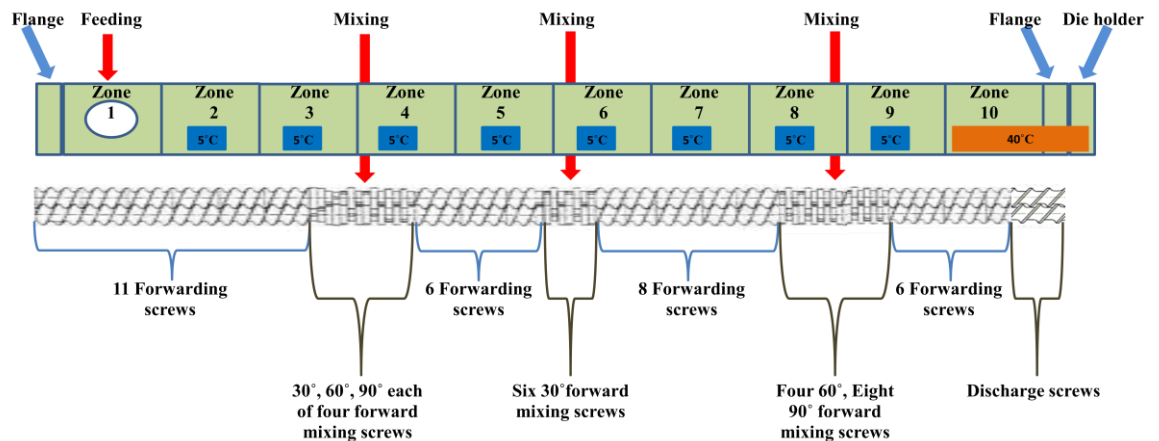
[Fig.4.3 Showing different zones of extrusion barrel with their corresponding temperature and position of mixing screws within the barrel]

Different Zones in Extruder Barrel	Zone 2	Zone 3	Zone 4	Zone 5	Zone 6	Zone 7	Zone 8	Zone 9	Zone 10	Die holder
Temperature of zones	5˚C	5˚C	5˚C	5˚C	5˚C	5˚C	5˚C	5˚C	40˚C	40˚C

[Table 4.4 Temperature profile used for LLC precursor powder production]

The different concentrations of Pluronic F127 solution containing CPM was fed into the extruder barrel using a Seko PR1 peristaltic pump. The observed extruder torque (%) and rise in temperature due to frictional heat generation was recorded.

> **Preliminary Batches for fixing variable levels**

There are number of variables in the process so we decided to use factorial design to understand effect of different independent variables on the properties of the final product. Preliminary batches were prepared with intention to decide the range of independent variables. The independent variables considered were:

a. Concentration of Pluronic F127 in the solution

b. MCC feed rate

c. Screw speed

Total 11 batches as shown in table 4.5 were prepared for the preliminary studies. Methylene blue was included as a marker compound in Batch 11 to understand uniformity of Pluronic F127 coating on the MCC surface.

The product obtained from various batches was evaluated for resistance to flow and compactness of the material by visual observation.

Batch no.	MCC feed rate for extrusion (gm/h)	Screw speed (RPM)	25% Pluronic F127 solution feed rate (gm/h)	Pluronic F127 solution : MCC (by weight)
1.	390	200	180	1: 2
2.	450	150	180	1: 2.5
3.	500	200	180	1: 2.78
4.	500	300	180	1: 2.78
5.	600	600	180	1: 3.33
6.	700	400	180	1: 3.89
7.	800	400	180	1: 4.45
8.	900	400	180	1: 5
9.	900	500	180	1: 5
10.	1000	500	180	1: 56
Batches with 25% Pluronic F127 containing methylene blue (10mg/ml of water)				
11.	1000	400	270	1:3.7

[Table. 4.5 Preliminary batches to determine range for independent variables.]

> **Factorial Design for LLC precursor processing**

On the basis of the preliminary batches the 3^3 factorial design studies was developed. The three factors (independent variables) and their levels are shown in Table 4.6. The numbers in parenthesis show coded levels where as those outside denote the actual values used in the

preparation of the batches. Total 27 batches were prepared (Table 4.7) and the centre point batch (0,0,0) was repeated thrice to get idea of the residual error in the processing and measurement.

Factorial design batches for Multiple regression analysis (3^3 factorial design study with three factors and three levels)			
Factors	Levels		
MCC feed rate (gm/hr) (variable X_1)	1400 (+1)	1200 (0)	1000 (-1)
Pluronic F127 concentration (variable X_2)	25% (+1)	22% (0)	19% (-1)
Screw speed (RPM) (variable X_3)	600 (+1)	500 (0)	400 (-1)

[Table. 4.6 The three factors considered and their three levels]

Batches	X1	X2	X3
F1	-1	-1	-1
F2	+1	-1	-1
F3	-1	+1	-1
F4	-1	-1	+1
F5	+1	+1	-1
F6	-1	+1	+1
F7	+1	-1	+1
F8	+1	+1	+1
F9	0	+1	+1

F10	0	-1	-1
F11	0	+1	-1
F12	0	-1	+1
F13	+1	0	+1
F14	-1	0	-1
F15	+1	0	-1
F16	-1	0	+1
F17	+1	+1	0
F18	-1	-1	0
F19	+1	-1	0
F20	-1	+1	0
F21	0	0	-1
F22	0	0	+1
F23	-1	0	0
F24	+1	0	0
F25	0	-1	0
F26	0	+1	0
F27	0	0	0
F28	0	0	0
F29	0	0	0

[Table. 4.7 Batches for factorial design study]

The Pluronic F127 solution was fed using peristaltic pump. The flow regulator control was maintained at fixed level to get constant feed rate for all Pluronic F127 solution concentration but still slight variation in the actual feed rate of the Pluronic F127 solution was there. The

flow was observed to be between 260 to 270 gm/hr depending on the Pluronic F127 solution concentration. To be precise the flow was 261, 268 and 270 gm/hr for 25, 22 and 19% respectively.

4.3 Characterisation

The following techniques were performed in the preliminary studies for physico-chemical characterisation of the starting material and the characterisation of processed LLC precursor.

4.3.1 Thermo gravimetric analysis (TGA)

Thermo Gravimetric Analysis was performed to check degradation onset temperature using a TA Instruments Q5000 Thermo Gravimetric Analyser (Crawley, UK), equipped with a RSC90 cooling unit. Each sample pan was tared to zero before loading the sample. Approximately, 8-10 mg sample was loaded with the nitrogen flow rate of 50 ml/min.

4.3.2 Differential scanning calorimetry (DSC)

DSC thermograms were obtained to check whether the system is able to detect heat flow changes during micellisation and cubic phase formation (gelation) as well as the melting temperature of the starting material. A TA Instruments Q2000 differential scanning calorimeter (Crawley, UK) equipped with an RSC90 cooling unit was used to produce the thermograms. The instrument was calibrated using an indium metal standard. Standard

aluminium DSC pans and lids were used for the DSC ramps with 5-6 mg of sample. A heating rate of 5 $^{\circ}$C/ min was selected and the nitrogen flow rate was kept at 50 mL/min.

4.3.3 Polarized light microscopy (PLM)

The formation of the mesophases (cubic phase) in the Pluronic F127 gel was confirmed using polarized light microscopy. An Olympus BX 41 microscope with the polarizing lens was used at 5X and 10X magnification.

4.3.4 Rotational rheometry

An Anton-Paar Physica MCR 301 rheometer was used to study the flow behaviour and complex viscoelastic characteristics of Pluronic F127 solution with or without CPM at different concentrations and temperatures. The gelation and gel melting temperatures were also detected by running temperature dependent frequency sweeps on the same rheometer system. For all the rheological measurements a cone and plate geometry with an angle of 1˚, a 0.049 mm central gap and of 50mm diameter was used.

4.3.5 Scanning electron microscopy (SEM)

Scanning electron microscopy was used to characterise the surface of the LLC coated precursor and to study the surface topography. The largest (710 - 355µm) and the smallest size (45 - 20µm) range of the LLC coated precursor was gold coated with a layer of 30 nm. SEM images were taken using an FEI Quanta 400 Scanning Electron Microscope operated under high vacuum and high voltage of 20KV. The images were taken at a working distance of 10mm at 1000X, 500X and 200X magnifications.

4.3.6 Particle size distribution

The particle size distribution was performed on the factorial design batches using a Retsch AS200 sieve shaker. The following sieves of pore size were employed: 710, 355, 250, 180, 150, 63, 45 and 20 μm. The powder precursor was shaken for 10 minutes at vibration amplitude of 2 mm/"g" without any interval. The weight retained on the sieves was recorded and plotted as a logarithmic probability distribution which then allowed the mean geometric diameter (d_g) to be determined.

4.3.7 Powder rheometer or flow analyser

The powder precursor's different batches of factorial design were tested for their flow behaviour by employing a TA.XT *Plus* powder rheometer (Stable Micro Systems, Surrey, U.K.). The powder rheometer was operated employing two cycles of compression–decompression tests while rotating before running a final cycle for analysis; the rheometer provides the rotational movement of the blades while traversing in the vertical direction. The following attachment was used: Rotor no. PFA/R2/SS (made of two blades with diameters and heights of 25 and 10 mm each, respectively) and the glass vessel (PFA/V/25G) with a diameter of 50mm. The glass vessel was filled up to the height of 70mm (35ml) for the analysis. Samples were studied in triplicate and the coefficient of variation was calculated for the area of decompression which represents the "work done for cohesion (WDC)" with the help of *Exponent* version 6 software for data analysis.

4.3.8 Ultra-Violet visible spectroscopy (UV-vis)

UV absorption spectra of Chlorpheniramine maleate was achieved using a Jasco V-630 UV-spectrometer. Samples were prepared in deionised water taken from ELGA Purelab ultra. UV cell made up of quartz having path length 1cm was used for experiment to load the samples. Spectra were recorded for each sample within the range 200 to 600 nm. Spectra manager 2 software was used to achieve the spectra.

4.3.9 Drug content, In-vitro drug release studies

A calibration curve was developed for the Chlorpheniramine maleate (CPM) in a phosphate buffer (pH = 6.8) within the concentration range of 5 - 40 μg/ml. The drug content of the processed LLC coated powder precursor was analysed by dissolving 416 mg of coated precursor into the refrigerated 10ml purified water and further diluted with phosphate buffer (pH=6.8). The drug content assay of specific batch for the dissolution study was done on selected particular size range of 150 - 63μm.

Dissolution studies were carried out using a USP type II dissolution test apparatus. For these dissolution studies, 900ml phosphate buffer of pH 6.8 (simulated intestinal fluid) was used as the dissolution medium and 416 mg of LLC coated powder precursor was loaded into the dissolution vessel maintained at $37 \pm 0.5°C$ and stirred at 80 rpm. Samples were collected after specific intervals and replaced with fresh dissolution medium. Collected samples were filtered using a 0.35 μm syringe filter. Samples were studied in triplicate and the coefficient of variation calculated. The obtained data was analysed using PCP-Disso software V3 (Poona College of Pharmacy, Poona, India).

4.4 New modulated DSC method development for Pluronic F127 solution cubic phase (gelation) detection

4.4.1 Aim

To develop a modulated DSC (MDSC) method for Pluronic F127 solution cubic phase detection by increasing the sensitivity of the conventional DSC system to detect these types of low enthalpic transitions.

4.4.2 Background

Pluronic F127 20-30% solution & gel (cubic phase) state is isotropically transparent in appearance as is water. Thus, to differentiate the cubic phase formation in comparison between the sol and the gel state using PLM is very difficult. This becomes an even greater challenge when the cubic phase powder precursor is in water. However differentiation of the different phases by PLM was found to be relatively straight forward using the classification established by Rosevear (1954) because of the complete anisotropy exhibited by the other two phases (lamellar phase and hexagonal phase) as compared to the cubic phase (see figures 2.5 and 2.6). Apart from small angle x-ray scattering (SAXS), PLM and rheometry no other technique has proved its calibre in LLC phase detection and inter-phase transition. Many other sophisticated analytical techniques have been employed in LLC examination but only in combination with the above mentioned technique is accurate identification of the liquid crystal phase ensured (Maheshwari et al., 2006). Cubic phase detection for the Pluronic F127 coated cubic phase powder precursor was found to be very difficult even with straight forward techniques like PLM for the obvious reason of isotropic transparent nature of the Pluronic

F127 cubic phase as is water. Rheometry cannot be applied to the Pluronic F127 coated powder precursor as undissolved MCC will interact with the measurement. Thus there is a need for a simple analytical method to detect LLC formation by powder precursor. As discussed earlier a conventional DSC system was found not to be sensitive enough to detect such low enthalpic (ΔH_{gel} = 0.73 J/g) cubic phase transitions (Cabana et al., 1997) as is evident from the conventional DSC thermogram shown in figure 5.3. Hence researchers have employed highly sensitive DSC systems to detect gelation (cubic phase) transition (Cabana et al., 1997, Nie et al., 2011) or they have utilised very low heating rate (1˚C) which was a compromise to obtain conditions in equilibrium between signal/noise ratio, where a specially developed indirect method was used to correct the base line to reduce noise (Barba et al., 2009).

4.4.3 Introduction

A conventional DSC system is based on the measurement of the difference in the heat flow between the sample and the inert reference as a function of temperature. Typically, in conventional DSC, a linear heating rate profile is applied for the both the sample and the inert reference. Modulated DSC (MDSC) works on the same principle as the conventional DSC system but the heating profile applied here is a sinusoidal modulation wave (oscillation) which is superimposed on the conventional linear heating ramp. Thus the combination yields a heating profile in which the average sample temperature continuously increases with time but in non-linear sinusoidal wave fashion. The advantage of applying such a complex heating profile on the sample is that this is equivalent to running two experiments simultaneously on the same sample. One profile will provide the average linear heating rate and the second provides a sinusoidal (instantaneous) heating rate.

➤ **Experimental parameters**

There are four experimental parameters for MDSC which must be fed into DSC system and their ranges, as recommended by TA Instruments – the instrument manufacturer, for getting accurate repeatable results are as follows –

- Sample size: Usually 10-20mg of sample is used for MDSC (Modulated DSC Theory, TA instruments TA-112B) which is almost 2 to 4 times the sample size used in conventional DSC in order to increase the sensitivity of the system.

- Underlying heating rate: A slower heating rate of 1 to 5˚C/min is used for MDSC (Modulated DSC Theory, TA instruments TA-112B) since, during a thermal event, at least 4-5 modulations should be allowed to occur for each detected thermal event.

- Temperature amplitude of modulation: ± 0.5 to 2˚C (Modulated DSC Theory, TA instruments TA-112B) is typically used. Larger amplitude corresponds to a larger heat flow response because the instantaneous heating rate is directly proportional to the amplitude (see equation 5.1).

$$dT/dt = \beta + A_T \, \omega \, \cos(\omega t)$$

Equation 5.1 Instantaneous heating rate equation.

Where: dT/dt = instantaneous heating rate (˚C/min)

β = underlying heating rate

A_T = modulation amplitude

ω = angular frequency = 2π/modulation period (min^{-1})

t = time (minutes)

Hence, the larger amplitude increases the sensitivity for transitions which have low enthalpy such as glass transition (T_g) or, in this case, the enthalpy of gelation. However the amplitude should not be set too large such that the material is unable to follow modulation. If the amplitude is too large to follow the modulation than the modulation waves gets distorted. This distortion can be used as a checkpoint to choose the maximum possible amplitude for a specific material or system.

- Period of modulation: 40 to 100 seconds (Modulated DSC Theory, TA instruments TA-112B). As evident from equation 5.1 the period and amplitude are inter-related terms. It is clear that with an increase in the period of modulation the range of acceptable amplitudes is also increased as the material has a longer time to respond. Smaller amplitudes are preferred with longer periods to ensure that the material has enough time to follow the smaller amplitude. This is since some materials are not strongly thermally conducting.

4.4.4 Material, methods & instrumentation

Pluronic F127, Chlorpheniramine maleate were used (see table 4.1 of chapter 4). Concentrations of 16, 19, 22 and 25% Pluronic solution containing CPM was prepared by the cold method specified in section 4.2.1. A TA Instruments Q2000 DSC (Crawley, UK) was used to perform the MDSC experiments. Different combinations of amplitude, period of modulation and heating rate were selected to optimise the system's sensitivity to detect the gelation and the nitrogen flow rate was kept at 50mL/min. T-zero aluminium hermetic pans and lids are used as reference pan (empty) and sample pan for Modulated DSC with approximately 35-40 mg of each sample. Temperature range for all samples was used within 5°- 40°C.

Chapter 5: Results and discussion

===

This chapter deals with understanding of twin screw extrusion process applied to produce cubic phase powdered precursor. The studies aimed to find out the significant variables and conditions which ensure smooth efficient processing, desired consistency of the final product and the pharmaceutical performance in terms of drug release.

The process design is based on the thermoreversible nature of the Pluronic F127 solution and the ability of the extrusion processing to cause uniform dispersion of the gel on the MCC particle surface. The challenge in the process is to achieve balance between coating of individual particle and generation of granules or small aggregates. Therefore development of this process required good understanding of the rheological behaviour of the Pluronic F127 solution which has been discussed in first part of this chapter. The second part mainly deals with the understanding of the effect of various processing variables and Pluronic F127 concentration on the generation of LLC coated MCC particles and their pharmaceutical performance. The important processing variables include screw rotation speed; MCC feed rate, barrel temperature, screw configuration and Pluronic F127 concentration.

5.1 Preliminary study

5.1.1 Thermo gravimetric analysis (TGA)

TGA thermograms of the Pluronic F127, CPM and MCC are shown in fig 5.1.
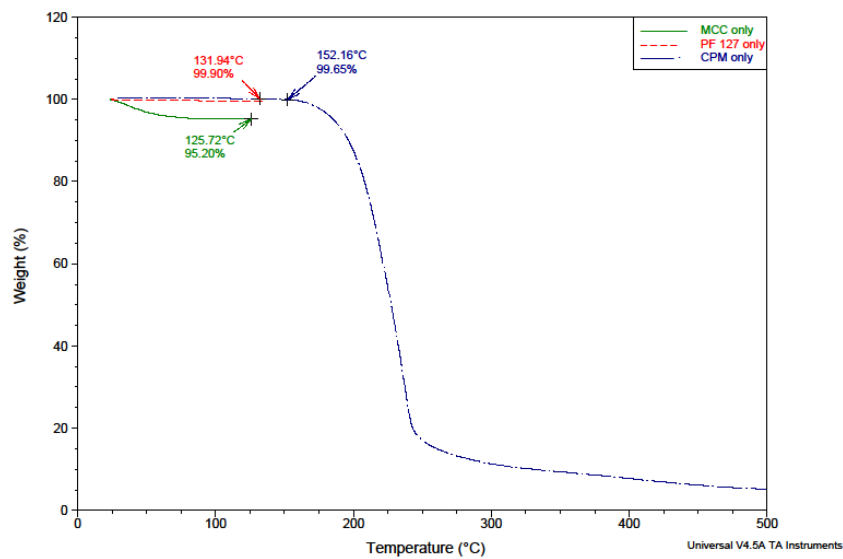
[Fig. 5.1 TGA thermograms of MCC, Pluronic F127 and CPM]

TGA thermogram shows that Pluronic F127, CPM and MCC are stable up to 100˚C which is expected to be much higher than the highest temperature which can be used during extrusion processing.

5.1.2 Differential scanning caloriemetry (DSC)

DSC thermograms of the drug, polymer and the Pluronic F127 solution saturated with CPM were obtained. The thermograms of Pluronic F127 and CPM are shown in fig. 5.2, it shows that Pluronic F127 is a crystalline polymer with melting point 55˚C and CPM melts at 132˚C.
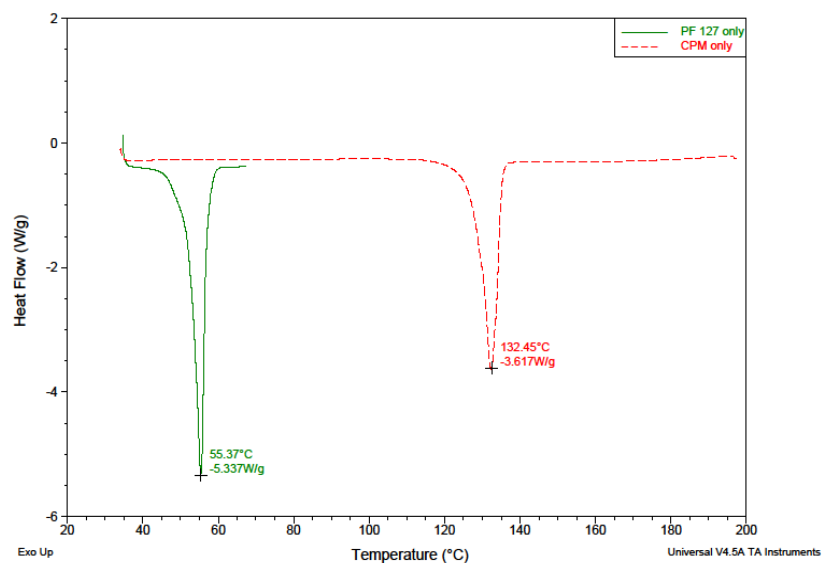
[Fig. 5.2 DSC thermograms of Pluronic F127 and CPM]

The DSC thermograms of the 22% and 25% w/w solutions are shown in Fig 5.3 The DSC thermogram show a small depression at around 3- 5˚C which represents the micellisation. The thermograms did not show any peak for gelation of the system. The enthalpy of gelation is very low which may not have been detected by the DSC we used. Cabana et al (Cabana et al., 1997) reported enthalpy of gelation for Pluronic F127 to be 0.73 J/g which was measured using high sensitivity DSC. Nie et al (Nie et al., 2011) also demonstrated use of high sensitivity DSC for measurement of enthalpy of gelation.
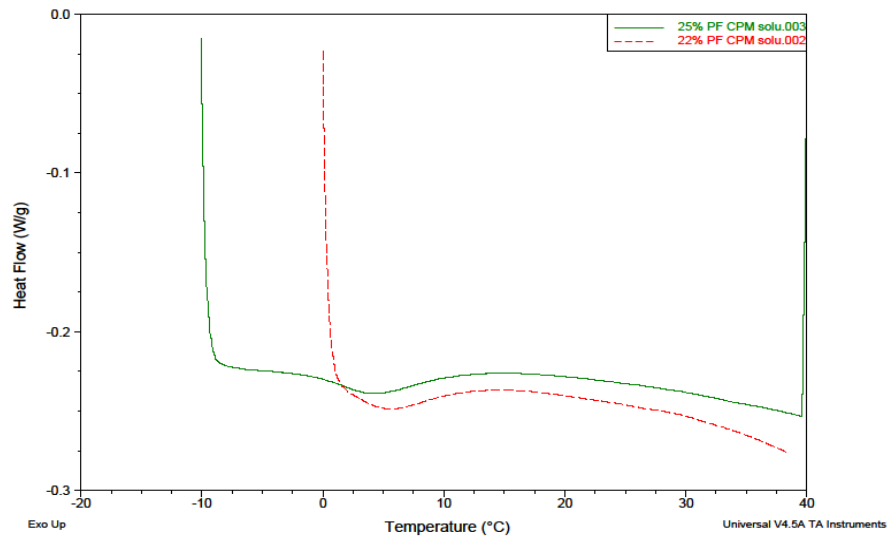
[Fig. 5.3 DSC thermograms of 22% and 25% Pluronic F127 containing CPM]

5.1.3 Rotational rheometry

As we are trying to coat the Pluronic F127 over the MCC, it is very important to explore Pluronic F127 solution's flow behaviour at various concentrations, temperatures and shears. Viscoelastic characteristic determination is also very important to optimise coating by selecting the best conditions for spreading the Pluronic F127 solution over the MCC surface and then to force sticking onto this surface.

➢ **Controlled shear rate test (CSR test)**

These tests were performed to investigate the change in viscosity (η) at specific temperatures at a defined shear rate. In this CSR test shear rate is the preset parameter and shear stress is the resultant parameter. Usually this test method is selected to probe the liquids with self-

levelling behaviour (Mezger, 2006). This method is used to mimic certain processes such as pipe flow, painting or spraying. Thus the CSR test will help in mimicking the flow through the peristaltic pump and within the extrusion barrel while coating and also provide insights to select the conditions to get Pluronic F127 solution easily spread over the MCC surface and to stick over the same. These tests also help to select conditions to feed Pluronic F127 solution through the peristaltic pump into the extruder barrel.

Figures 5.4 - 5.8 show the CSR test results for different Pluronic F127 concentration (15 - 35%). As it is been already been reported that at 20 - 30% concentrations the Pluronic F127 exhibits thermoreversible gelation which is due to gradual micelle formation and their arrangement to form cubic lattice with the increase in temperature and vice-versa (BASF Technical Bulletin, 2006 and Brown et al., 1991). This micellisation process is very temperature sensitive as the amount of micelles formed is directly proportional to the temperature after a critical micelle concentration (CMC) has been passed. Therefore with the gradual increase in temperatures there is an increase in the number of micelles formed which is evident by an increase in viscosity with temperature (see figs. 5.4 - 5.8) except for the higher Pluronic F127 concentrations (25 - 35%) where the viscosity remains almost constant at moderate to higher temperatures (25 - 40˚C for 25%, 20 - 40˚C for 30%, 15 - 40˚C for 35%). This exceptional constant viscosity of higher Pluronic F127 at moderate to higher temperature is due to saturation of micellisation at 25˚C or above (see figs. 5.6, 5.7 and 5.8). The temperature at which micelle formation gets saturated decreases with increasing Pluronic F127 concentration (see fig. 5.6, 5.7, 5.8).

The results from figures 5.4 - 5.8 illustrate that the Pluronic F127 system exhibits shear thinning behaviour at all temperatures where micellisation has occurred irrespective of concentration. From the literature it is evident that Pluronic F127 is very sensitive towards

temperature dependent thermoreversible gelation which is the consequence of cubic lattice arrangement of micelles (BASF Product Brochure, 1997). The amount of micelles formed at a specific Pluronic F127 concentration is directly proportional to the temperature. Therefore with the application of increasing shear rate at a specific temperature which favours the micellisation the material exhibits shear thinning due to the shear induced alignment of micellar structures with the flow direction within the gelation range of the Pluronic F127 at a particular concentration. With increasing shear more and more micelles are getting aligned with the flow direction which accounts for the decrease in viscosity of the system. The viscosity function curves at 15, 20 and 25% Pluronic F127 concentrations (see fig. 5.4, 5.5 and 5.6) shows that at 5˚C the system behaves as a Newtonian fluid due to the absence of micelles at this lower temperature. At a higher concentration of 30%, even at 5˚C, the system exhibits shear thinning up until a low shear rate of ($\dot{\gamma}$) of 1 sec^{-1} (see fig. 5.7) which is due to higher amount of Pluronic F127 (30%) polymer chain presence which has forced formation of fewer micelles at such low temperature. Once the shear rate increases beyond $\dot{\gamma}$ of 1 sec^{-1} the system exhibits Newtonian behaviour which confirms' the complete alignment of micelles by the applied shear in the direction of flow. Above the thermoreversible gelation concentration range (i.e. 35%) at which the system maintains its gel state even at low temperatures, the system experiences shear thinning up until $\dot{\gamma}$ of 200 sec^{-1} even at the lowest temperature (5˚C) (see fig. 5.8) which is because of the higher concentration of Pluronic F127 being responsible for the greater extent of micellisation even at 5˚C. Beyond this $\dot{\gamma}$ of 200 sec^{-1} the system starts behaving as a Newtonian fluid. This Newtonian behaviour beyond $\dot{\gamma}$ = 200 sec^{-1} at 5˚C is again because of the complete alignment of the available micelles by the applied shear.
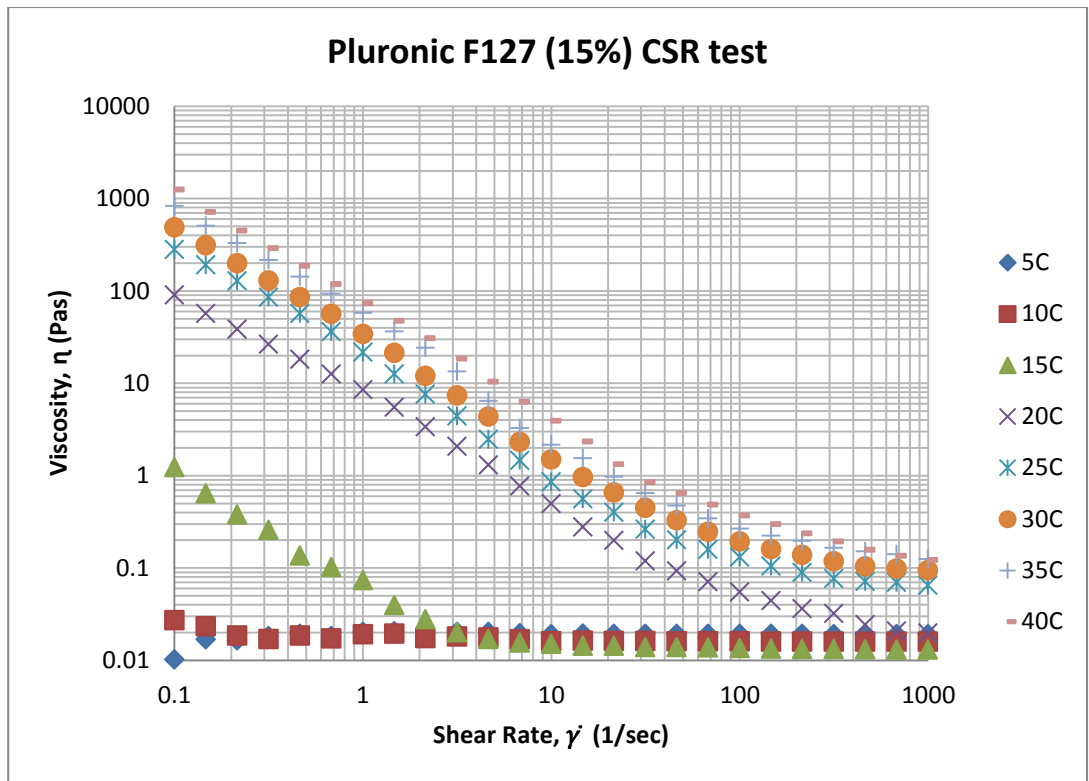
[Fig. 5.4 Viscosity function curve of Pluronic F127 15 % solution at specific temperatures]

The figure above clearly depicts that the system is transforming towards Newtonian fluid beyond $\dot{\gamma}$ of 100 sec^{-1} at temperatures of 20°C or above which is again due to a lower extent of micellisation at low Pluronic F127 concentration (15%). The system is showing shear thinning behaviour with the increase in shear rate from moderate to higher temperature.
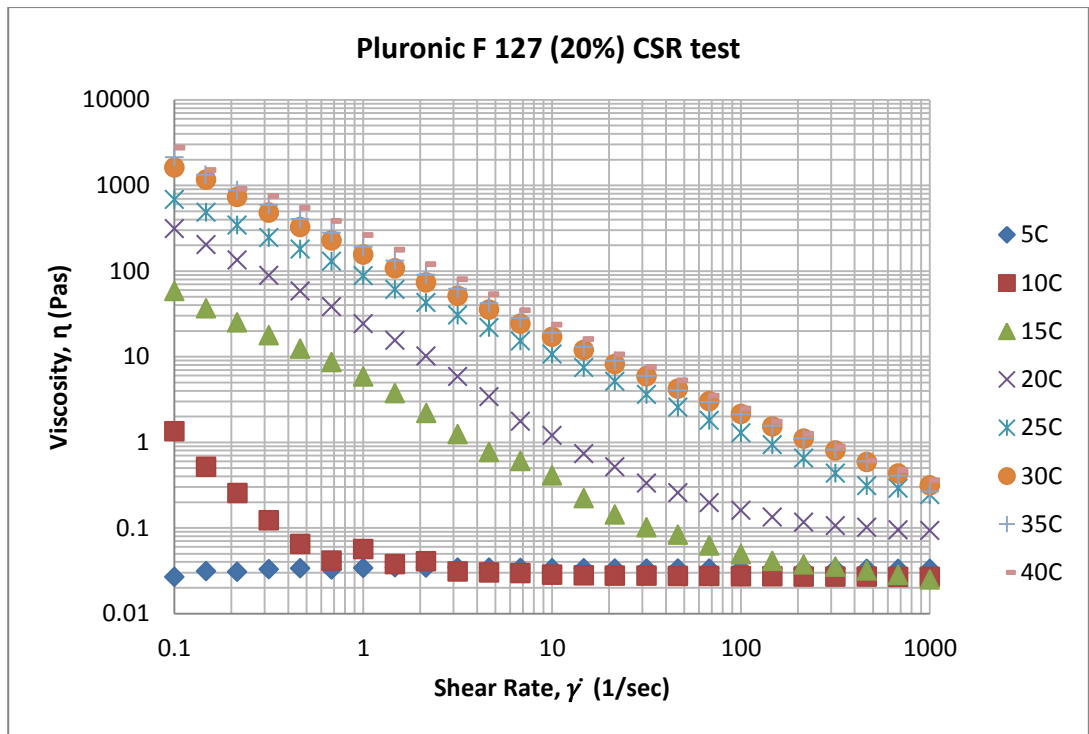
[Fig. 5.5 Viscosity function curve of Pluronic F127 20% solution at specific temperatures]

The above figure illustrates that with increasing temperatures there is increase in micellisation which is the reason for the stepwise increase in viscosity. At 25°C and above the viscosity curves become almost identical owing to saturation of micellisation. At higher concentrations of 25% (see fig. 5.6), 30% (see fig. 5.7), and 35% (see fig. 5.8) the viscosity at moderate to higher temperatures (25 - 40°C) is almost identical at all shear rates. Even the viscosity at slightly lower temperatures (20°C and 15°C) at higher concentrations (25%, 30% and 35%) has moved up due to gradual achievement of the micelle saturation level (see fig. 5.7, 5.8).
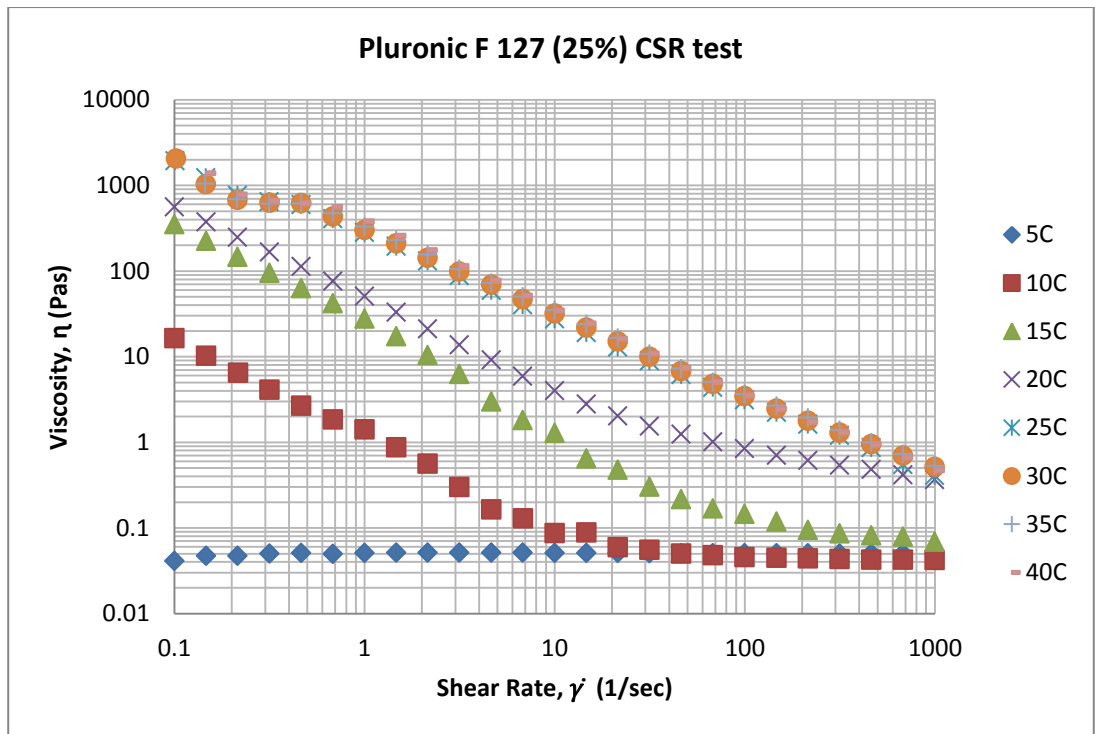
[Fig. 5.6 Viscosity function curve of Pluronic F127 25 % solution at specific temperatures]

At higher concentrations (25- 35%) and moderate to high temperatures (25 - 40˚C for 25% (see fig. 5.6), 20 - 40˚C for 30% (see fig. 5.7), 15 - 40˚C for 35 % (see fig. 5.8)) an initial plateau of Newtonian behaviour is found at low shear rates up to $\dot{\gamma}$ of 1 sec^{-1} (see fig. 5.6 to 5.8). This Newtonian behaviour at such a low shear rate is due to the highly compact arrangement of the large number of micelles which are tough enough to resist such a low shear to restrict micellar alignment in the direction of flow (see figs. 5.6, 5.7 and 5.8).
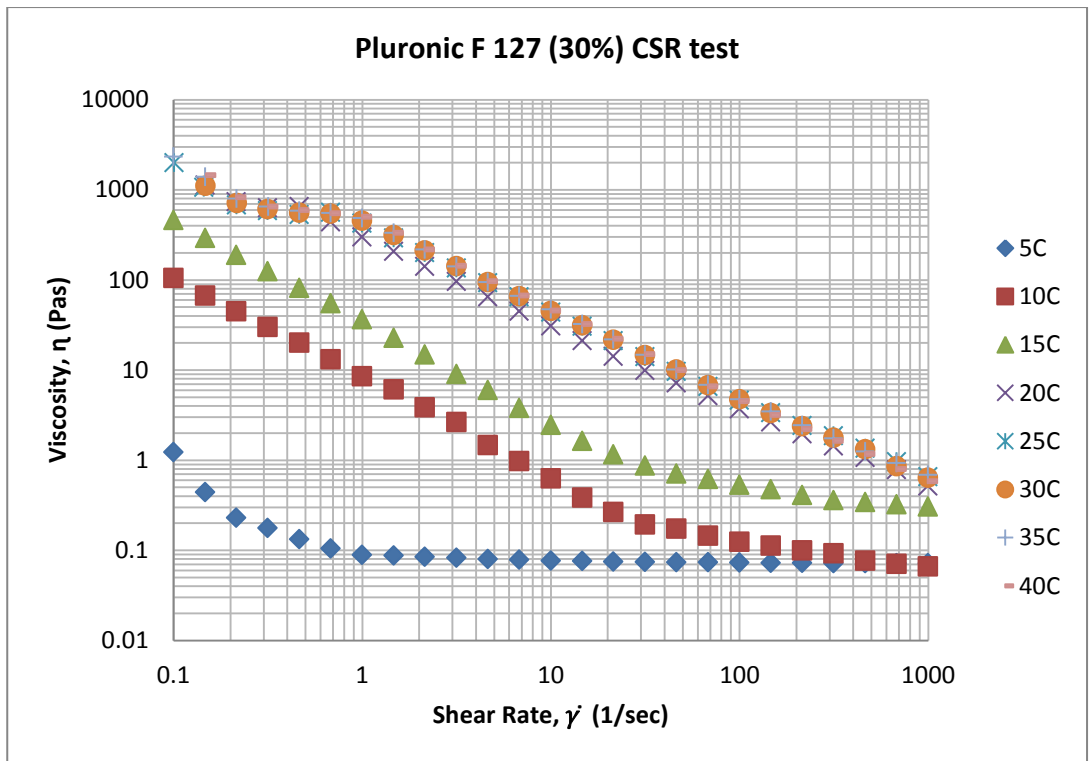
[Fig. 5.7 Viscosity function curve of Pluronic F127 30 % solution at specific temperatures]
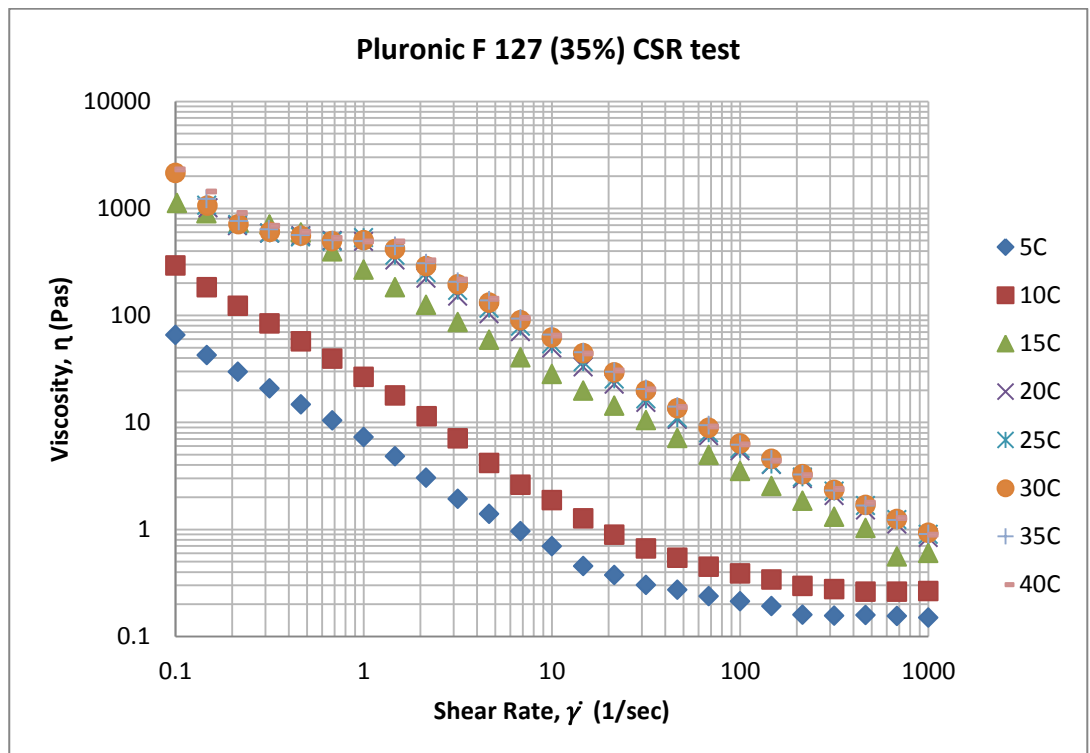
[Fig. 5.8 Viscosity function curve of Pluronic F127 35 % solution at specific temperatures

All the thermoreversible gelation concentration range (including 15%) displays dual behaviour i.e. shear thinning and Newtonian behaviour at moderate or intermediate temperatures (15˚C, 20˚C). Interestingly with the rise in the Pluronic F127 concentration from 15 to 20% at 10˚C and the system also started experiencing shear thinning and also gets transformed to a Newtonian system beyond a certain critical shear rate ($\dot{\gamma}$). The reason behind this shift in behaviour is due the formation of micelles with the increase in Pluronic F127 concentration to 20% at low temperature of 10˚C which was not there with 15% concentration at same temperature of 10˚C (compare fig. 5.4 and 5.5 for 10˚C). This reason also accounts for the increase in the shear rate limit with the increasing Pluronic F127 concentration beyond which the system starts behaving as a Newtonian fluid at a particular temperature (see figs. 5.9 and 5.10).
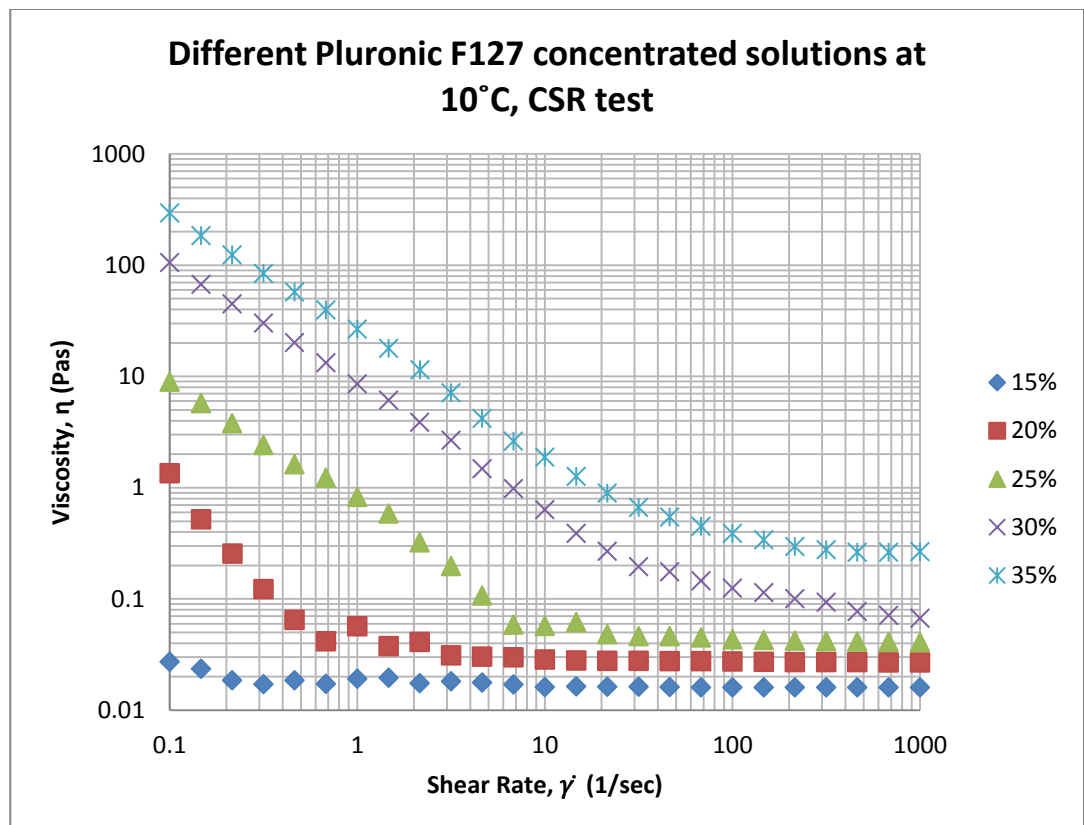
[Fig. 5.9 Viscosity function curve of different concentrations of Pluronic F127 at 10˚C]
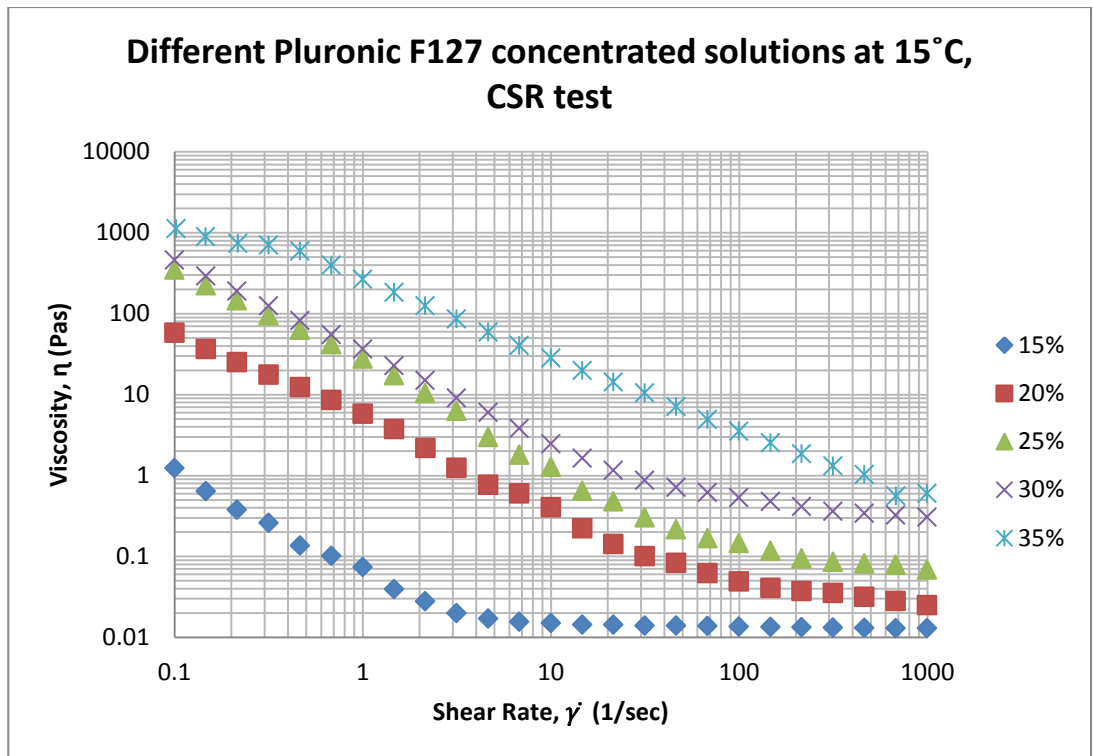
[Fig. 5.10 Viscosity function curve of different concentrations of Pluronic F127 at 15˚C]
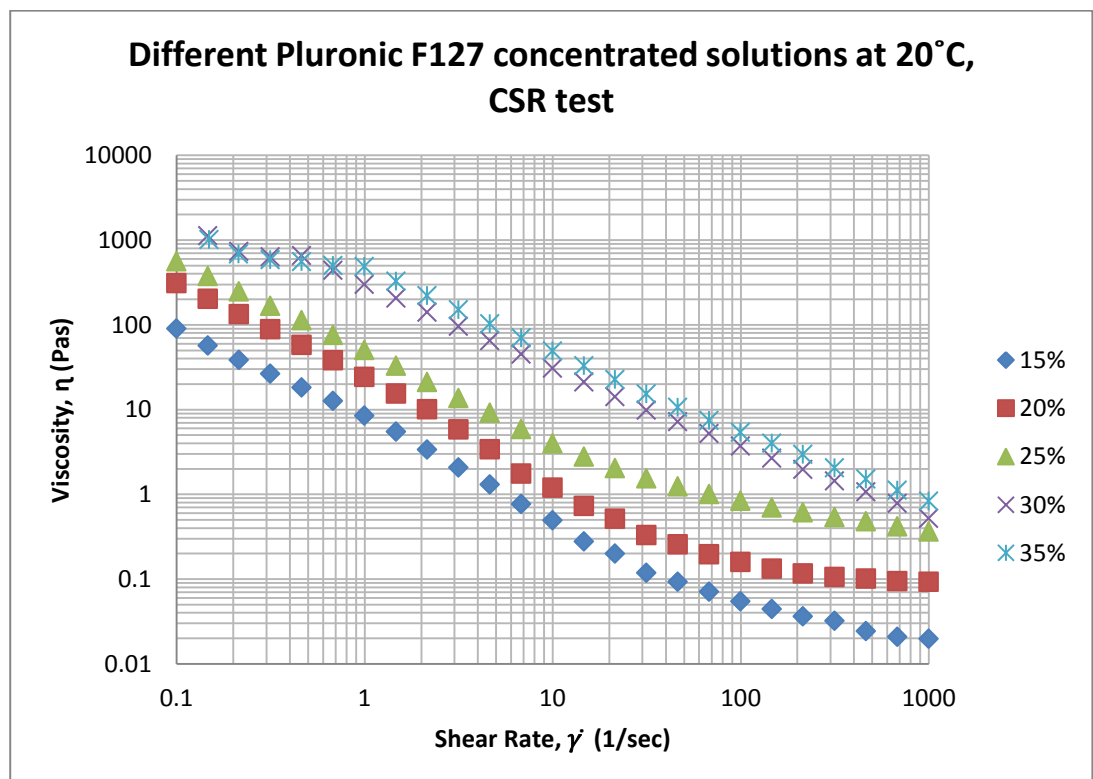
[Fig. 5.11 Viscosity function curve of different concentrations of Pluronic F127 at 20˚C]

From all the above discussed results it can be concluded that Pluronic F127 solution's flow behaviour is very sensitive towards temperature and the Pluronic F127 concentration. Thus to feed any specific concentration of Pluronic F127 solution within the thermoreversible range, lower temperatures are the most suitable. Although they can also made to flow by applying shear at higher temperatures (cubic phase gel state), but for that, specific amount of shear needs to be applied to get Newtonian flow. This is because of shear thinning behaviour.

> **Shear strain amplitude sweep**

These tests are performed to investigate the linear viscoelastic range (LVR) under which the reliable repeatable viscoelastic results are ensured before moving on to frequency sweeps to measure the complex viscoelastic characteristics of the material where the applied strain (deformation strength) within these oscillatory tests is kept under the LVR (Mezger, 2006). The analysis of the viscoelastic character of the material should be designed to preserve the structure of the material, so that measurements can provide insights into the inter particle and inter molecular forces inside the material (Martin, 1993). Within LVR the deformation is reversible and will not destroy or alter the structure of the material during the measurement. This oscillatory test is performed in controlled shear deformation (CSD) mode where the deformation strain ($\dot{\gamma}$) is preset and the resultant shear stress (τ) is measured. Within the CSD amplitude sweeps the frequency (ω) is kept constant and variable strain amplitude is applied.

The results from the strain amplitude are presented in figure 5.12 to 5.16 which illustrates that with the increase in temperature and the concentration both the storage modulus (G') and loss modulus (G'') increases. With all the concentrations tested, at all temperatures, linear viscoelastic behaviour is found until a shear strain of 1% after which both the G' & G'' starts to disobey the linear trend which suggests the beginning of structural deformation.

From the strain amplitude sweeps it can be concluded that shear strains up to 1% are safe to maintain the linear viscoelastic character of the materials under test. Thus shear strain of 1% can be applied to carry out the frequency sweeps ensuring no potential structural deformation.
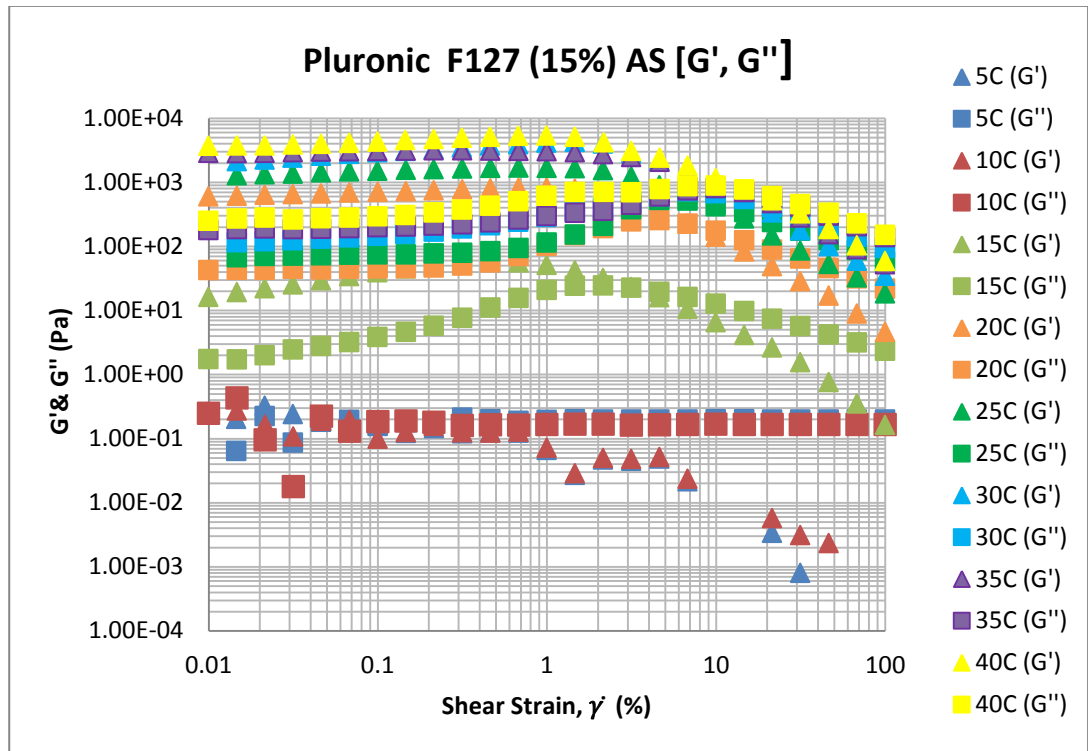
[Fig. 5.12 Strain amplitude sweep plot of 15 % Pluronic F127 at various temperatures]
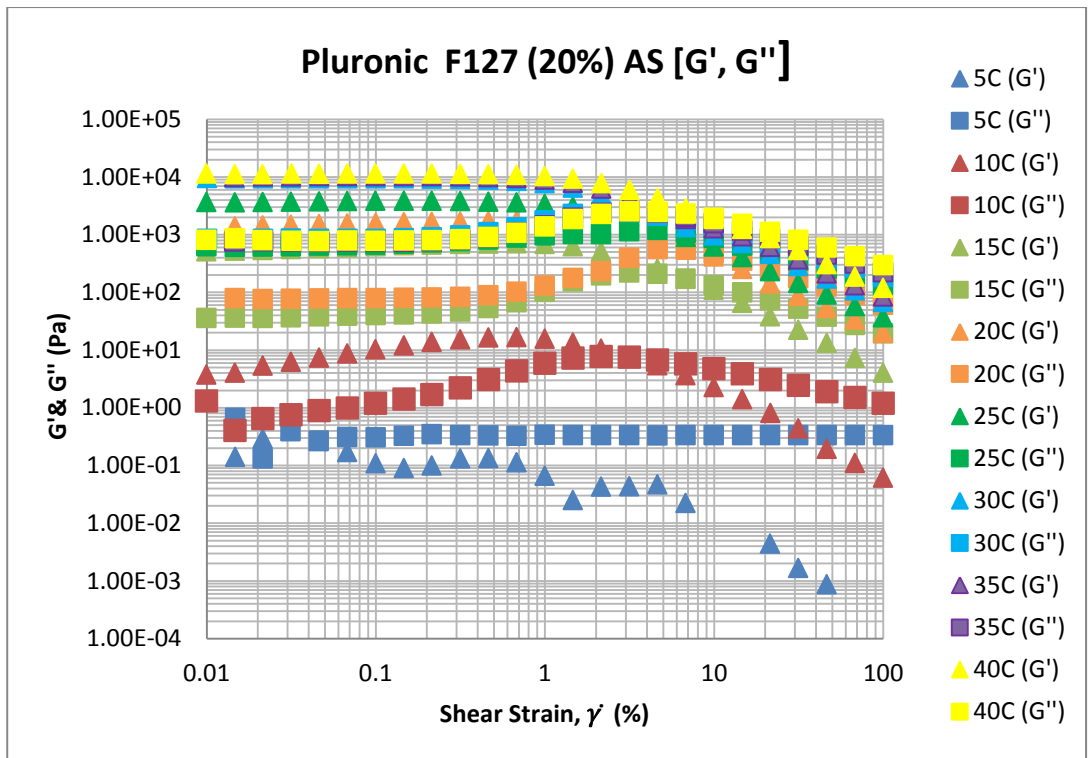
[Fig. 5.13 Strain amplitude sweep plot of 20 % Pluronic F127 at various temperatures]
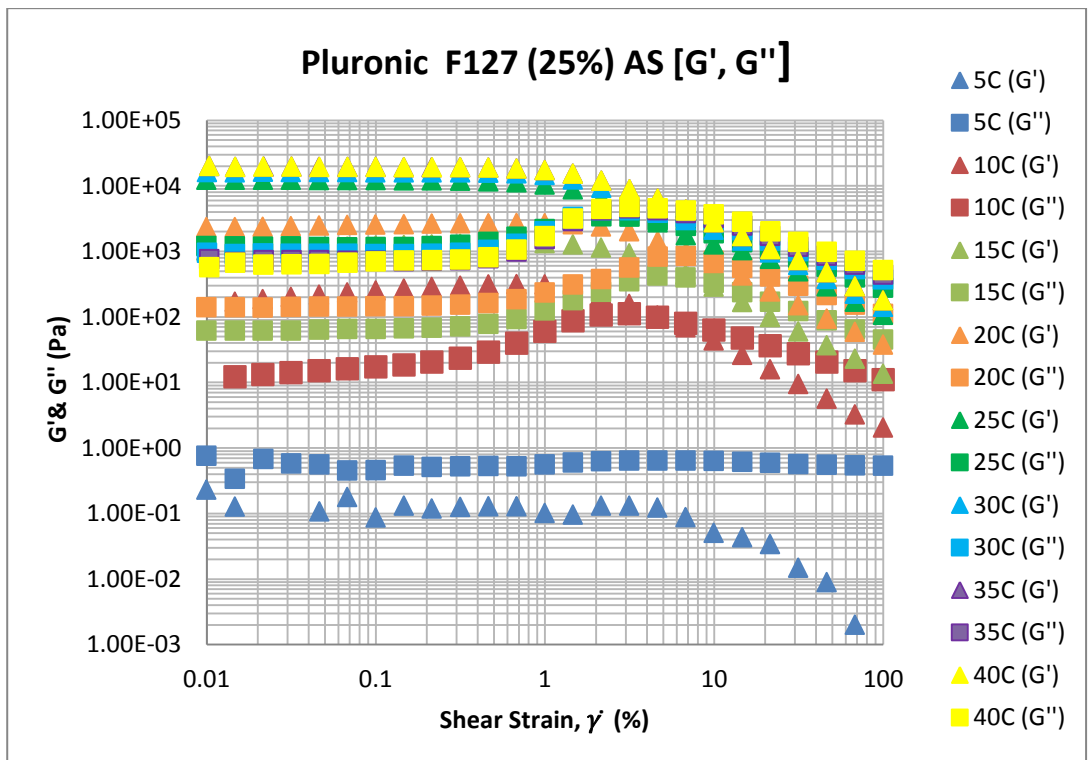
[Fig. 5.14 Strain amplitude sweep plot of 25 % Pluronic F127 at various temperatures]
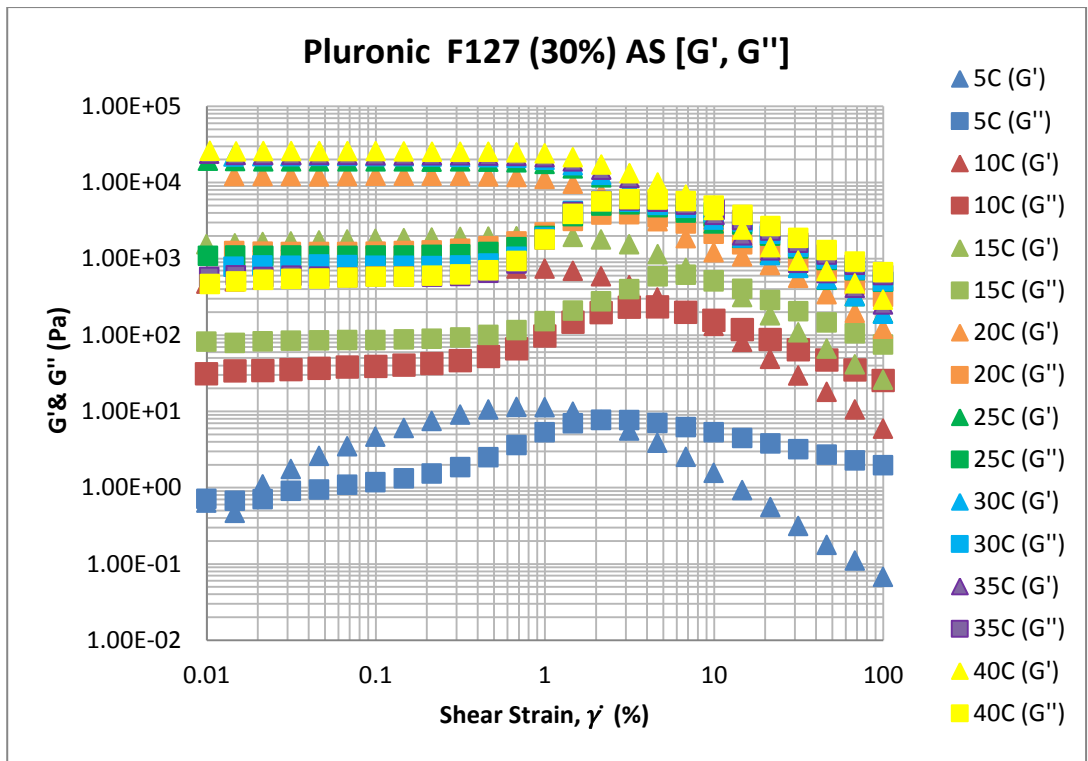
[Fig. 5.15 Strain amplitude sweep plot of 30 % Pluronic F127 at various temperatures]
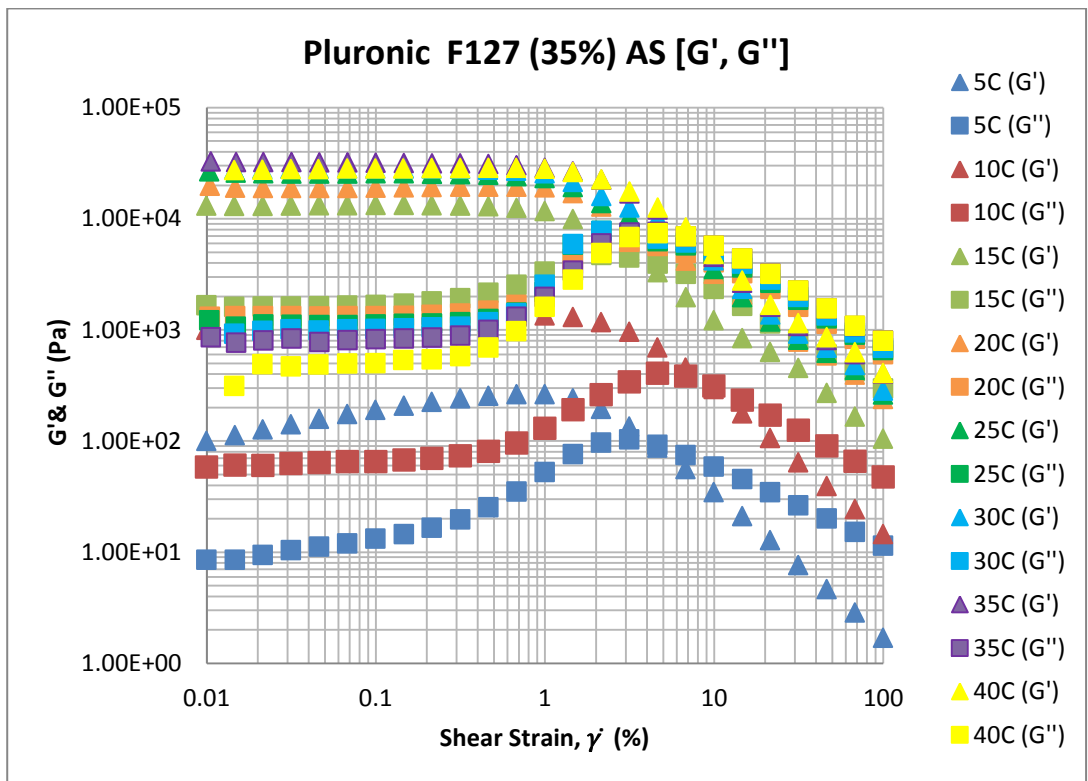
[Fig. 5.16 Strain amplitude sweep plot of 35 % Pluronic F127 at various temperatures]

➢ Frequency sweeps

These tests are performed to investigate the complex viscoelastic behaviour with a constant shear strain (%) under below the limit of the LVR as quantified by the preceding amplitude sweep tests. This oscillatory test is performed in CSD test mode where again shear strain ($\dot{\gamma}$) is preset and the resultant outcome is shear stress (τ). Thus frequency sweeps in CSD modes are performed with constant amplitude under the LVR limit at variable frequencies. From the frequency sweep results the storage modulus (G') and loss modulus (G'') have been plotted for discussion.

The results of the storage modulus against the variable frequencies are shown in figures 5.17 - 5.21. The storage modulus is the measure of the energy stored during deformation by the material. This stored deformation energy is then available to the material to act as the driving force for structural reformation. This energy may or may not be sufficient enough to completely restore the deformed structure. Materials which completely restore the deformation energy display their reversible deformation behaviour after the shear load removal and then eventually acquire an unchanged structure. Hence G' accounts for the elasticity or the elastic behaviour of the test sample (Mezger, 2006). It has been clearly observed that storage modulus is increased with rise in temperature and concentration which means that elasticity of the material is increased (see fig. 5.17 - 5.21). The storage modulus is shown to be constant throughout the frequencies except for the 5˚C, 10˚C and 15˚C for 15%, 5˚C and 10˚C for 20 % and 5˚C for both 25% and 30% solutions. A constant G' value at all frequencies is evidence of the genesis of fairly rigid structure which in this case is the cubic phase gel from moderate to higher temperatures at specific concentrations. However there are temperatures at specific concentrations where the G' is not constant but still manages to follow a trend with increase in frequency such as 15˚C for 15%, 10˚C for 20% and 5˚C for 25

and 30% solutions. This behaviour at low temperatures is due to the absence of the rigid structural formation (gel) though the micelles are still responsible for a limited storage of deformation energy. At the lowest temperatures G' is unable to follow any trend and displays the lowest values due to the absence of micelles. Here the sample is in its sol state.

From the above discussed results of the storage modulus, it can be concluded that at higher temperatures at specific concentrations within the thermoreversible range, the system is transformed to a gel which is fairly rigid and elastic. This gel state of Pluronic F127 is not suitable for spreading to form a coat over the MCC surface. Thus the sol state should be maintained for coating by maintaining the refrigerated temperature (5˚C).
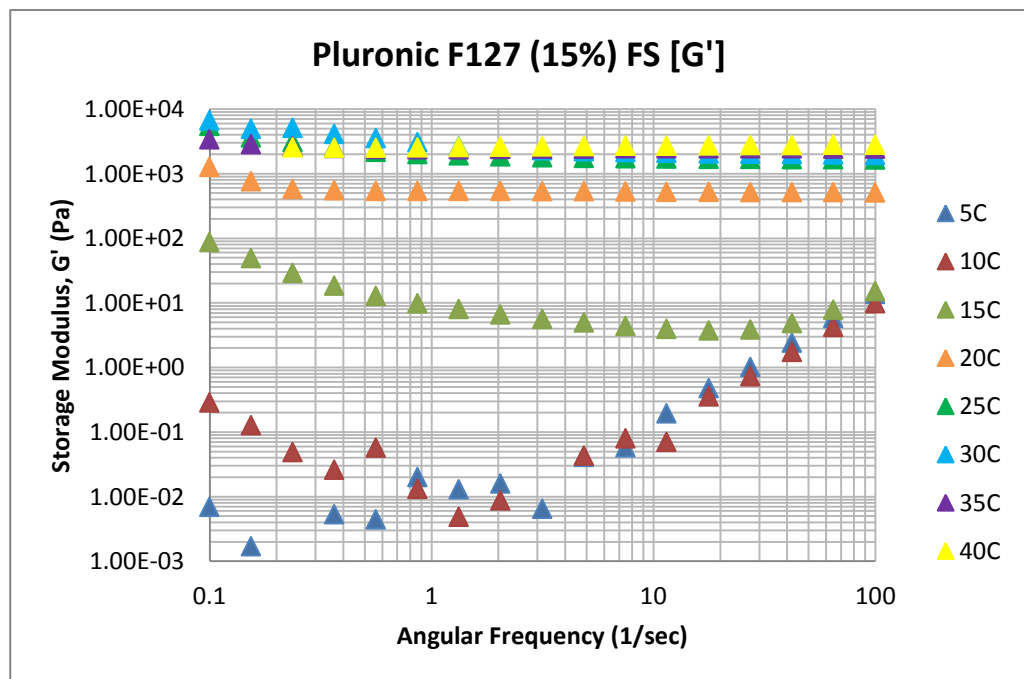
[Fig. 5.17 Frequency sweep plot of 15 % Pluronic F127 at various temperatures with storage modulus against angular frequency]
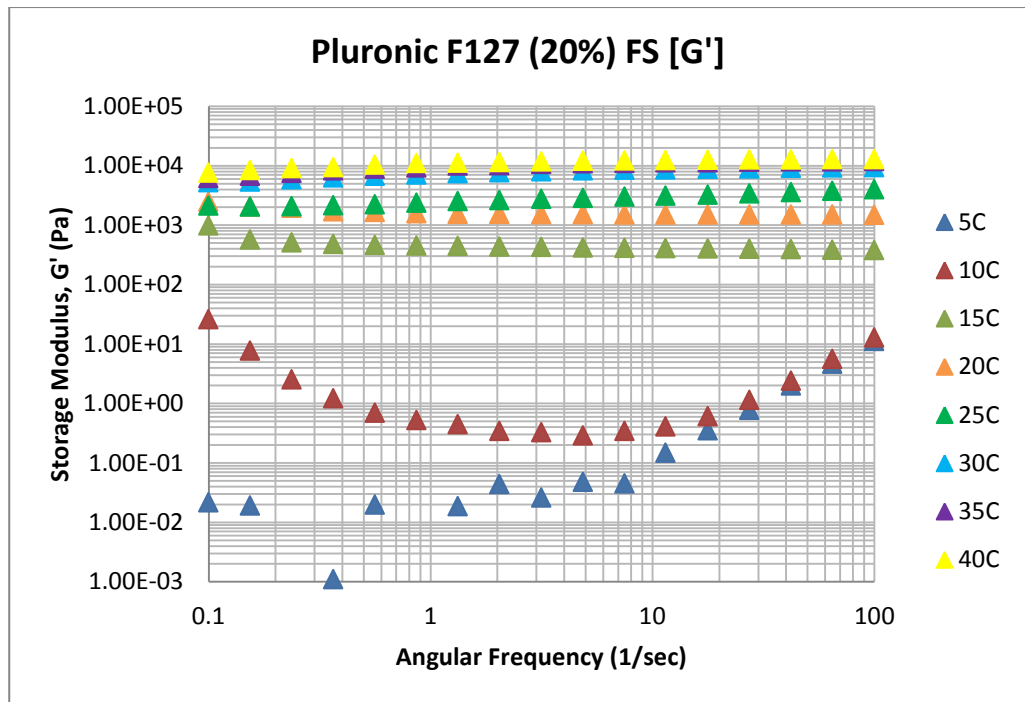
[Fig. 5.18 Frequency sweep plot of 20 % Pluronic F127 at various temperatures with storage

modulus against angular frequency]
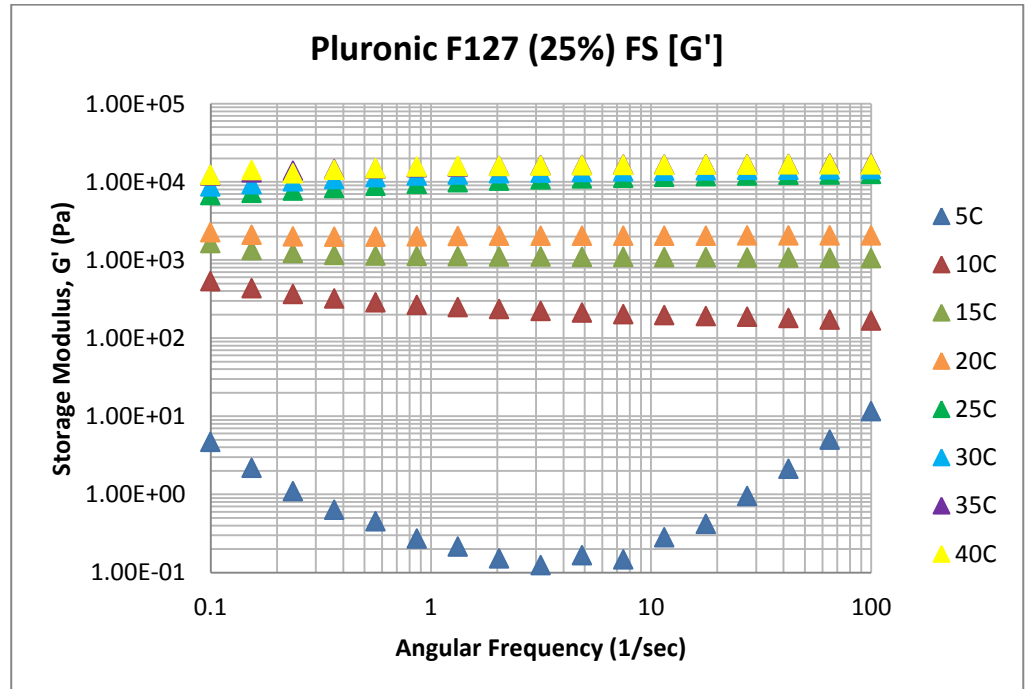
[Fig. 5.19 Frequency sweep plot of 25 % Pluronic F127 solution at various temperatures with

storage modulus against angular frequency]

[Fig. 5.20 Frequency sweep plot of 30 % Pluronic F127 solution at various temperatures with

storage modulus against angular frequency]

[Fig. 5.21 Frequency sweep plot of 35 % Pluronic F127 at various temperatures with storage

modulus against angular frequency]

Figures 5.22 - 5.26 display the loss modulus (G'') data against the variable frequencies from the frequency sweeps. The loss modulus is the measure of deformation energy lost after shear removal or used up by the sample during the shear process. This lost or used energy is responsible for the structural changes or deformation. Thus the material which loses energy exhibits irreversible deformation behaviour because they retain the changed or deformed structure after a load cycle. Therefore G'' accounts for the viscous behaviour of the sample (Mezger, 2006). Figures 5.22 - 5.26 illustrates that loss modulus increases with increasing temperatures and concentrations at all frequencies. This can be interpreted as, with the increase in temperature and concentration the viscous character of the sample is increased which is due to the higher extent of micellisation. There is a very slight decrease in G'' values with increase in frequency at moderate to higher temperatures with all concentrations except for the 5˚C, 10˚C and 15˚C for 15% and 30%, 5˚C, 10˚C, 15˚C and 20˚C for 20% and 25%, 5˚C and 10˚C for 35%. This slight decrease in G'' with frequencies at moderate to higher temperatures indicates a maximum possible micellisation. Thus, we can say that the Pluronic F127 gel structure doesn't lose its viscous character even at higher frequencies. However there are temperatures at specific concentrations where a steep drop in viscous character (G'') is observed because of lesser extent of micellisation which is not enough to provide rigidity to the system such as 15˚C for 15 - 30%, 20˚C for 20% and 25%, 10˚C for 25% and 30% and lastly 5˚C and 10˚C for 35%. Meanwhile at low temperatures of 5˚C (15 - 30%) and 10˚C (15% and 20%) G'' does not follow the trend line with increase in frequency hence confirming the absence or very limited micellisation (see figs. 5.22 - 5.26). Thus, this confirms that a smaller amount of deformation energy is lost or used up in the destruction of fewer micelles.

From the above discussed results of the loss modulus the following conclusion can be drawn. At higher temperatures and higher concentrations, where the system is unaffected by the frequency, the material exhibits highly viscous characteristics which will be beneficial for the Pluronic F127 solution for sticking to the MCC surface after being spread.
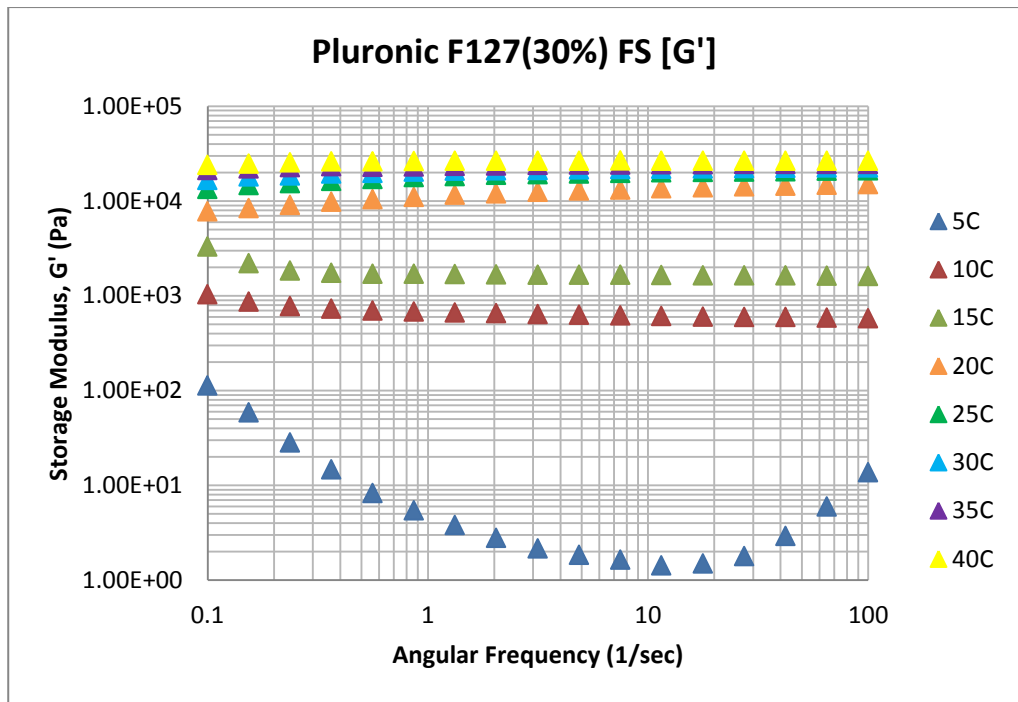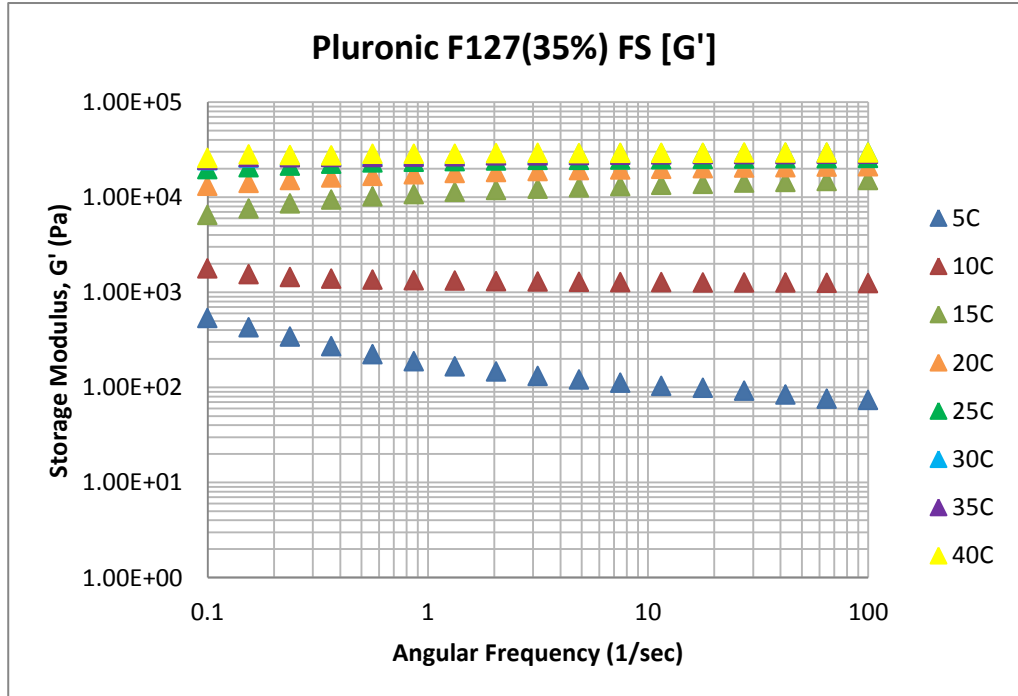

[Fig. 5.22 Frequency sweep plot of 15 % Pluronic F127 at various temperatures with loss modulus against angular frequency]

[Fig. 5.23 Frequency sweep plot of 20 % Pluronic F127 solution at various temperatures with

loss modulus against angular frequency]
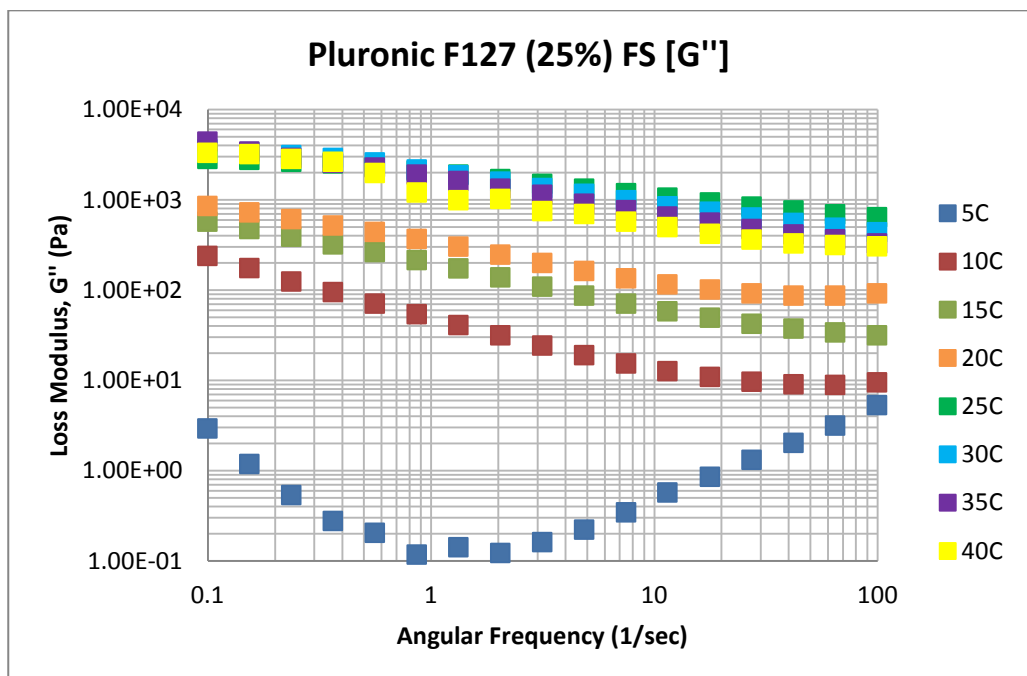
[Fig. 5.24 Frequency sweep plot of 25 % Pluronic F127 at various temperatures with loss

modulus against angular frequency]
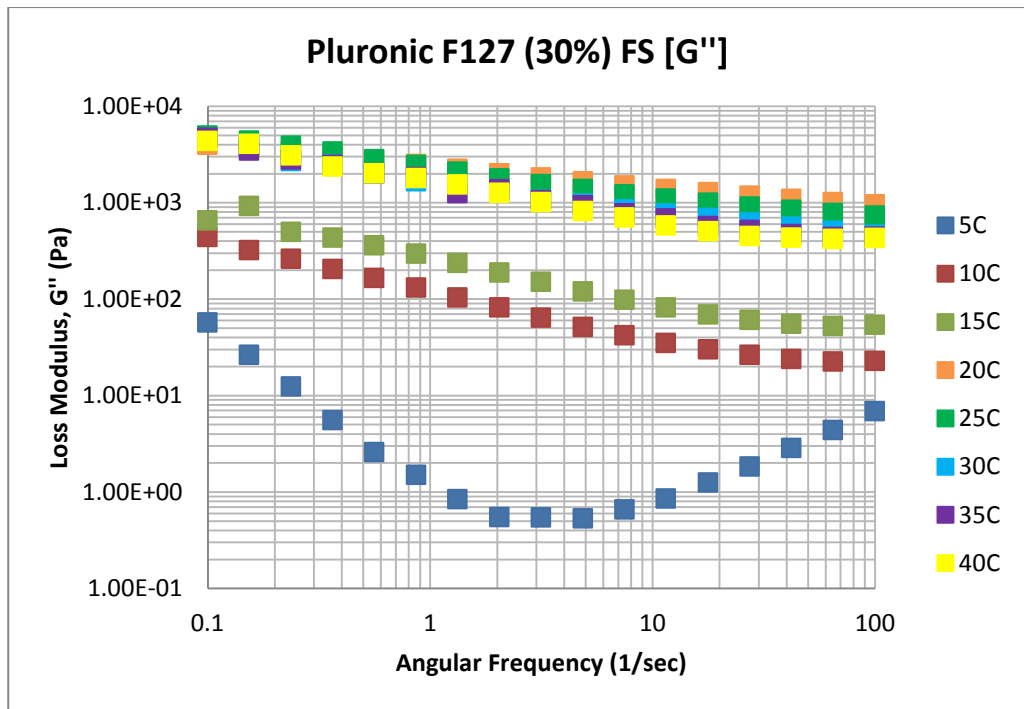
[Fig. 5.25 Frequency sweep plot of 30 % Pluronic F127 at various temperatures with loss

modulus against angular frequency]
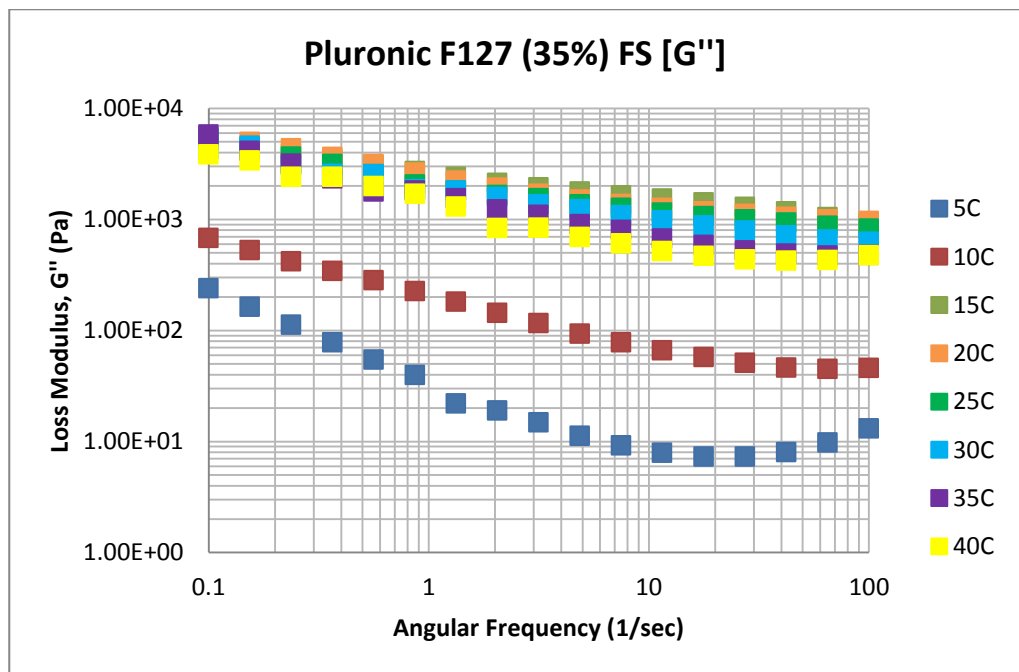
[Fig. 5.26 Frequency sweep plot of 35 % Pluronic F127 solution at various temperatures with
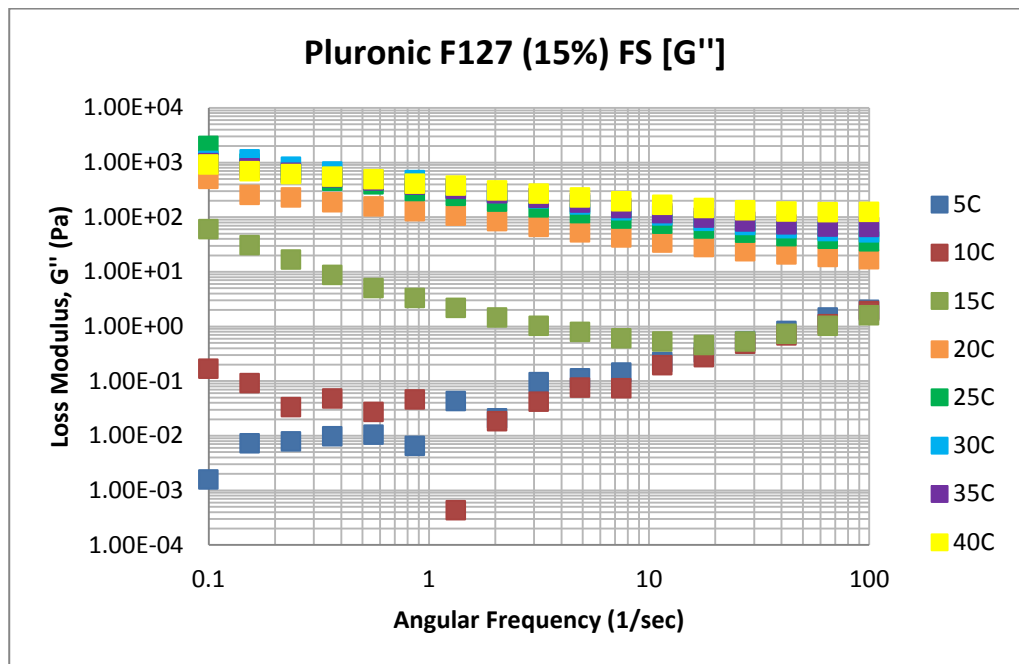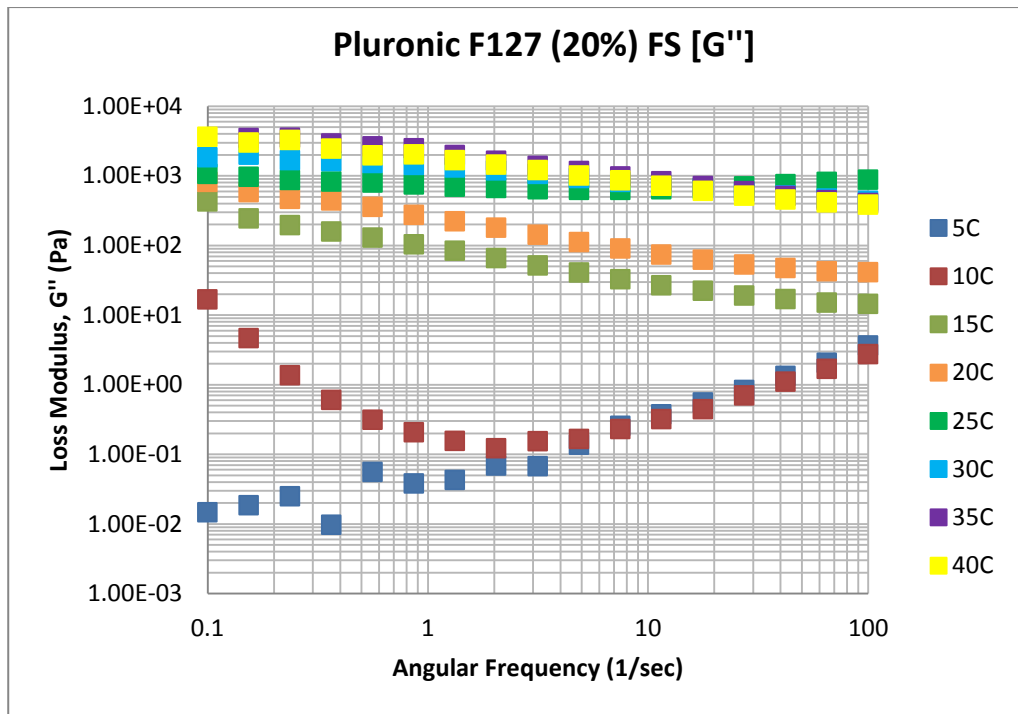
loss modulus against angular frequency]

Finally from the results of the frequency sweep tests, the following conclusions may be drawn. The gel state of the Pluronic F127 is not suitable for spreading, therefore the Pluronic F127 concentration should be kept within the thermoreversible range where, at lower temperatures, the system is in the sol state and behaves as a Newtonian fluid. This Newtonian behaviour is suitable for spreading or coating the Pluronic F127 solution over the MCC surface. However at higher temperatures and concentrations, the system exhibits viscous characteristics which will be very helpful for sticking the Pluronic F127 solution over the MCC surface. Thus after spreading of the thermoreversible concentration range of Pluronic F127 on to the MCC (at a low temperature) the temperature should be raised up to 40°C to force the Pluronic F127 to stick over the surface.

> **Temperature dependent oscillatory tests at constant dynamic mechanical conditions**

These types of oscillatory tests are performed at constant frequency and amplitude where the only variable parameter is the temperature. Thus a measuring temperature profile is preset while a constant dynamic-mechanical shear is applied throughout the measurement. These types of tests are referred to as "dynamic-mechanical thermoanalysis or DMTA tests". The purpose of performing the DMTA tests here is solely the determination of the gelation temperature. The DMTA tests are performed in a CSD mode with constant amplitude of 0.5% which is well within the pre-determined LVR (see fig. 5.12 - 5.15) and at a constant frequency of 10Hz both restricting deformation or change in structure.
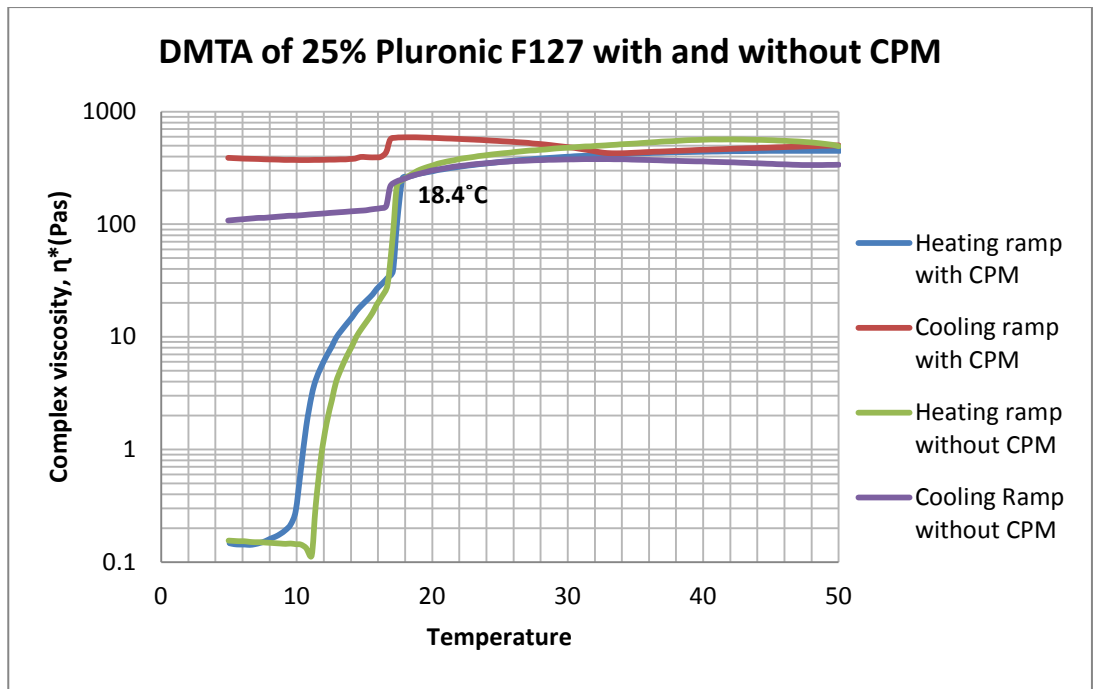
[Fig. 5.27 DMTA test of 25 % Pluronic F127 solution with and without CPM, both for

heating and cooling ramps]
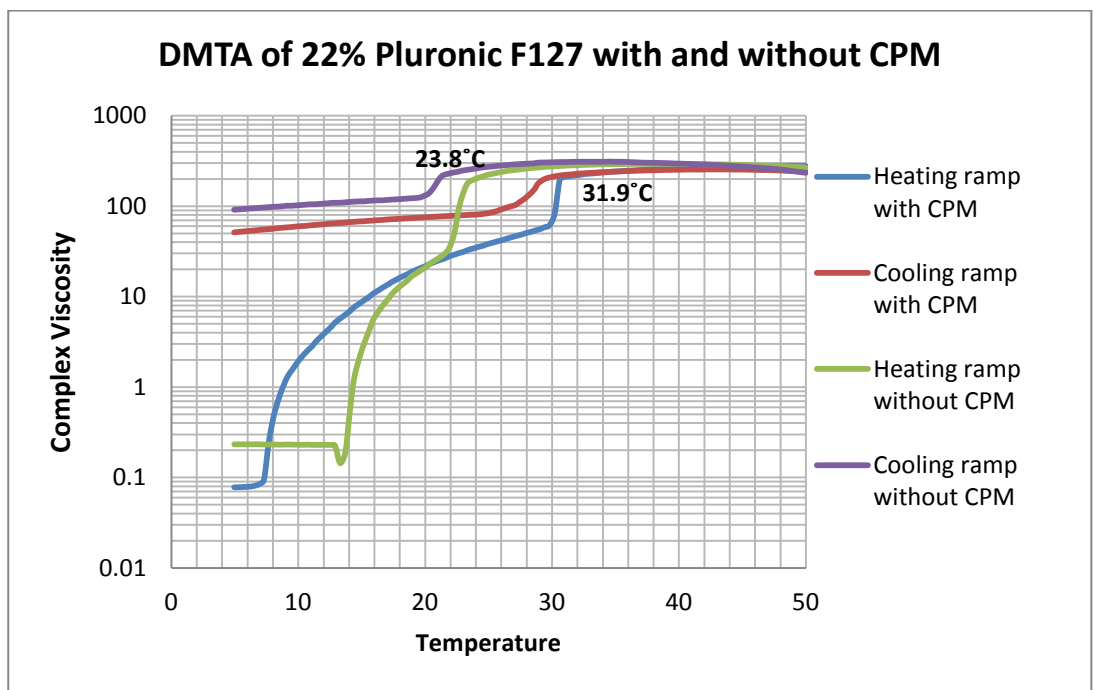
[Fig. 5.28 DMTA test of 22 % Pluronic F127 solution with and without CPM, both for

heating and cooling ramps]
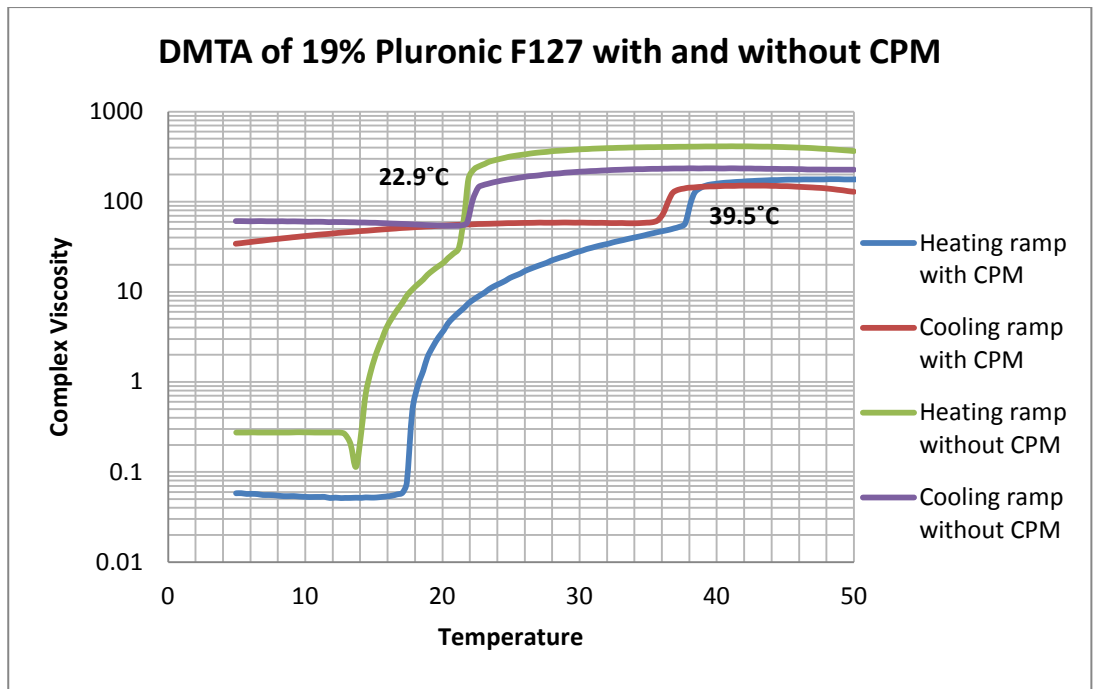
[Fig. 5.29 DMTA test of 19 % Pluronic F127 solution with and without CPM, both for

heating and cooling ramps]
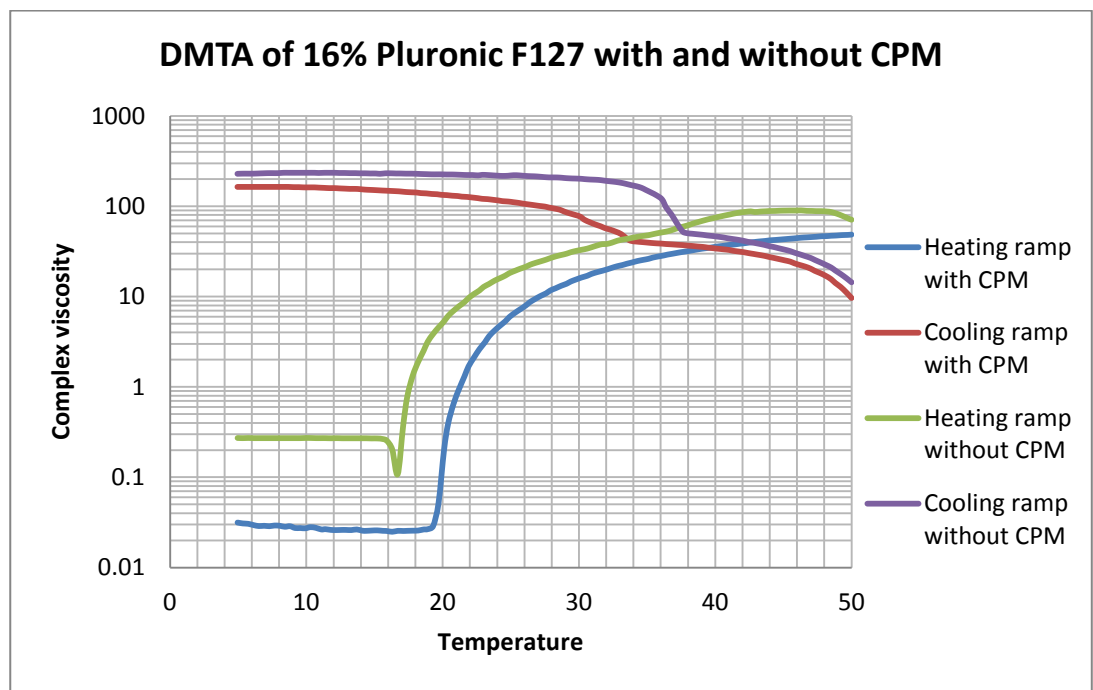
[Fig. 5.30 DMTA test of 16 % Pluronic F127 solution with and without CPM, both for

heating and cooling ramps]

For heating ramps in the DMTA tests at all concentrations with or without CPM, a gradual increase in the complex viscosity (η^*) was found. This proves gradual micellisation with increasing temperature (see figs. 5.27 - 5.30). In a heating ramp, at a particular temperature, the viscosity increases dramatically before becoming constant at higher temperatures (see figs. 5.27 - 5.29). This temperature can be easily recognised as the gelation temperature. To cross check this gelation temperature, the cooling ramp DMTA tests were performed to check whether the viscosity falls at the same temperature or not. As expected the viscosity is suddenly reduced at approximately the same temperature. However in the case of the 16 % Pluronic F127 solution with and without CPM, there is an absence of the sudden changes in viscosity in both the heating and cooling ramps which suggests the absence of gelation at 16% Pluronic F127 concentrations. This is well in accordance with the previous reports (Brown et al., 1991 and BASF Technical Bulletin, 2006).

Pluronic F127 concentration	Gelation temperature without CPM	Gelation temperature with CPM	Change in gelation temperature
25%	18˚C	18˚C	No change
22%	24˚C	32˚C	6˚C
19%	23˚C	40˚C	7˚C

[Table. 5.1 Showing gelation temperature of different Pluronic F127 concentration with and without CPM determined by DMTA tests (see fig. 5.27 to 5.29)]

For 25 % Pluronic F127 solution with or without CPM the gelation temperature is almost identical at approx. 18˚C (table 5.1). With the addition of CPM to Pluronic F127 at particular concentrations of 22% and 19%, there was an increase in the gelation temperature from 24˚C to 32˚C and 23˚C to 40˚C for 22% and 19% respectively (table 5.1). It can be speculated that this change in gelation temperature is due to difficulties in micellisation in the presence of the

CPM molecule at a particular temperature where the amount of micelles formed are relatively less in comparison to the pure Pluronic F127 solution. With the higher Pluronic F127 concentration the molecules are forced by the densely populated vicinity molecules to form micelles to engulf CPM containing water and form a cubic lattice arrangement as in the case of the 25 % Pluronic F127 solution, where no change in gelation temperature was found with addition of CPM.

5.2 Preliminary Batches

The eleven preliminary batches were obtained with aim to explore: a. Feasibility of the extrusion processing, b. Challenges in processing and trouble shooting, c. Set range for independent variables for next stage of factorial design experiments.

The powder product obtained was inspected visually for presence of agglomerates, compactness of the material and torque during processing was noted. The observations about the batches are summarised in table 5.2.

Initial batches for the process optimization with 25 % Pluronic F127 solution with the feed rate of 180 gm/hr					
Batch no.	MCC feed rate for extrusion (gm/h)	Screw speed (RPM)	Pluronic F127 solution : MCC (by weight)	Observed product consistency	% Torque
1.	390	200	1: 2	Few compacted granules	50-60
2.	450	150	1: 2.5	Large compacted granules	50-60
3.	500	200	1: 2.78	Extruder choked	80-90
4.	500	300	1: 2.78	Few compacted granules	70-80
5.	600	600	1: 3.33	Few compacted granules	70-80
6.	700	400	1: 3.89	Few compacted granules	80-90
7.	800	400	1: 4.45	Few compacted granules	80-90
8.	900	400	1: 5	No signs of compaction	70-80
9.	900	500	1: 5	Few compacted granules	80-90
10.	1000	500	1: 56	No signs of compaction	80-90

Batch with 25% Pluronic F127 containing methylene blue (10mg/ml of water)					
11.	1000	400	1:3.7	Few compacted granules	70-80

[Table. 5.2 Initial batches to optimize the free flowing powdery consistency showing observed powder consistency and torque (%) during processing]
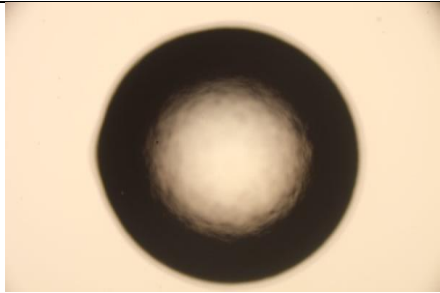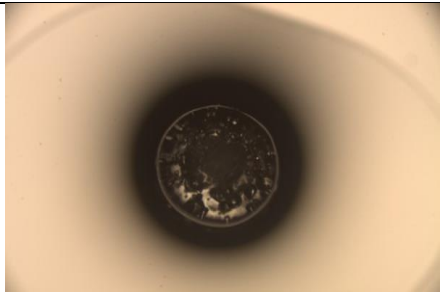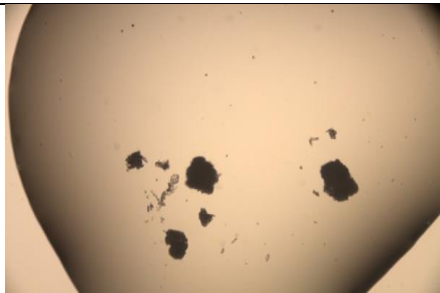
From these initial batches (batch 1-10) it was found that to get the desired consistency the ratio of the MCC should be more than three times that of the weight of the Pluronic F127 solution and the RPM of the screws should be 400 or above. For all these initial batches (batch 1-10) the torque (%) was very high (50 – 90% of the extruder's capability) and the processing very noisy. Furthermore in most of the batches compacted granules were found. It was thought that the reason for these issues might be the inability to achieve the refrigerated temperature (5˚C) along the barrel thus not helping the Pluronic F127 solution to mix and spread on the MCC surface. That is, processing the material at ambient temperature was inducing the elastic behaviour due to which the Pluronic F127 solution tends to restore and will certainly not aid in its spreading instead tending to retain its original structure. This rigid elastic Pluronic F127 gel with MCC along with rotating screws having some compression zones will produce compacted granules. The compacted granules provide resistance to powder flow along the barrel which causes high torque production and frictional heat generation which makes the process even more difficult to attain the desired consistency. To check the mixing and the spreading efficiency of the standard mixing configuration (see table 4.7) a separate batch-11was processed (see table 5.2) with 25 % Pluronic F127 containing methylene blue dye to check colour dispersal within the precursor. The methylene blue colour was found to be well dispersed displaying adequate mixing and spreading efficiency of the standard mixing configuration (see fig. 5.31).

[Fig. 5.31 Batch -11 showing uniform colour dispersal of Methylene blue over the MCC through twin screw extrusion using standard mixing configuration]

5.2.1 Polarised Light Microscopy (PLM)
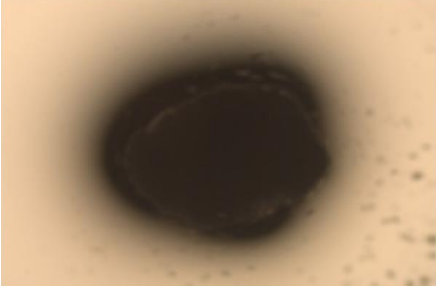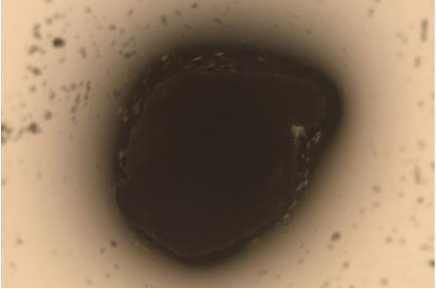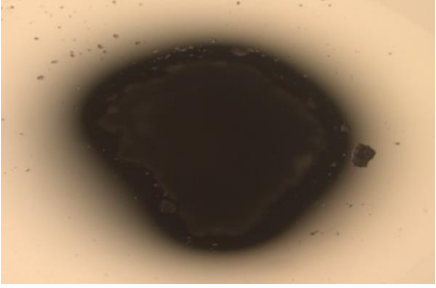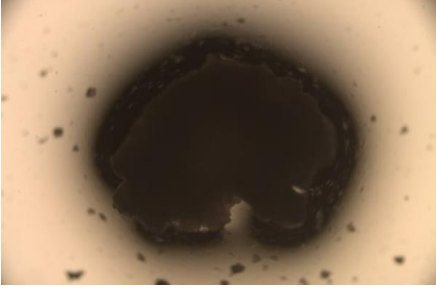
The PLM images for Pluronic F127 and some of the processed batches are shown below. In figures 5.32 images a) and b) are for drop of 25 % w/w Pluronic F127 solution and a solid Pluronic F127 particle undergoing hydration respectively. The generation of cubic phase was confirmed by the dark black colour edge surrounding the clear central part. This is confirmation with the observation by Rosevear (Rosevear, 1954). Image c) is for MCC particle under hydration which failed to show presence of any mesophase structure.
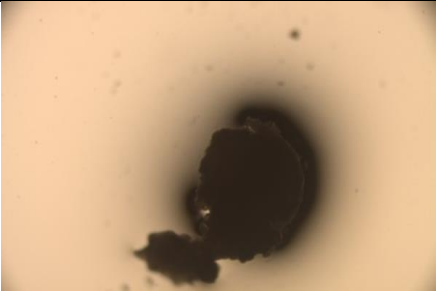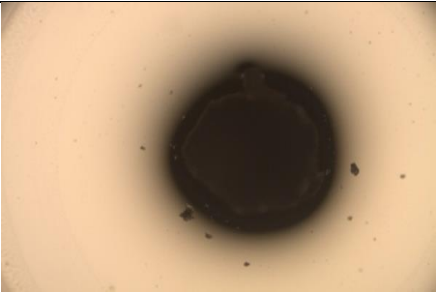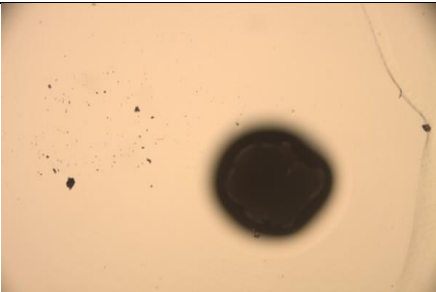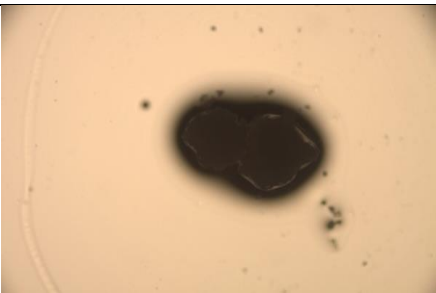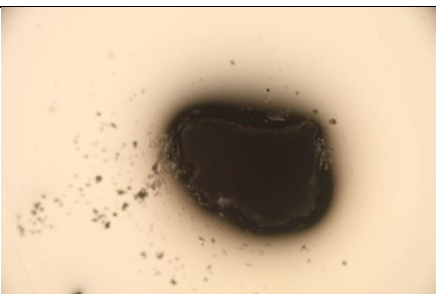
Pic .No.	Picture description with batch no.	Picture
a.	PLM image at 5x magnification of 25% Pluronic F127 gel at 40˚C with water, showing a uniform dark black colour at the circumference of the drop and isotropic (clear) at the centre confirming cubic phase liquid crystal formation according to the classification established by Rosevear (1954).	
b.	PLM picture at 5x magnification of Pluronic F127 particle at 40˚C with water, showing uniform dark black colour at the circumference of the particle confirming cubic phase liquid crystal formation according to the classification established by Rosevear (1954).	
c.	PLM picture at 5x magnification of uncoated MCC particles with water at 40˚C. Unable to form cubic phase because of absence of Pluronic F127 coating.	
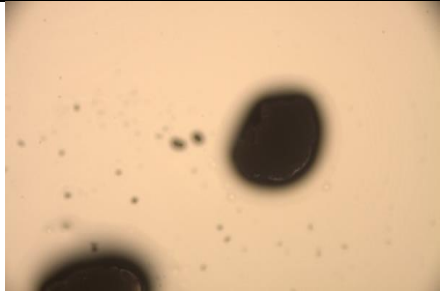
[Figures 5.32 PLM images of Pluronic F127 gel, hydrating Pluronic F127 and MCC particles]

Figures 5.33 provide images of hydrating particles in size range of 63 − 150 μm from 10 batches. The particles showed development of dark edge, absence of birefringence indicates

that the phases forming are not other than cubic phase. Another indication is there are highly compacted particles having uniform coating on the surface. There is also chance that the coating solution could have been squeezed to the surface of the agglomerate due to high shear during extrusion.

Pic .No.	Picture description with batch no.	Picture
a.	PLM picture at 10x magnification of Pluronic F127 coated MCC particle of batch-1 at 40˚C with water, showing uniform dark black colour at the circumference of the particle confirming cubic phase liquid crystal formation according to the classification established by Rosevear (1954).	
b.	PLM picture at 10x magnification of Pluronic F127 coated MCC particle of batch-2 at 40˚C with water, showing uniform dark black colour at the circumference of the particle confirming cubic phase liquid crystal formation according to the classification established by Rosevear (1954).	
c.	PLM picture at 10x magnification of Pluronic F127 coated MCC particle of batch-3 at 40˚C with water, showing uniform dark black colour at the circumference of the particle confirming cubic phase liquid crystal formation according to the classification established by Rosevear (1954).	
d.	PLM picture at 10x magnification of Pluronic F127 coated MCC particle of batch-4 at 40˚C with water, showing uniform dark black colour at the circumference of the particle confirming cubic phase liquid crystal formation according to the classification established by Rosevear (1954).	

e.	PLM picture at 10x magnification of Pluronic F127 coated MCC particle of batch-5 at 40˚C with water, showing discontinued uniform dark black colour at the circumference of the particle confirming cubic phase liquid crystal formation according to the classification established by Rosevear (1954). But the discontinuity is due to uncoated part on the MCC surface.	
f.	PLM picture at 10x magnification of Pluronic F127 coated MCC particle of batch-6 at 40˚C with water, showing uniform dark black colour at the circumference of the particle confirming cubic phase liquid crystal formation according to the classification established by Rosevear (1954).	
g.	PLM picture at 10x magnification of Pluronic F127 coated MCC particle of batch-7 at 40˚C with water, showing uniform dark black colour on the folds at the circumference of the particle confirming cubic phase liquid crystal formation according to the classification established by Rosevear (1954).	
h.	PLM picture at 10x magnification of Pluronic F127 coated MCC particle of batch-8 at 40˚C with water, showing uniform dark black colour on the folds at the circumference of the particle confirming cubic phase liquid crystal formation according to the classification established by Rosevear (1954).	
i.	PLM picture at 10x magnification of Pluronic F127 coated MCC particle of batch-9 at 40˚C with water, showing uniform dark black colour on the folds at the circumference of the particle confirming cubic phase liquid crystal formation according to the classification established by Rosevear (1954).	

j.	PLM picture at 10x magnification of Pluronic F127 coated MCC particle of batch-10 at 40˚C with water, showing uniform dark black colour on the folds at the circumference of the particle confirming cubic phase liquid crystal formation according to the classification established by Rosevear (1954).	

[Figures 5.33: PLM images of preliminary batches with description and batch]

> **Challenges and troubleshooting**

1. For the Pluronic F127 solution feeding for the initial optimisation batches, a 10ml pipette was used. This proved very difficult to maintain a precise flow rate with the pipette. A SEKO PR1 peristaltic pump was later employed for the factorial design batches.

2. The extruder was unable to achieve the refrigerated temperature profile along the barrel with the conventional water cooling system for the initial optimisation batches. Thus a chiller with suitable coolant was plumbed into the extruder for achieving the low temperature set profile along the barrel for the factorial design batches (see section 5.3).

3. Difficulties in keeping the Pluronic F127 in the sol state within the pumping pipe owing to its extreme temperature sensitivity and the control of its feed rates owing to temperature induced viscosity changes posed further problems. To ensure the exposure of Pluronic F127 solution outside the ice bath within the pumping tube for the minimum time, the tubing length was kept to a minimum by locating the peristaltic pump near to the hopper. Even with this change the highest Pluronic F127 concentrated solution (25%) was still sometimes fed in a very close to gel like consistency.

4. While feeding the MCC and the Pluronic F127 solution with the feeder and the pump respectively from the same hopper, after a few seconds of processing it was found that the
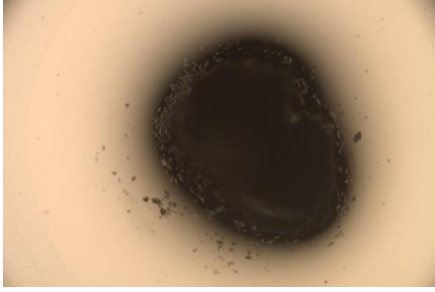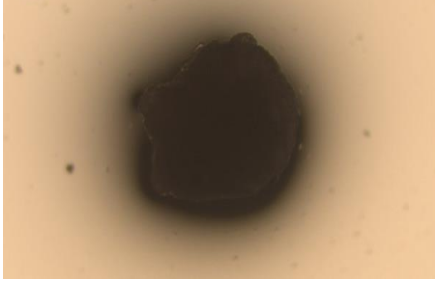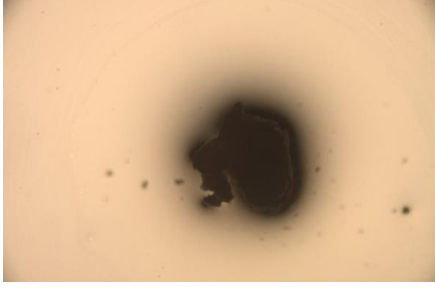
MCC was forming a lump on the feeding throat of the barrel by adsorbing the Pluronic F127 solution, thereby obstructing material entry onto the screws. This problem was solved by dividing the hopper cavity with the help of a plastic sheet to restrict the contact between Pluronic F127 solution and the MCC outside the barrel.

5.3 Factorial design batches

After the addressing the challenges found during preliminary studies 3^3 Central composite design batches were processed using various set variables for each batch. The processing of the batches was smooth and did not face any of the problems observed in preliminary batches. The use of chiller reduced torque as well as formation of compacted mass (granules) which is undesirable. It can be attributed to the reduced elasticity and Newtonian behaviour of Pluronic F127 at low temperatures. By comparing the values of "d_g" and % torque of the factorial design batches of all three concentrations, it was found that with the decrease in the Pluronic F127 solution concentration (increase in the amount of water) the tendency of compaction was found to increase which is also responsible for the increase in the torque.

The product obtained from different batches was subjected to particle size distribution study using sieve analysis (see section 4.3.6) and measurement of "work done for cohesion (WDC)" using texture analyser. The particles were also evaluated using PLM and SEM. The drug release behaviour was also checked for some batches.

5.3.1 Polarised light microscopy

Pic .No.	Picture description with batch no.	Picture
a.	PLM picture at 10x magnification of Pluronic F127 coated MCC particle of batch-F6 at 40˚C with water, showing uniform dark black colour at the circumference of the particle confirming cubic phase liquid crystal formation according to the classification established by Rosevear (1954).	
b.	PLM picture at 10x magnification of Pluronic F127 coated MCC particle of batch-F9 at 40˚C with water, showing uniform dark black colour at the circumference of the particle confirming cubic phase liquid crystal formation according to the classification established by Rosevear (1954).	
c.	PLM picture at 10x magnification of Pluronic F127 coated MCC particle of batch-F8 at 40˚C with water, showing uniform dark black colour at the circumference of the particle confirming cubic phase liquid crystal formation according to the classification established by Rosevear (1954).	

[Figures 5.34: PLM images of factorial design batches with description and batch]

The PLM images of the hydrated powder from batches containing lower, medium and high amounts of MCC are shown in figures 5.34. By comparing the figures 5.34 a), b) and c), It clearly shows that there is thick coat on the surface of particle from batch having lower MCC where as the coat was incomplete when MCC levels were high (see image (c) from figures 5.34) . This indicates there is uniform distribution of gel during extrusion process but there needs to be balance between amount of gel and number Of MCC particles. At lower MCC amounts it may lead to formation of the thick layer providing slow release but at the same

time increases chances of particle agglomeration because of bridging action of excess gel on the surface.

5.3.2 Scanning electron microscopy (SEM)
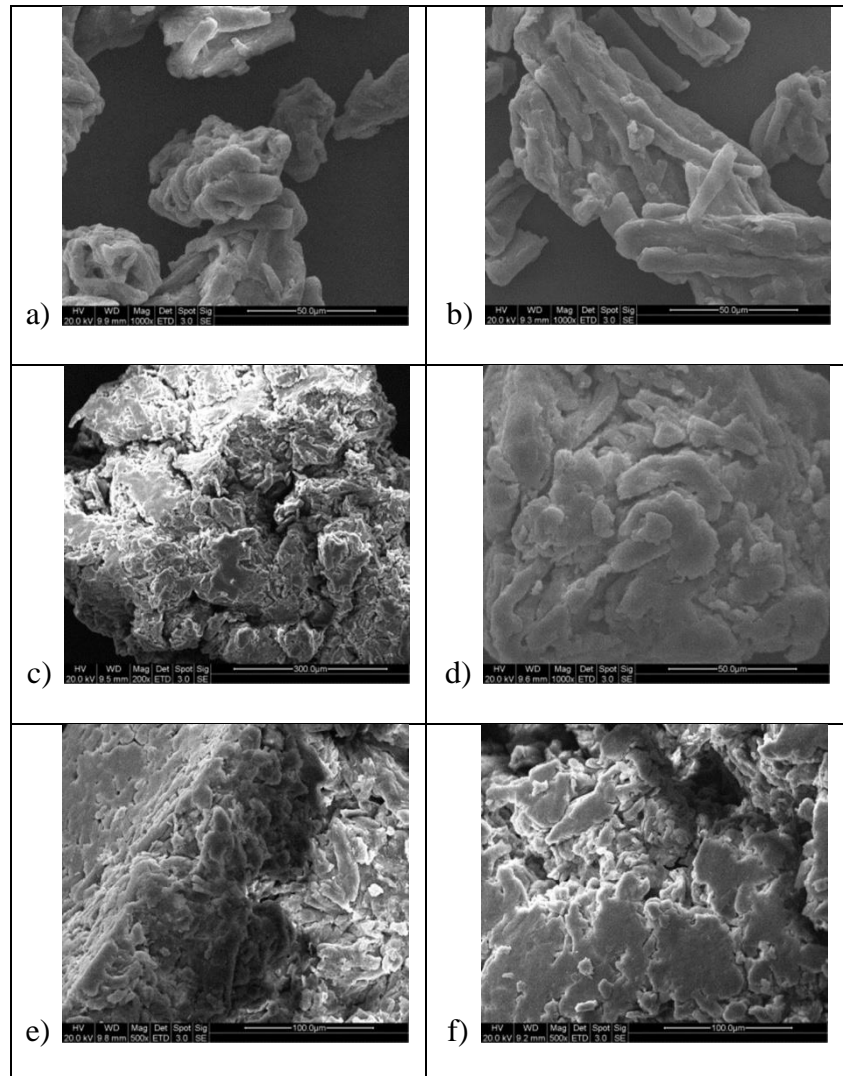
[Figures 5.35 SEM images from factorial design batches]

The SEM photographs of uncoated MCC before and after extrusion are shown in images a) and b) of figures 5.35. The fibrous MCC was found to be stretched and elongated during extrusion process due to the applied shear during processing. The images c), d), e) and f) show effect of amount of MCC and Pluronic F127 on the surface properties of the particles.

At higher percentage of Pluronic F127 (25%), the particle surface is smoother showing significant coating on the surface especially when amount of MCC was low (Image d). At lower percentage of Pluronic F127 the particle surface was not fully coated and shows crevices on the surface (Image c). At the same time the individual particles look to be more flattened then elongated indicating plastic deformation of the material due to thin or no coating (Image e and f).

5.3.3 Particle size distribution

The particle size distribution was carried out by sieving and Geometric mean diameter (d_g) was calculated using log- probability plot.

The idea behind plotting the log normal distribution on the probability scale is that it gives a linear relationship (see figs. 5.36 - 5.37) which is advantageous to characterise this normal distribution curve by the slope of the line and a reference point (Martin AN, 1993). The reference point used here is the logarithm of the particle size which is equivalent to 50% on the probability scale i.e. the 50% size. This is known as the Geometric mean diameter (d_g). The d_g was found to be the highest for Batch-F1 i.e. 500 µm. This means that for batch-30 50% of particles are less than 500 µm. The log probability plot of all the batches are not shown but the d_g value of each batch was shown in table 5.3. The particle size of all the batches from the factorial design study has been quantified by this log probability plot method to calculate "d_g".
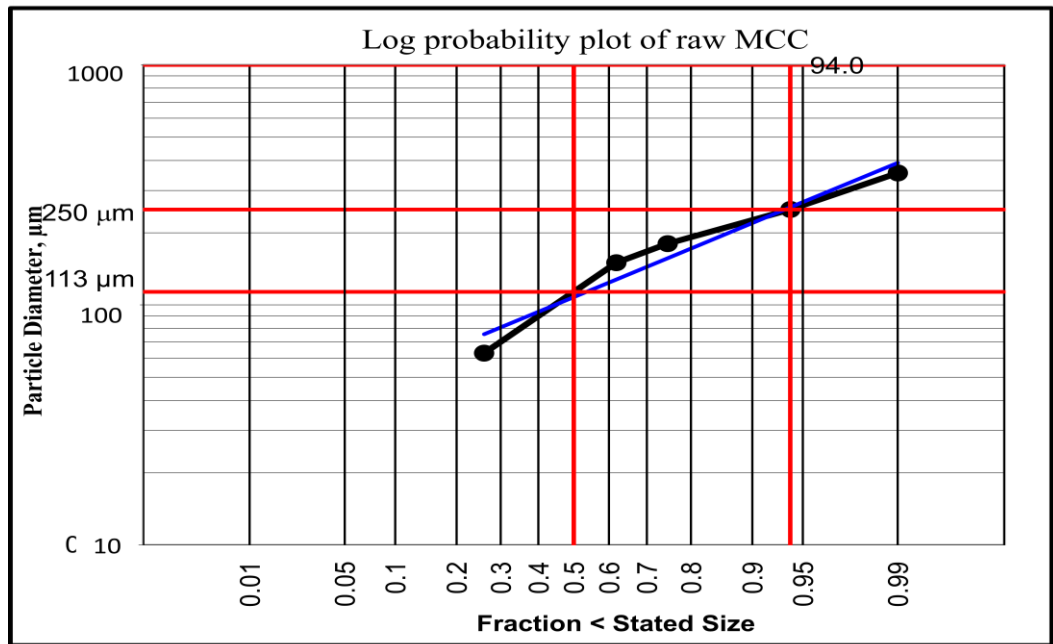
[Fig. 5.36 Log probability plot of raw unprocessed MCC showing the Geometric mean
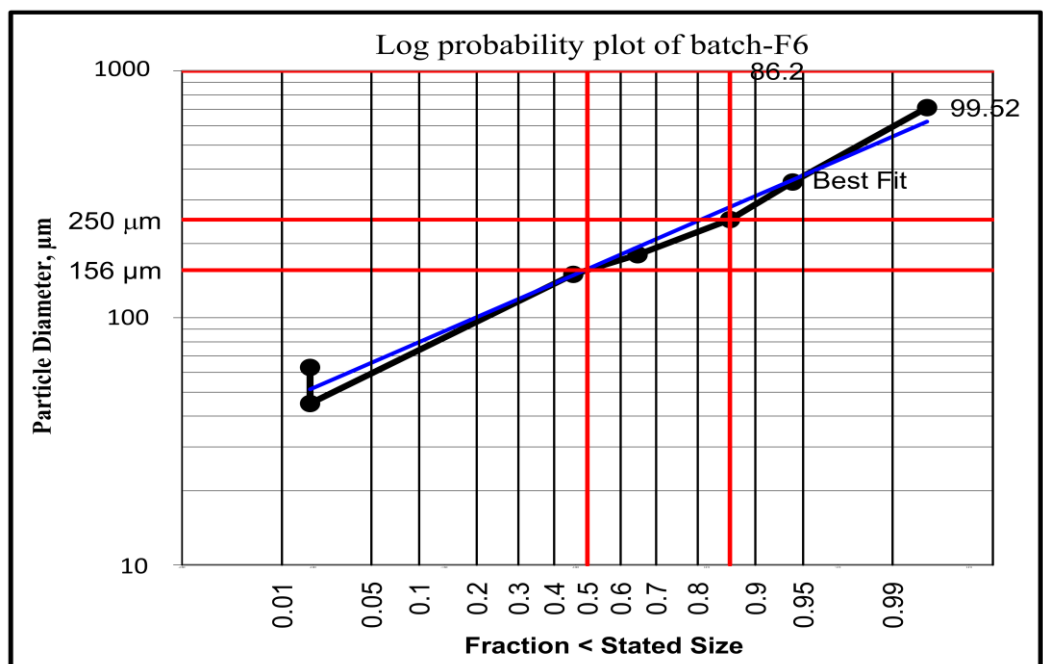
diameter (d$_g$)]

[Fig. 5.37 Log probability plot of batch-F6 of factorial design study showing the Geometric

mean diameter (d$_g$)]

Geometric mean diameter (d_g) was used as the dependent variable for modelling the relationship with the help of regression analysis which was performed on the factorial design batches to investigate and develop the surface response curve based on independent variables or factors (MCC feed rate (X_1), Pluronic F127 concentrations (X_2) and screw speed (X_3)) or their combinations which were significant in effecting the dependent variable "d_g".

5.3.4 Powder flow analysis

The powder flow analysis was performed using a TA.XT *Plus* powder rheometer (Stable Micro Systems, Surrey, U.K.) as described in section 4.3.7 to check the coating efficiency of the processed powder precursor. A typical force time profile obtained using powder flow analyser is shown in fig. 5.38. Unprocessed MCC was found to be very cohesive in powder flow which is also evident from the larger negative area (see fig. 5.38) (indicative of WDC as specified in section 4.3.7) than for the processed batches (see figure 5.38). Thus, it might be expected that if the MCC particles become coated with the Pluronic F127 the cohesion between the particles will decrease. The negative area in the figure 5.38 from the powder analyser represents the decompression cycle of the rotor blade which measures the work performed (energy required) to overcome the cohesion forces to bring the rotor blade out of the column of the powder bed while rotating and traversing upwards (decompression cycle). The work done for cohesion (WDC) was found to be highest for the raw uncoated MCC (WDC = 425 gm.sec) in comparison with the Pluronic F127 granules (WDC = 269 gm.sec) and the processed batches. Here it is important to note that the units for WDC that is 'gm.sec' is proportional to the units of the 'Work Done' because the seconds here is quantified in terms of the distance moved by blade while traversing in the vertical direction with the speed of 30 mm/sec (see section 4.3.7) and gm is the force experienced by the rotating blade in terms of

weight. Thus 'gm' is representative of force and 'seconds' represents the distance travelled. Batch-F1 with the maximum compaction (highest "dg") has the highest WDC = 307.048 gm.sec among all the factorial design batches which indicates that most of the Pluronic F127 was utilised by the particles to form the compacted mass. Thus, there will remain a smaller quantity of Pluronic F127 left for coating of the remaining particles. Hence less number of coated particles is present. Therefore the coating which is acting as barrier between the particles surface to restrict their sticking together due to the cohesion force is not available. This might be potential reason for such high WDC of Batch-F1 (highest "dg") among all the factorial design batches. The calculated WDC for all the factorial design batches is summarized in table 5.3.
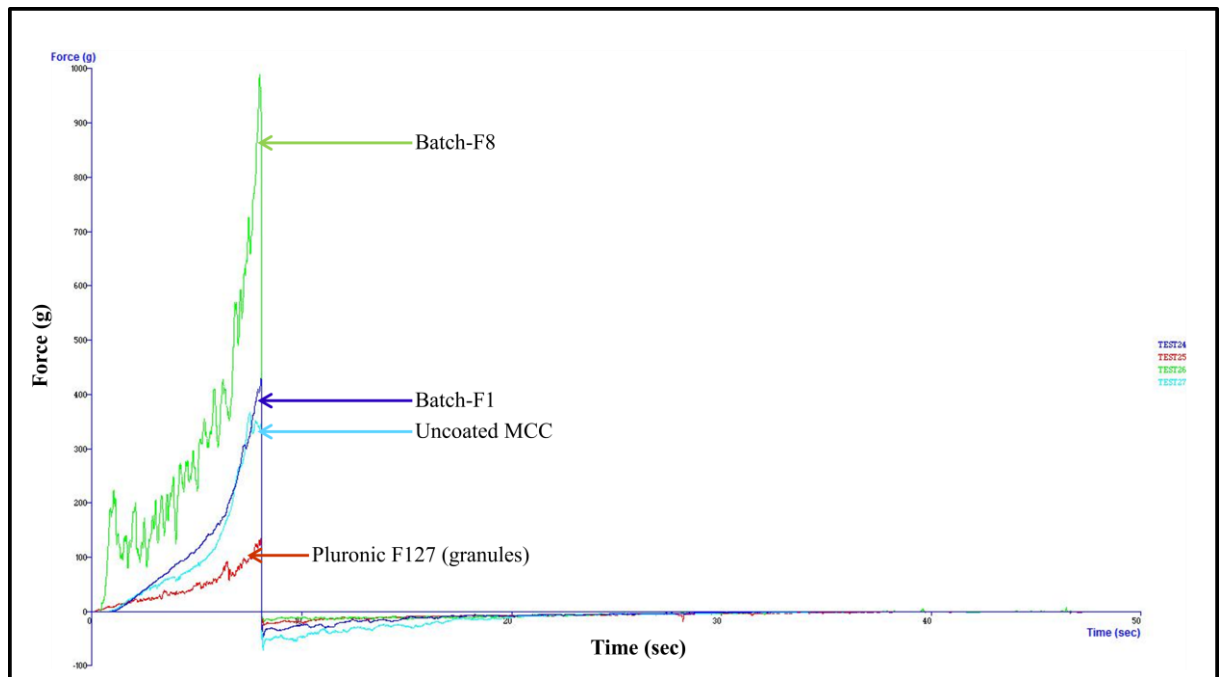
[Fig. 5.38 Sample powder rheometer graphs of uncoated MCC, Pluronic F127 granules and processed batches with highest (batch-F1) & relatively low (batch-F8) "WDC". For "WDC" information refer to tables 5.7]

5.3.5 Regression Analysis

The three quantitative evaluation parameters reflecting dependent properties were considered for regression analysis and plotting response surface. The data of dependent variables for the twenty nine batches of the factorial design are summarised in Table 5.3.

Batches	% Torque	"d_g" (µm)	Work done for cohesion (gm.sec)
F1	45	500	307
F2	15	175	161
F3	45	440	176
F4	15	232	143
F5	25	251	209
F6	15	156	183
F7	15	105	97
F8	15	145	133
F9	15	133	156
F10	45	440	271
F11	45	500	201
F12	15	238	121
F13	10	156	108
F14	45	470	220
F15	15	156	143
F16	35	277	152
F17	15	205	183
F18	35	490	184

F19	25	250	181
F20	15	224	178
F21	15	200	156
F22	15	148	136
F23	25	490	173
F24	15	228	163
F25	15	140	176
F26	15	135	173
F27	15	163	157
F28	25	280	202
F29	25	302	210

[Table 5.3 Showing observed data of Torque, "dg" and WDC for factorial design batches]

The torque values ranged from as low as 10% to 45% which indicate that all batches were processed smoothly with resistance to flow in a processable limit. The values of "d_g" were between 105 μm to about 500 μm but for most of the batches values were below 300 μm. This size is significantly larger than the average particle size of the MCC particle. This may be due to formation of small agglomerates and increase in size due to coat of Pluronic F127 on the surface. The WDC ranged approximately between 100 to 300gm.sec. The batch F7 showed lowest values for almost all the parameters when screw speed was lowest when other two factors were at higher level.

The data was then subjected to multiple regression analysis treatment. The model fitted was in the equation below.

$$\hat{y} = \beta_o + \beta_1 X_1 + \beta_2 X_2 + \beta_3 X_3 + \beta_{11} X_1{}^2 + \beta_{22} X_2{}^2 + \beta_{33} X_3{}^2 + \beta_{12} X_1 X_2 + \beta_{13} X_1 X_3 + \beta_{23} X_2 X_3 + \beta_{123} X_1 X_2 X_3$$

Where, $\hat{y}$ indicates predicted value of the dependent variable, β_o is constant and β_i denotes regression coefficients for respective independent variables. In the equation X1, X2 and X3 represent linear terms whereas the square terms indicate quadratic and cross terms indicate interaction between the variables.

The multiple regression analysis was carried out using Microsoft Excel package. The Analysis of Variance (ANOVA) or F test was carried out to check significance of each parameter. The final equation and coefficient of determination was determined. The significance of coefficient of determination was checked on the basis F test at 95 % confidence that is p value was set to be less than 0.05. The backward elimination method was used to arrive at the final equation.

Once the final regression equation was obtained, it was used to generate response surfaces indicating effect of various parameters on the dependent variables. The surface can be plotted in maximum three dimensions therefore only two variables can be illustrated at any one time. When more than two variables were significant then one of the variable was set at constant level and effect of other two variables was represented in the response surface.

The regression analysis and ANOVA data for the three variables is summarised in Table 5.4.

Coefficients	Torque	"d_g"	Work done for cohesion
β_o	20.45454545	262.7241379	174.8656552
β_1	-6.944444444	-88.77777778	-18.66711111
β_2	-8.055555556	-85.66666667	-34.162
β_3	-	-	-
β_{11}	-	-	-
β_{22}	4.267676768	-	-
β_{33}	-	-	-
β_{12}	-	-	-
β_{13}	-	-	-
β_{23}	-	-	21.96858333
β_{123}	-	-	-
r^2	0.551041417	0.567142533	0.620822234
F- value	10.22814126	17.0329808	13.64404533
Significance	0.000141043	1.87277×10^{-05}	1.79947×10^{-05}

[Table. 5.4 Showing ANOVA data for Torque, "d_g" and WDC]

The regression analysis data shows that the coefficient determinations for all three variables were in the range of 55 – 62%. Though these values are low, the significance is high as degree of freedom is high and due to repeated centre point batches the error has been well estimated. The coefficient of determination indicates contribution of the independent variables for the variance observed in the dependent variables. Therefore we can say on an average around 60% variation in the three parameters was attributed to the factors which are found significant in the regression analysis. In other word 40% variation has to be attributed to unknown variables. Though experiments are well controlled to minimise the unknown variables still

there are chances that some variables may be unintentionally introduced especially because of the limitations in instrumentation. For example, as explained in the previous section the amount of Pluronic F127 solution added varied slightly with the concentration because of the limited control capability of the peristaltic pump used. This variation would have definitely contributed to the error term in the equation.

The response surfaces present good way to understand effects as compared to the equations alone. The response surfaces showing effect of different variables are shown below.

➢ Torque

The variation in % torque during processing indicates lower load on the rotating shaft because of resistance to flow. The regression analysis negative values of regression coefficients for X1 and for X2 where as positive coefficient for the quadratic term $X2^2$. This suggests that the negative coefficients for linear term that is torque decreases with increase in amount of percentage of Pluronic F127 and MCC feed rate.
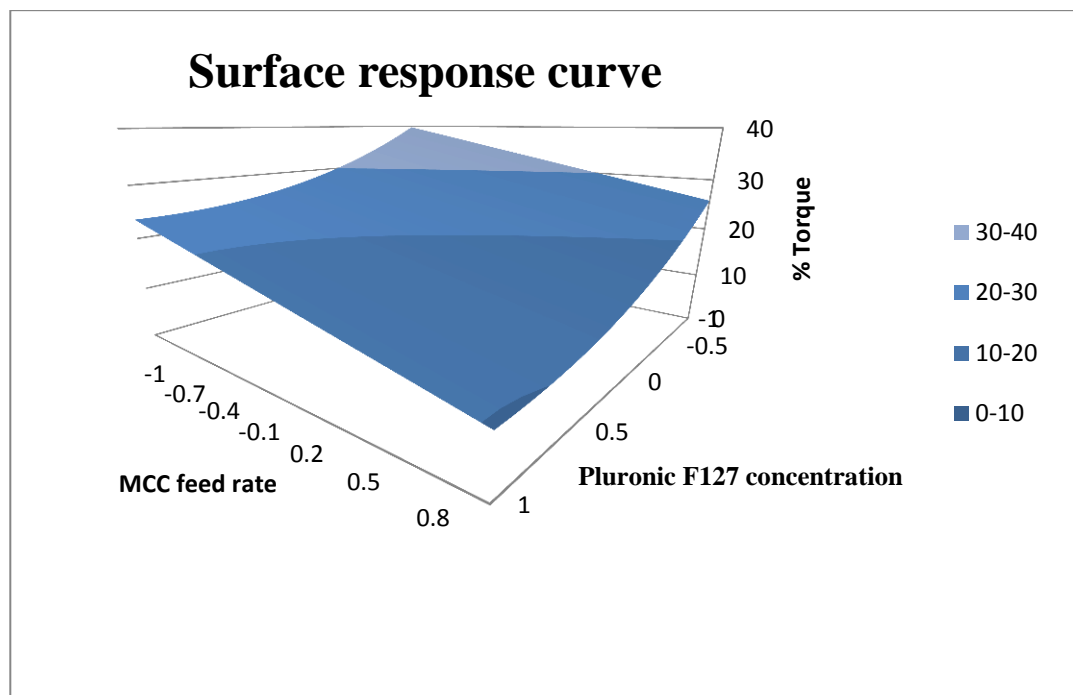
[Figure. 5.39 Response surface curve showing effect of PF127 concentration and MCC feed rate.]

As Pluronic F127 concentration in the solution increases the viscous layer coates uniformly MCC particles which will reduce friction and in turn torque experienced will be reduced. The surface smoothening of particles with increase in Pluronic F127 concentration has also been observed in the SEM photographs. Similarly this can also be supported on the basis of better coating because enhanced viscoelastic behaviour at higher Pluronic F127 concentrations was

observed in the rheological study. The high viscoelastic cubic phase of that higher Pluronic F127 concentrations can resist any structural damage due to shear applied during processing maintaining surface smooth uniform coating.

The effect of Pluronic F127 concentration is interesting as it shows negative coefficient for linear term and positive coefficient of the quadratic term. This suggests that as Pluronic F127 concentration increases torque decreases upto certain feed rate and increases with further increase in Pluronic F127 concentration. This is responsible for the negative saddle shape of the response surface. Lower Pluronic F127 concentration doesn't provide viscous lubrication effect due to which generated friction will be more and hence the torque. Increase in Pluronic F127 concentration upto a certain level provides good lubrication which reduces the torque till the system's viscoelasticity is bearable. At the highest Pluronic F127 concentration the viscoelasticity is increased further thereby will produce some aggregates which is responsible for friction and increase in torque again but only up to a certain level.

> **Mean geometric diameter "d_g"**

The regression analysis data showed that variables X1 and X2 that is MCC feed rate and Pluronic F127 concentration have significant effect on the "d_g" of the product. The coefficients for both the parameters are negative and contribute to around 57% variation in the "d_g". As Pluronic F127 concentration in the solution increases there is increase viscosity and slight decrease in the amount of water incorporated in the system. The low viscosity solution at lower concentration of Pluronic F127 will favour particle agglomeration leading to higher "d_g" values. No doubt at higher concentrations of Pluronic F127 the thickness of Pluronic

F127 layer will be higher but its contribution to increase in "d_g" value will be dominated by agglomeration caused by low viscosity of Pluronic F127 solution.

As MCC increases the coating thickness of Pluronic F127 decreases which is also due to the amount of water soaked in by MCC also increases due to the hygroscopic nature of MCC. This provides a uniform coating with lesser surface hydration which reduces agglomeration leading to decrease in the "d_g" value.
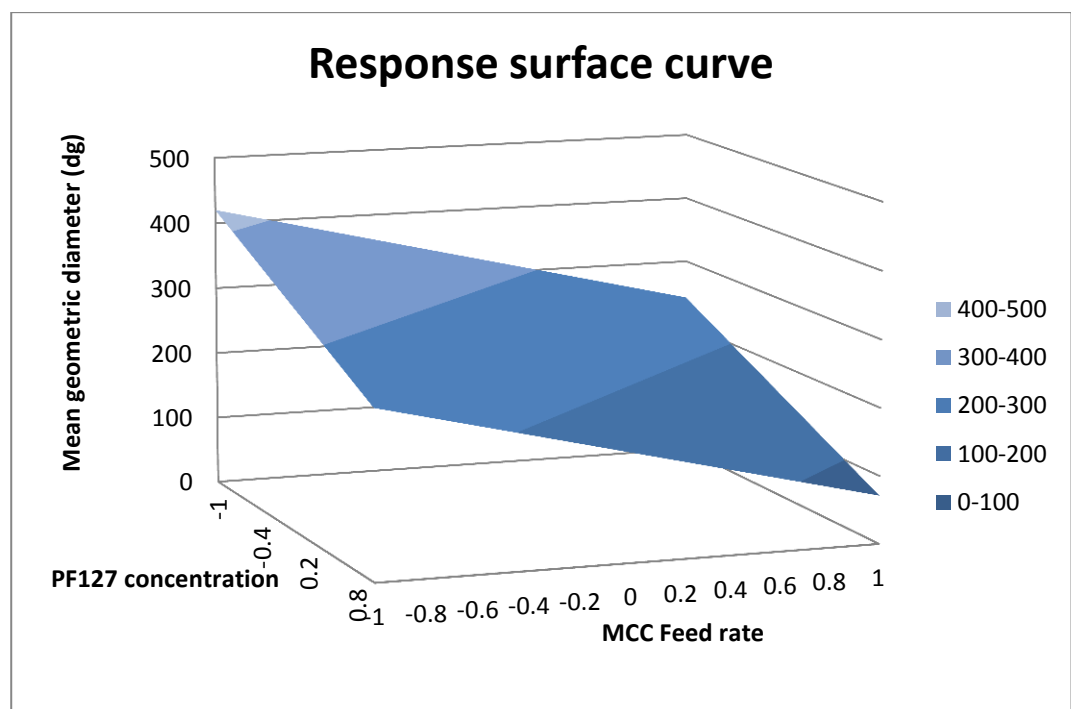
[Figure. 5.40 Response surface curve showing effect of PF127 concentration and MCC feed rate.]

> **Work done for cohesion (WDC)**

The WDC indicates the work required to overcome the cohesion between the particles. The regression analysis data shows that apart from the two linear terms X1 and X2 and interaction

term X2X3 is also significant. It suggests that as there is decrease in WDC with increase in Pluronic F127 concentration and screw speed. WDC is dependent on various particle properties such as particle size, surface smoothness, moisture content, stickiness of the surface and friability of the particle. In other words this parameter is a complex one and is dependent on number of particle properties.

As discussed above with increase Pluronic F127 concentration a uniform and smooth coat is provided on the particle surface reducing friction between the particles which lead to the decrease in the work required to be carried out on the powder during decompression stage. In the same way increase in screw speed must be causing surface smoothening because of even coating on the particle surface. Though a factor need to be taken into consideration is increased number of fines generated at higher screw speed may cause increased friction and should have shown higher WDC values at higher screw speeds though percentage of fines are high particle surface may be smoother overcoming the effect due to increased area of contact. To certain extent the positive value of interaction term X2X3 supports the above discussion. The presence of interaction term X2X3 in the equation indicates that the trends of WDC are opposite at higher and lower levels of X2X3 as shown in fig. 5.44 to 5.45.
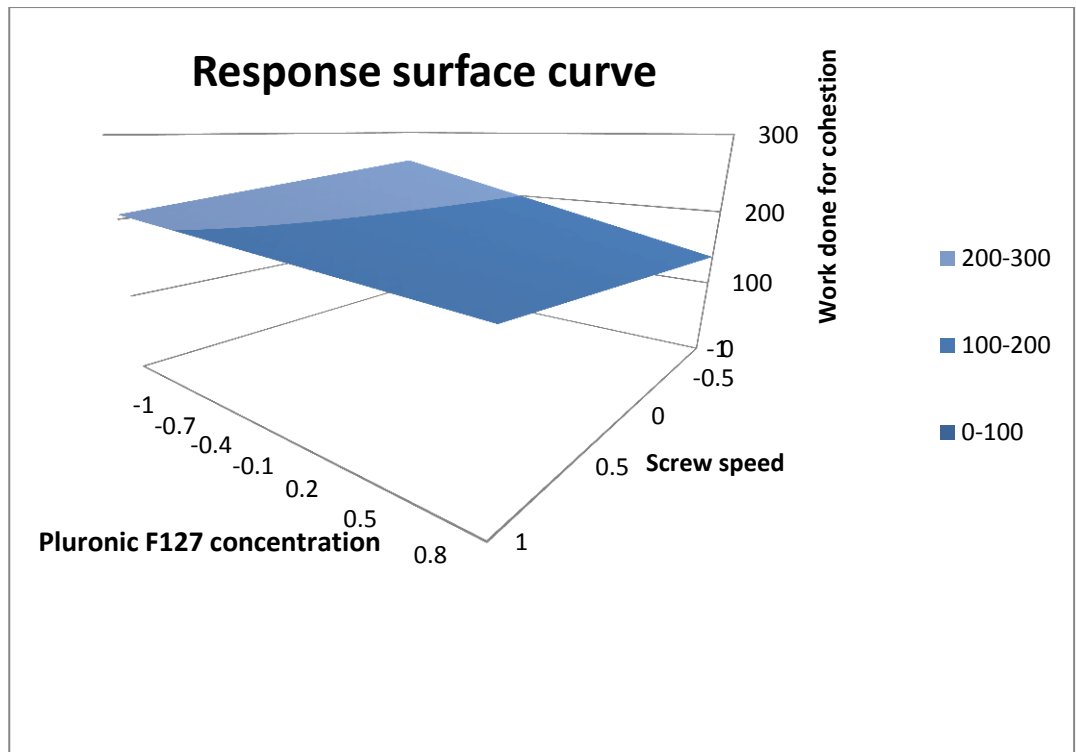
[Figure. 5.41 Response surface curve showing effect of Pluronic F127 concentration and screw speed at X1 = -1]
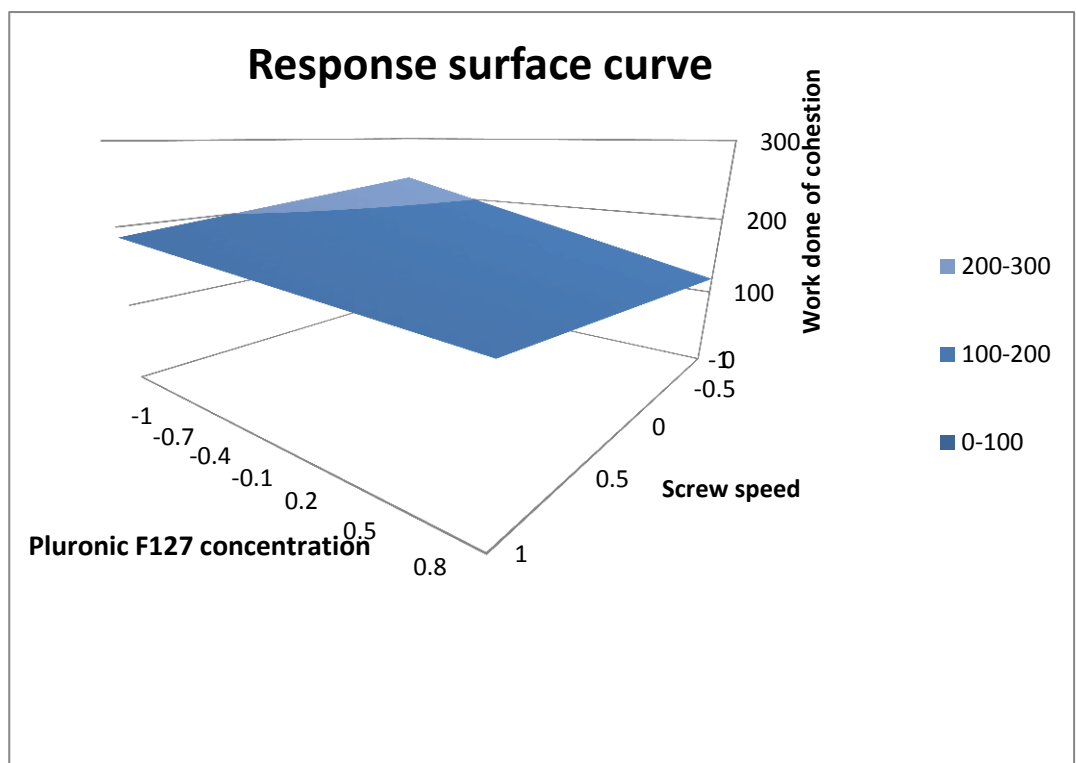
[Figure. 5.42 Response surface curve showing effect of Pluronic F127 concentration and screw speed at X1 = 0]
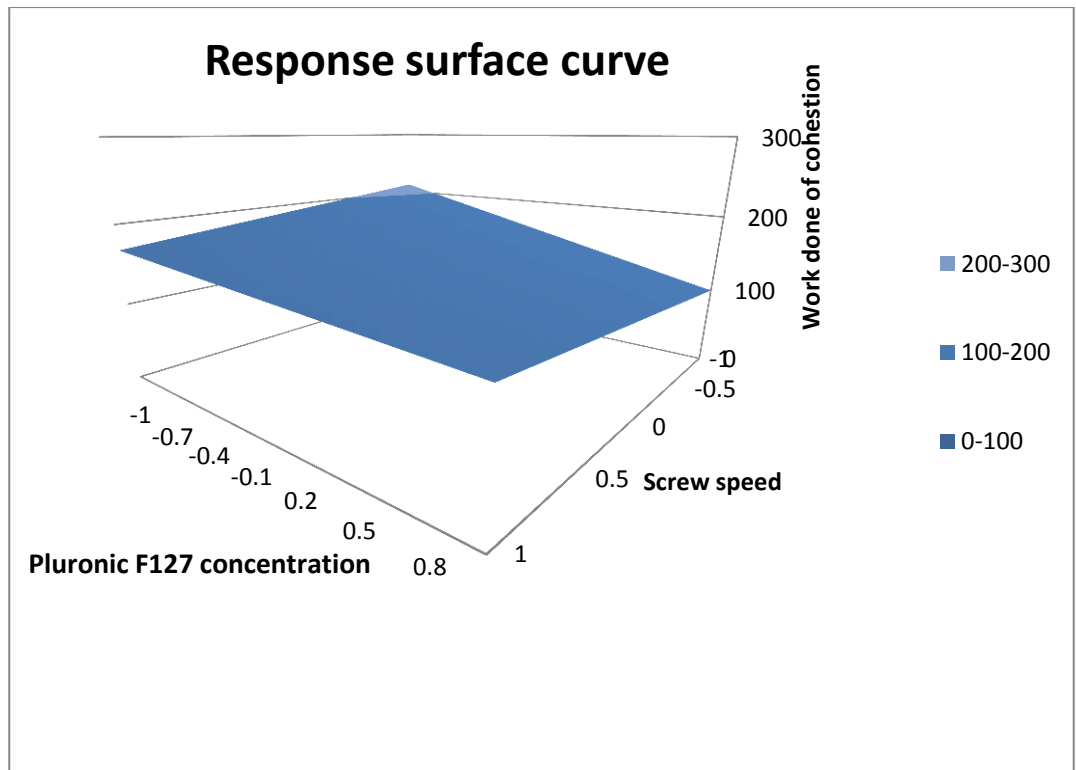
[Figure. 5.43 Response surface curve showing effect of Pluronic F127 concentration and screw speed at X1 = +1]
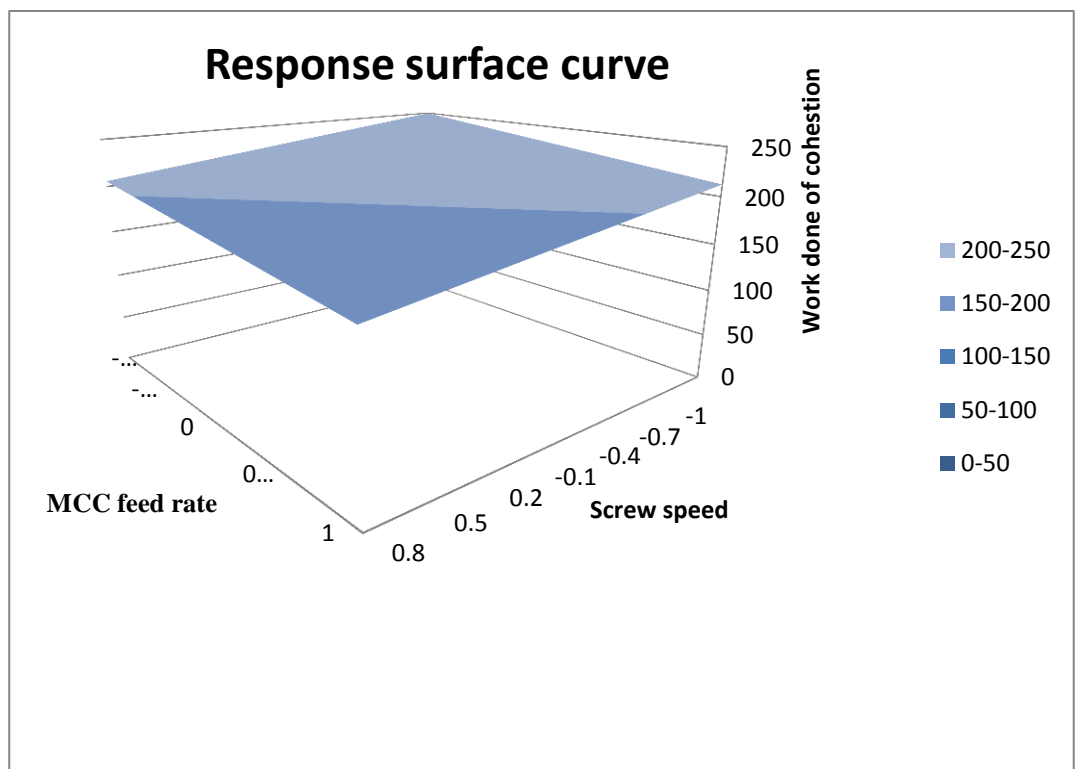
[Figure. 5.44 Response surface curve showing effect of MCC feed rate and screw speed at X2 = -1]
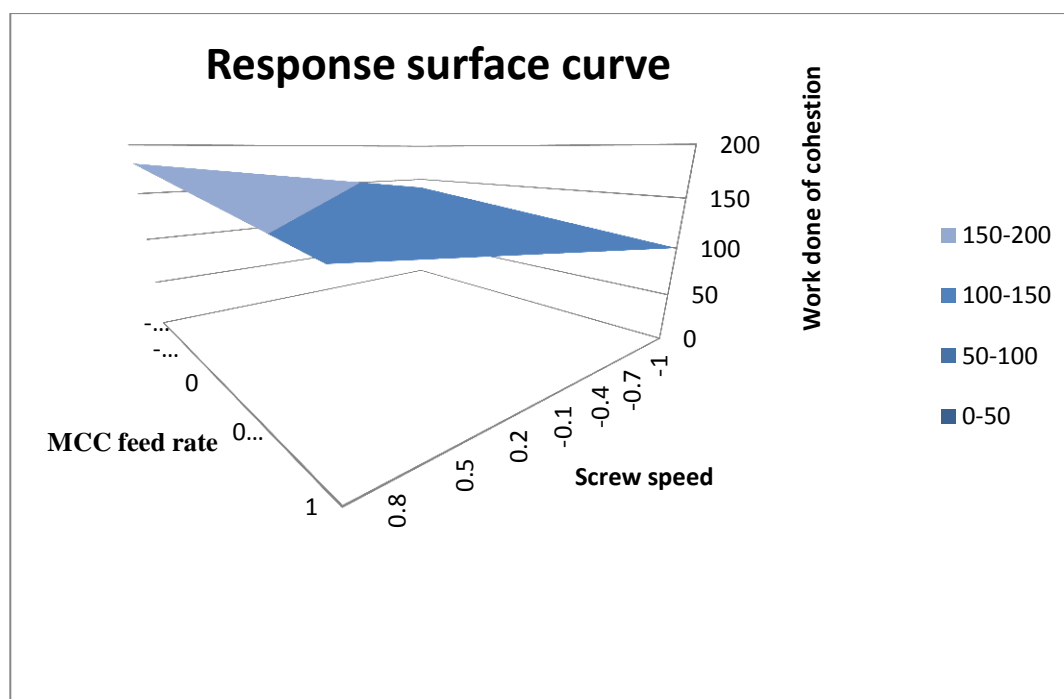
[Figure. 5.45 Response surface curve showing effect of MCC feed rate and screw speed at X2 = +1]

5.3.6 In-vitro drug release studies

The pharmaceutical performance of the cubic phase coated powder precursor prepared through twin screw extrusion was analysed through in-vitro drug release studies. Initial trials were performed using batch-F4 from the factorial design batches was selected as this batch was expected to produce a 'good' controlled release profile since it contained the maximum Pluronic F127 concentration and lowest MCC proportion when compared with the other batches. The particle size range chosen was in between 150 - 63µm as this forms the major portion in all the batches as well as for the unprocessed MCC. Around 416 mg of processed LLC precursor was taken for dissolution studies containing around 3.33mg (quantified by assay, see section 4.3.9) of CPM.
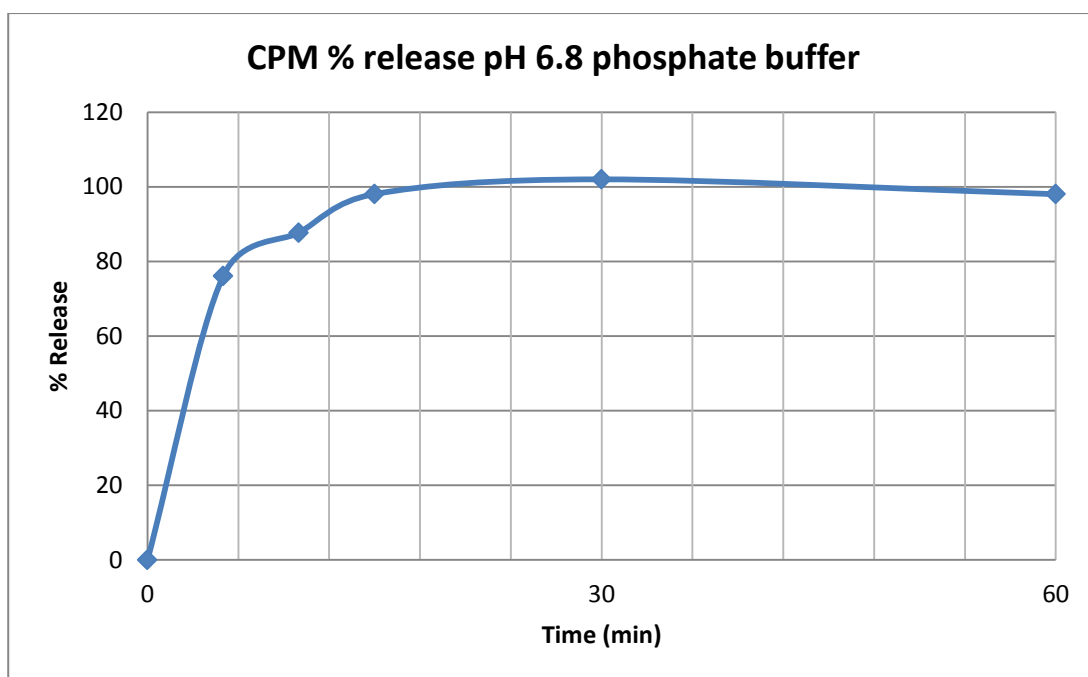
Fig. 5.46 CPM % release profile from LLC coated precursor of batch-F4 (factorial design batches) within the particle range of 150-63µm.

The drug release profile was found to be very disappointing since 100% of CPM was released within 15minutes (see fig. 5.46) in comparison to expected 100% release within 4-6 hours as found by (Shah and Paradkar, 2005). This poor performance might be due to the very thin coating of Pluronic F127 as the proportion of MCC was high (almost four times the Pluronic F127 solution or above). It is also possible that the dissolution media containing buffer salts (Potassium Dibasic Phosphate and Sodium Hydroxide) might be restricting the gelation (cubic phase formation) by the LLC coated precursor as is also reported for various other salts by (Pandit and Kisaka, 1996).To further investigate the possibility of gelation restriction by buffer salts another dissolution test was performed on the same particle size range of batch-F4 but without the buffer salts (only de-ionised water as dissolution media).

CPM % Release without buffer
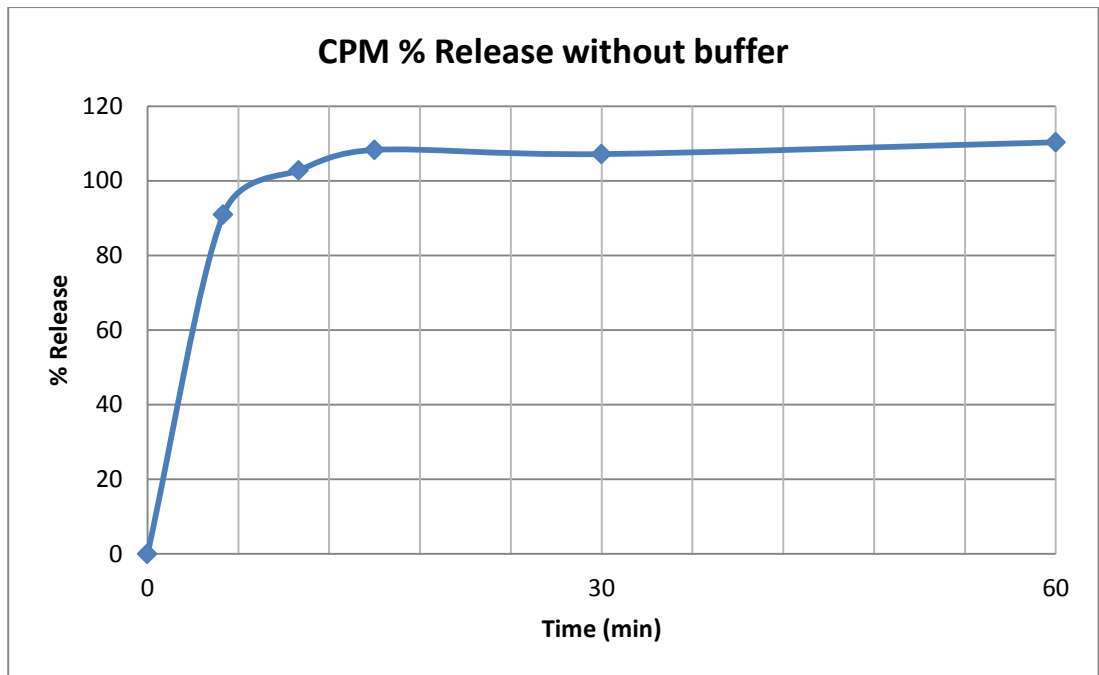
Fig. 5.47 CPM % release profile from LLC coated precursor of batch-F4 (factorial design batches) within the particle range of 150-63μm - de-ionised water.

Again the dissolution profiles reveals (see fig. 5.47) that 100% CPM was released after approximately 15 minutes which refutes the buffer salts being responsible for the burst CPM release by the LLC coated precursor.

It was found that even with maximum levels of Pluronic F127 containing CPM coated precursor was unable to provide controlled release of CPM. Instead 100% CPM was released in approximately 15 minutes. Thus it can be speculated that the very thin Pluronic F127 coating is responsible for the observed burst release profile.

5.4 Results and discussion of new modulated DSC method development for Pluronic F127 solution cubic phase (gelation) detection

The gelation temperature of the Pluronic F127 was confirmed by DMTA as discussed in section 5.1.3. The DMTA results are also used here to plot "Damping factor (tanδ)" with change in temperature which can be used to compare with the MDSC thermograms. The gelation temperature of the 25%, 22% and 19% Pluronic F127 containing CPM was found to be approx 18˚C, 32˚C and 39˚C respectively. No gelation temperature was found for 16% Pluronic F127 containing CPM as it doesn't gel at this concentration as previously reported (BASF Technical Bulletin, 2006(Pisal et al., 2004) (see figures 5.27 to 5.30). For the MDSC thermograms only the non-reversible heat flow curves are shown here since the effect of structural arrangement and crystallization can only be seen in the non-reversible heat flow (Modulated DSC Theory, TA instruments TA-112B).

Initially maximum amplitude of ± 2˚C was chosen to achieve high sensitivity. A moderate period of modulation of 50 seconds and a linear heating rate of 1˚C/min on the 25% Pluronic F127 solution system containing CPM showed no significant transformations (see figure 5.48). A modulation period of 60 seconds was then attempted with the rest of the parameters being held constant. This change did not significantly affect the thermogram (see figure 5.48).
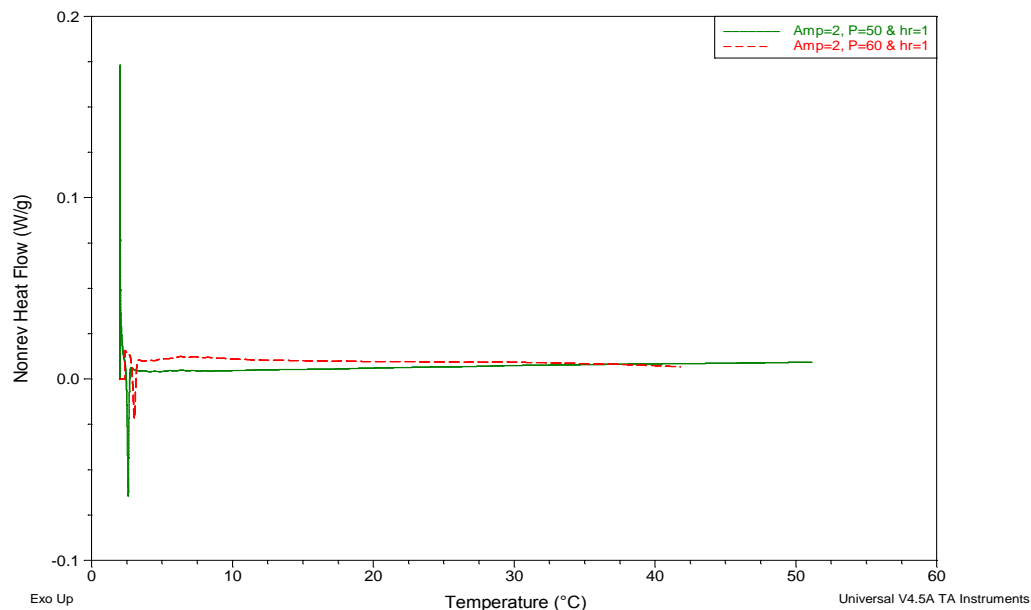
[Fig. 5.48 MDSC thermogram of 25% Pluronic F127 solution containing CPM, showing non-reversible heat flow]

Higher amplitudes of 2.5˚C and 3˚C were then tried with the lowest period of modulation (40 seconds) and heating rate of 1˚C/min after which a micellisation endothermic plateau was found (at approximately 7 to 8˚C) with 2.5˚C of amplitude. With the further increase in amplitude (to 3˚C) the micellisation plateau became transformed into a peak suggesting an increase in the sensitivity of the system (see figure 5.49). However no signs of any thermal event at the gelation temperature for this system of 18˚C were apparent (see figure 5.49).

Graph axis labels: Nonrev Heat Flow (W/g) vs Temperature (°C)

Legend:
Amp=3, P=40 & hr=1
Amp=2.5, P=40 & hr=1

Annotations on graph:
7.74°C
-0.01577W/g

7.37°C
-0.01834W/g

Exo Up

Universal V4.5A TA Instruments
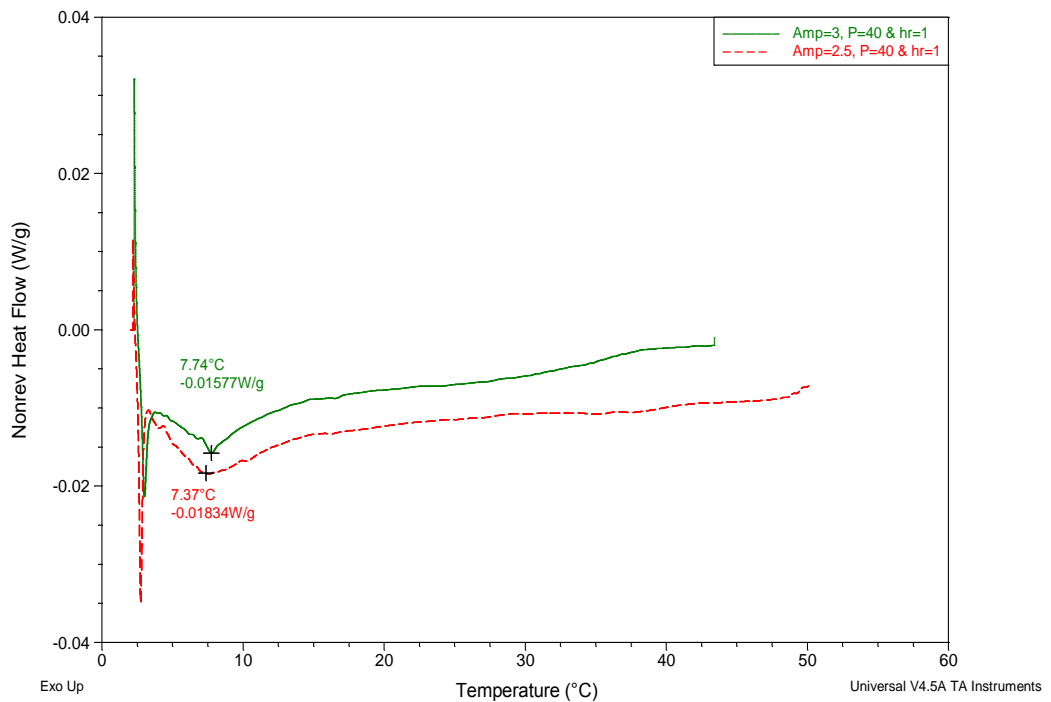
[Fig. 5.49 MDSC thermogram of 25% Pluronic F127 solution containing CPM, showing non-reversible heat flow]

The gelation peak or the cubic phase transition is undetectable by the MDSC heating ramps at such high amplitude of modulation is due to the gradual micellisation of the Pluronic F127 solution which is evident from the results of DMTA heating ramps (see figures 5.27 to 5.30) where complex viscosity was found to be gradually increasing with increase in temperature for all the concentrations of Pluronic F127 solution both with and without CPM. Thus the low micellisation enthalpy along with gradual consumption of thermal energy for micellisation is undetectable even at higher amplitudes of modulation. However it is clear that the amount of thermal energy required to force already formed micelles to arrange into a cubic phase lattice will be very low in comparison with the energy required to form the micelles. Therefore it

becomes very difficult for the MDSC heating ramp even at higher amplitudes to detect the difference in the heat flow for the cubic phase arrangement (gelation).

➤ **Effect of heating and cooling ramp**

To overcome the above problem an MDSC cooling ramp was performed for comparison with the heating ramp at the same parameters. By carefully studying the DMTA results of heating ramps shown in figures 5.27 to 5.29 (for 25%, 22% and 19% Pluronic F127 with without CPM) the complex viscosity was found to increase gradually till gelation temperature where it shouts up suddenly and becomes constant afterwards. This gradual increase in viscosity is due to gradual micellisation which is a temperature dependent higher enthalpy phenomenon in comparison with cubic lattice arrangement of micelles. Thus sudden low enthalpy cubic phase arrangement at specific temperature might have got shadowed by the higher enthalpy gradual micellisation while measuring the heat flow difference by DSC system. However while cooling (DMTA results of cooling ramps, see figures 5.27 to 5.29) the complex viscosity remains almost constant throughout except for the gel melting temperature where it drops suddenly which represents that no other thermal event is happening except for the destruction of cubic lattice arrangement of micelles at gel melting temperatures. Thus this low enthalpy gel melting thermal event might be detected by using cooling ramps.
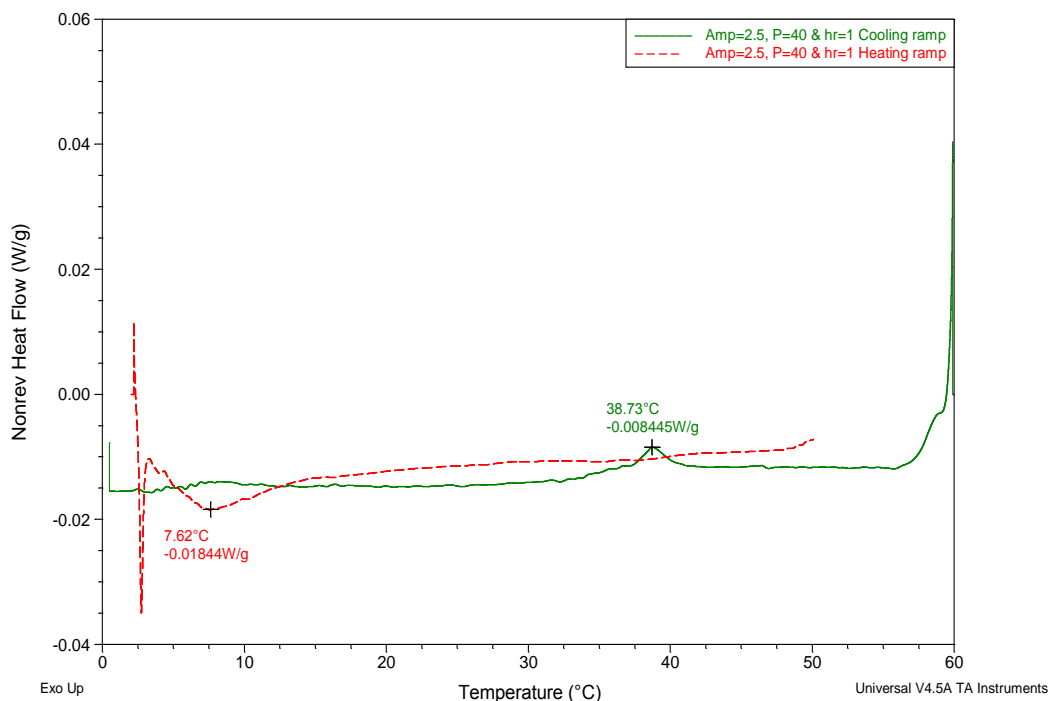
[Fig. 5.50 MDSC thermogram of 25% Pluronic F127 solution containing CPM, showing

heating (red) and cooling (green) ramps of non-reversible heat flow at 2.5˚C amplitude, 40sec

period and 1˚C/min heating rate]

The results from the above thermogram show that a peak at 38˚C is detected by the cooling

ramp but its corresponding temperature doesn't match with the gelation temperature of 25%

Pluronic F127 containing solution which might due to less suitable MDSC parameters which

is also evident by lack of micelle melting exotherm at 7-8˚C. The amplitude (2.5˚C) used for

the cooling ramp was relatively high while the period of modulation was relatively low and

hence not offering enough time for the material to react to such a large amplitude of

modulation. Although the above result indicates that MDSC cooling ramps should be used for

the further analysis to detect the gelation because of the detection of peak at around 38˚C

which was found to be absent in the heating ramp (see fig. 5.50).

➢ **Effect of sample size**

To study whether the amount of sample size used (40 mg) influenced the gelation detection is crucial in this case as the sample is a mixture of Pluronic F127 with water containing CPM. Thus the heat capacity (thermal conductivity) of all three components (Pluronic F127, water and CPM) will influence the heat flow within the system. Thus to gain an understanding about the effect of sample size an MDSC ramp with half the sample weight (20 mg) was performed (see figure 5.51).
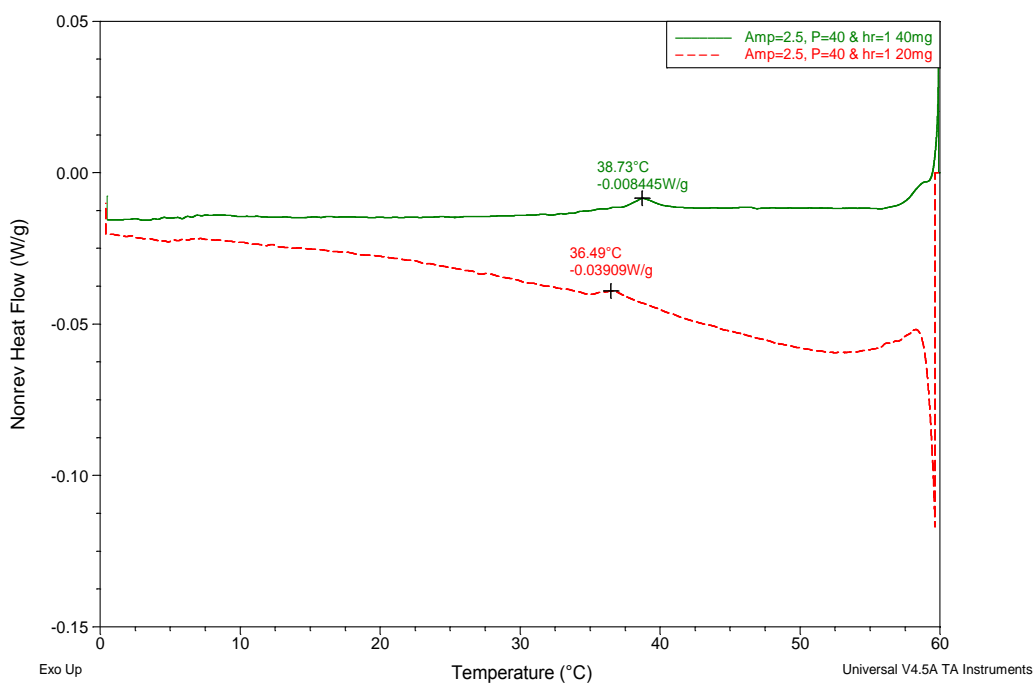

[Fig. 5.51 MDSC thermogram of 25% Pluronic F127 solution containing CPM, showing cooling ramps of non-reversible heat flow at 2.5°C amplitude, 40sec period and 1°C/min heating rate of 40mg (green) and 20mg (red) sample weight]

From the above MDSC thermogram it is evident that a larger sample weight (40 mg) is preferable for making the transition detectable as the peak at 36 - 38˚C becomes supressed by the reduction in the sample size (20mg).

> **Effect of water content (Pluronic F127 concentration) or "C_P" of the system**

MDSC cooling ramps at a high amplitude of 2.5 ˚C, a low period of modulation (40 seconds) and a cooling rate of 1˚C/min were used to understand the effect of increasing concentration.
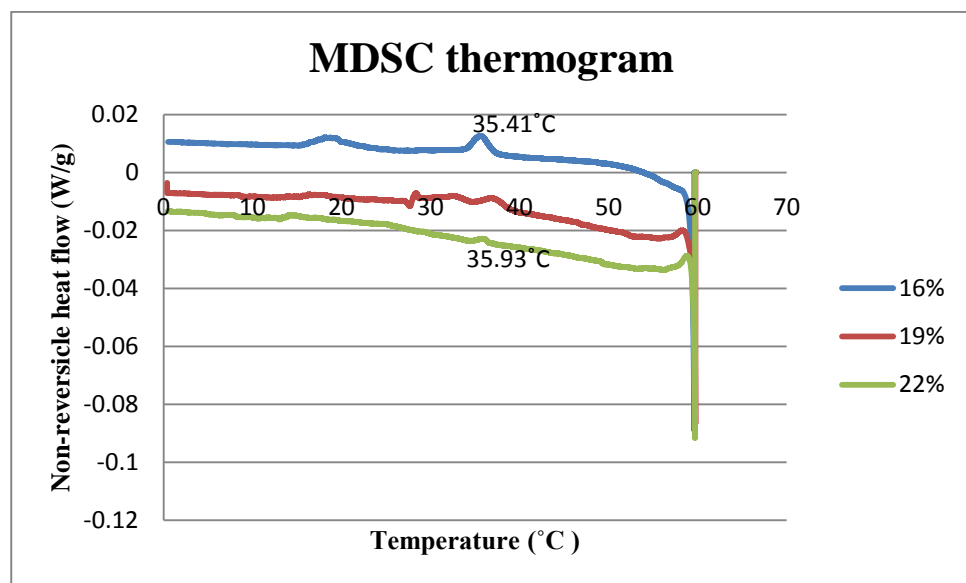
[Fig. 5.52 MDSC thermogram of various Pluronic F127 concentrated solution containing CPM, showing non-reversible heat flow at 2.5˚C amplitude, 40sec period and 1˚C/min cooling rate of 16% (blue), 19% (red) and 22% (green)]

The results from the above figure 5.52 illustrates that, for 16% Pluronic F127 solution containing CPM with higher water content even this low period of modulation (40 seconds) was enough to observe an exothermic peak at 35.41˚C which corresponds to the temperature at which a significant change in the "Damping factor (tanδ)" of the rheological DMTA test occurred (see figure 5.53). Aluminium has high thermal conductivity (C_p = 0.897 J/g.K) and

water (C_p = 4.1813 J/g.K) is almost five times more thermally conductive than Aluminium if we compare their "C_p". Therefore with the increase in amount of water the thermal conductivity of any system will increase significantly. Thus due to the high water content, the heat capacity of the 16% Pluronic F127 solution system is bound to be very high in comparison to the higher concentration of Pluronic F127 which enables the system to follow such high modulation amplitude (2.5˚C) within very short span of time (period of 40sec) to produce accurate results which corresponds to structural change ("Damping factor (tanδ)") temperature. However with the decrease in amount of water as the Pluronic F127 concentration increases the ability of the Pluronic F127 solution system to follow the high amplitude continues to decrease owing to the decrease in "C_p" of the system with the decrease in water content. Thus, this effect can be observed on the MDSC non-reversible heat flow curve as peaks are getting blunt distorted with the increase Pluronic F127 concentration.
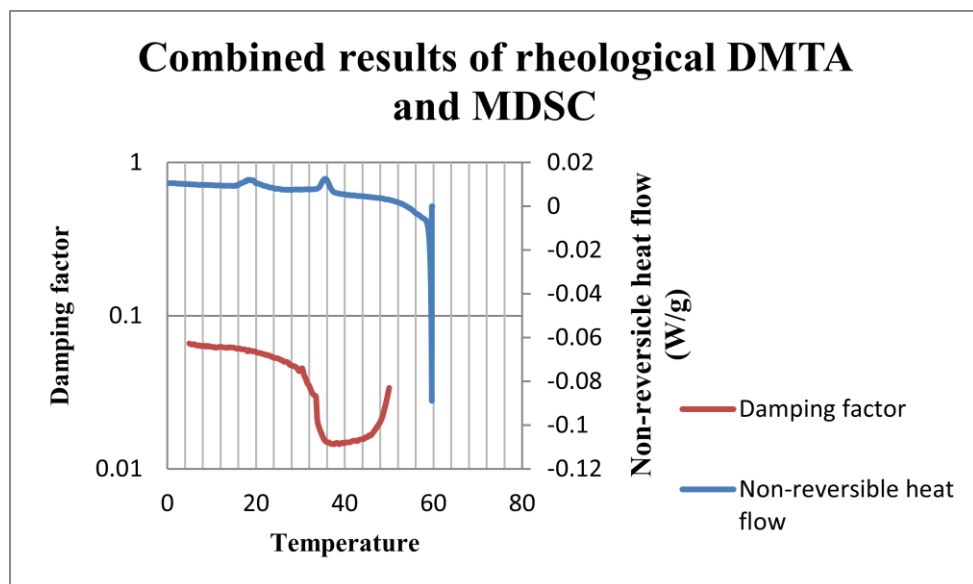
[Fig. 5.53 Combined results from DMTA & MDSC, showing thermogram of 16% Pluronic F127 concentrated solution containing CPM and "Damping factor (tanδ)" with respect to temperature]

The above discussed results suggest that there is a need to optimise the parameters for the MDSC according to the "C_p" (concentration and composition of the system) to detect such low enthalpy transitions bearing in mind that each component will have its contribution to the overall "C_p" of the system. That is, for each specific concentration of Pluronic F127 the parameters should be optimised accordingly. Based on the results shown in figure 5.52, it was decided to reduce the amplitude of modulation and allow more time (50 seconds) for the highest Pluronic F127 concentration of 25 % (lowest "C_p" value within the range of 16-25% Pluronic F127 solutions tested (lowestwater present) containing CPM so that the sample would have enough time to accurately follow the complex modulation cycle at a slightly lower amplitude (2˚C). The results from figure 5.54 reveal that three peaks were observed: a prominent peak at 6˚C and two others at 15˚C and 31˚C. The prominent peak at 6˚C is the indicative of the micelles melting. By comparing the MDSC results with DMTA results, as shown in figure 5.55, it was found that the peak at 15˚C exactly corresponds to the viscosity drop of the DMTA results which is indicative of the gel melting (cubic phase melting). Another small peak found at around 31˚C also corresponds to the slight change in the viscosity which is indicative of the structural reorganisation. Thus for the highest Pluronic F127 concentration (25%) 2˚C amplitude of modulation, a 50 seconds period of modulation and a 1˚C/min linear cooling ramp was able to detect such a low enthalpic transition.
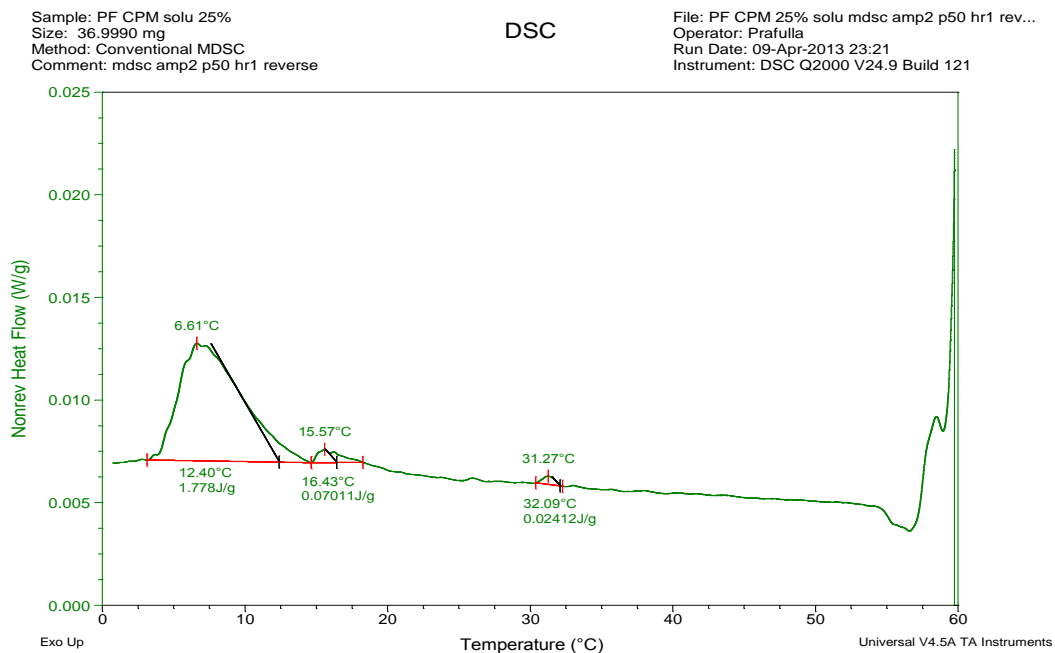
[Fig. 5.54 MDSC thermogram of 25% Pluronic F127 solution containing CPM, showing

cooling ramps of non-reversible heat flow at 2˚C amplitude, 50sec period and 1˚C/min

heating rate]

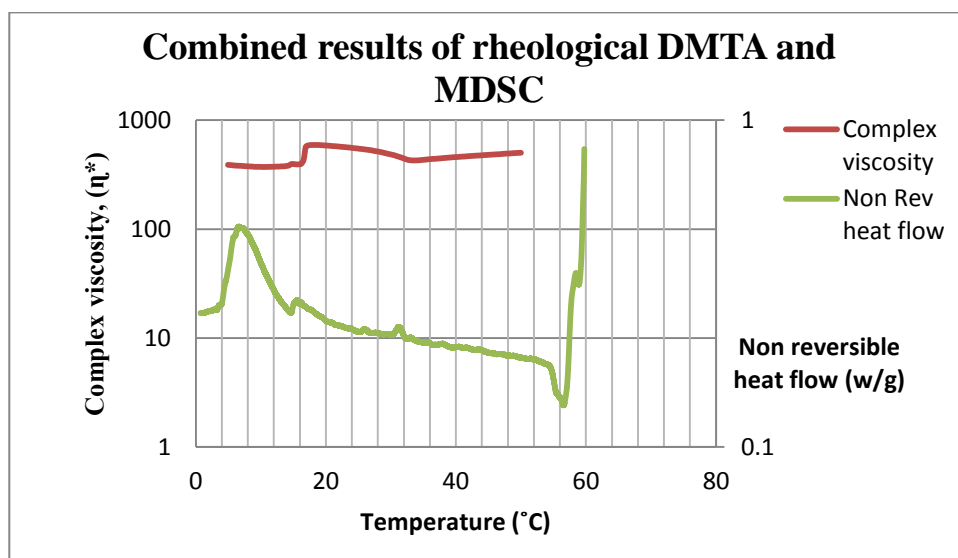[Fig. 5.55 Combined results from DMTA & MDSC, showing thermogram of 25% Pluronic

F127 concentrated solution containing CPM and "Complex viscosity (η^*)" with respect to

temperature]

5.4.1 Conclusion

MDSC can be utilised to detect low enthalpy cubic phase transition by optimising its parameters to increase the sensitivity of the system. However while selecting the parameters the material's overall thermal conductivity ("C_p"), its sample size and its behaviour under heating or cooling should also be considered accordingly.

Chapter 6: Conclusion

==

Following conclusions can be drawn from the present study:

- The present work demonstrates feasibility of producing drug loaded liquid crystal precursor of a PluronicF127 coated MCC particles using sub ambient extrusion processing.

- The PluronicF127 solution showed thermoreversible behaviour and formed a viscous cubic phase system with concentration dependent change in the elasticity.

- The cubic phase of Pluronic F127 was not found to suitable for the coating because of its elastic behaviour. The sol state of the Pluronic F127 was found to be Newtonian which is been exploited for coating it over the MCC surface by twin screw extruder.

- The amount of CPM has influenced the gelation temperature. This effect was found be most prominent on the lowest concentration of thermoreversible range of the Pluronic F127 and least on the highest concentration of thermoreversible range Pluronic F127 in terms of shifting gelation temperature to higher level.

- The standard mixing screw configuration was found to be more than sufficient enough to get the Pluronic F127 solution containing CPM uniformly dispersed over the bulk of the MCC.

- To get rid of the compacted particles the MCC to Pluronic F127 solution ratio should be five times or above at refrigerated temperature and the screw speed should be more than 400 RPM.

- The tendency of the twin screw extrusion process to produce compacted particles was found to increase with the increase in the amount of water

- The Polarized light microscopy (PLM) and SEM study confirms the coating of the Pluronic F127 on the MCC particles to form LLC coated powdered precursor through twin screw extrusion. But as the amount of MCC was increased the coating was found to be incomplete. The powder flow analysis study on the LLC coated precursor coating was also found in agreement with the PLM and SEM studies.

- From the factorial design study it was found that only Pluronic F127 concentration and MCC feed rate was having a significant linear relationship with the amount of compacted particles produced (d_g). The tendency to produce compacted particles was found to increase with the decrease in Pluronic F127 concentration and MCC feed rate.

- % Torque was found to have significant linear relationship with Pluronic F127 concentration and MCC feed rate and quadratic for term $X2^2$.

- The WDC was found to have significant linear relationship with the Pluronic F127 concentration, MCC feed rate and the interaction of MCC feed rate and screw speed. The W.D. for cohesion was found to increase with the decrease in Pluronic F127 concentration and MCC feed rate.

- The LLC coated powdered precursor through twin screw extrusion was unable to produce controlled release profile instead they offered burst release profile. Within 10-15min 100% CPM was released.

Chapter 7: Future work

===

The future work will be focused on to investigate the reasons for the failure to produce the controlled release profile by LLC coated powdered precursor prepared through twin screw extrusion which was found to be very unusual, after the coating confirmation. There might certain other reasons for such a burst release profile such as the coating thickness of Pluronic F127 might be very thin which gets eroded very quickly by dissolution media. Thus Atomic force microscopy (AFM) studies can be done to investigate the thickness. Dissolution studies of the compacted tablet prepared by LLC coated powdered precursor should be done to compare the release profile with the LLC coated powdered precursor. Lastly, developed MDSC method should be used on the prepared LLC coated powdered precursor investigate the cubic phase formation. The MDSC parameters optimization should also be explored for 22% and 19% Pluronic F127 concentration to detect gelation.

References:-

AitkenNichol, C., Zhang, F. and McGinity, J. W. (1996) Hot melt extrusion of acrylic films. *Pharmaceutical Research,* 13 (5)**,** 804-808.

Aquafeed, A. A. F.-V. t. s. e. i. f. (2008) *Versatile twin screw extruder ideal for aquafeed.* Available from: http://www.allaboutfeed.net/Processing/Extruding--Expanding/2008/9/Versatile-twin-screw-extruder-ideal-for-aquafeed-AAF011376W/ (Accessed 21 November).

Barba, A. A., d'Amore, M., Grassi, M., Chirico, S., Lamberti, G. and Titomanlio, G. (2009) Investigation of Pluronic (c) F127-Water Solutions Phase Transitions by DSC and Dielectric Spectroscopy. *Journal of Applied Polymer Science,* 114 (2)**,** 688-695.

Barrel-parallel_twin_screw03, P. t. s. a. *Parallel_twin_screw03.* Available from: http://www.ymscrew.com/en/ProductShow/parallel_twin_screw03_ID571.html (Accessed 02/12/2013).

BASF Wyandotte, 1997. Pluronic Surfactants, Product Brochure. BASF Corporation, Mount Olive, New Jersey.

BASF, 2006. Pluronic F127 Surfactant Viscosity as a function of Temperature & Concentration, Technical Bulletin. BASF Corporation, Florham Park, New Jersey.

BASF, 2012. Pluronic F127 block Copolymer Surfactant, Technical Bulletin. BASF Corporation, Florham Park, New Jersey.

Benton, W. J., Miller, C. A. and Fort, T. (1982) SPONTANEOUS EMULSIFICATION IN OIL-WATER-SURFACTANT SYSTEMS. *Journal of Dispersion Science and Technology,* 3 (1)**,** 1-44.

Breitenbach, J. (2002) Melt extrusion: from process to drug delivery technology. *European Journal of Pharmaceutics and Biopharmaceutics,* 54 (2)**,** 107-117.

Brown, W., Schillen, K., 1991. Micelle and gel formation in a Pluronic triblock co-polymer in water: dynamic and static light scattering and oscillatory shear measurements. J. Phys. Chem. 95, 1850–1858.

Cabana, A., Aït-Kadi, A. and Juhász, J. (1997) Study of the Gelation Process of Polyethylene Oxidea–Polypropylene Oxideb–Polyethylene OxideaCopolymer (Poloxamer 407) Aqueous Solutions. *Journal of Colloid and Interface Science,* 190 (2)**,** 307-312.

Caffrey, M. (2003) Membrane protein crystallization. *Journal of Structural Biology,* 142 (1)**,** 108-132.

Carvalho, F. C., Campos, M. L., Peccinini, R. G. and Gremião, M. P. D. (2013) Nasal administration of liquid crystal precursor mucoadhesive vehicle as an alternative antiretroviral therapy. *European Journal of Pharmaceutics and Biopharmaceutics,* 84 (1)**,** 219-227.

Community, E. P. *Extrusion.* Available from: http://www.plastics.com/extrusion-whatis-pg2.html (Accessed 02/12/2013).

Crowley MM, Physicochemical and mechanical characterisation of hot melt extruded dosage forms, University of Texas at Austin, PhD Thesis (May 2003.)

Crowley, M. M., Schroeder, B., Fredersdorf, A., Obara, S., Talarico, M., Kucera, S. and McGinity, J. W. (2004) Physicochemical properties and mechanism of drug release from ethyl cellulose matrix tablets prepared by direct compression and hot-melt extrusion. *International Journal of Pharmaceutics,* 269 (2)**,** 509-522.

Crowley, M. M., Zhang, F., Repka, M. A., Thumma, S., Upadhye, S. B., Battu, S. K., McGinity, J. W. and Martin, C. (2007) Pharmaceutical applications of hot-melt extrusion: Part I. *Drug Development and Industrial Pharmacy,* 33 (9)**,** 909-926.

Czarnecki R.F. & D.L. Williams, 1993. Sustained released delivery system for use in the periodontal pocket. Copley Pharmaceutical Inc., USA Patent 5,230,895

DiBiase, M. D. and Rhodes, C. T. (1996) Formulation and evaluation of epidermal growth factor in pluronic F-127 gel. *Drug Development and Industrial Pharmacy,* 22 (8)**,** 823-831.

Engström, S., Nordén, T. P. and Nyquist, H. (1999) Cubic phases for studies of drug partition into lipid bilayers. *European Journal of Pharmaceutical Sciences,* 8 (4)**,** 243-254.

Follonier N, Doelkar E, Cole ET, Evaluation of hot melt extrusion as a new technique for the production of polymer based pellets for sustained release capsules containing high loadings of freshly soluble drugs, Drug Dev Ind Pharm. 8 (1994) 1323-1339.

Friberg, S., Jansson, P. O. and Cederberg, E. (1976) SURFACTANT ASSOCIATION STRUCTURE AND EMULSION STABILITY. *Journal of Colloid and Interface Science,* 55 (3)**,** 614-623.

Gamlen M, Continuous extrusion using Baker Perkins MP50 (multipurpose) extruder,   Drug development Ind. Pharm. 12 (1986) 1701-1713.

Gruner SM, Tate MW, Kirk GL, So PTC, Turner DC, Keane DT, et al. X-ray diffraction study of the polymorphic behavior of N-methylated dioleoylphosphatidylethanolamine. Biochemistry 1988;27:2853–66.

He, C., Kim, S. W. and Lee, D. S. (2008) In situ gelling stimuli-sensitive block copolymer hydrogels for drug delivery. *Journal of Controlled Release,* 127 (3)**,** 189-207.

Hyde ST. Identification of lyotropic liquid crystalline mesophases. In: Holmberg K, editor. Handbook of applied surface and colloid chemistry. New York: Wiley; 2001. p. 299–332.

Jain, H., Ghule, R., Joshi, G., Maurya, J., and Trivedi, N. (2011) Liquid crystal as accelerant in drug absorption from topical formulations. *International Research Journal of Pharmacy,* 2 (4), 86-89.

Kim, J.S., Kim, H.K., Chung, H., Sohn,Y.Y.,Kwon, I.C., Jeong, S.Y., 2000. Drug formulations that form a dispersed cubic phase when mixed withwater. Proc. Int. Symp. Control. Rel. Bioact. Mater. 27, 1118–1119.

Kumar, K. M., Shah, M. H., Ketkar, A., Mahadik, K. R. and Paradkar, A. (2004) Effect of drug solubility and different excipients on floating behaviour and release from glyceryl monooleate matrices. *International Journal of Pharmaceutics,* 272 (1-2)**,** 151-160.

Maheshwari, M., Paradkar, A., Yamamura, S. and Kadam, S. (2006) Preparation and characterisation of Pluronic-colloidal silicon dioxide composite particles as liquid crystal precursor. *Aaps Pharmscitech,* 7 (4).

Modulated DSC Theory; Thermal Analysis Review; TA Instruments Technical Paper TA-211B.

Martin AN. Physical Pharmacy. 4th ed. Philadelphia, PA: Lea & Febiger; 1993.

Mezger TG, 2006. The rheological handbook,Hannover, Vincentz Network GmbH & Co. KG.

Nie, S., Hsiao, W. L. W., Pan, W. and Yang, Z. (2011) Thermoreversible Pluronic (R) F127-based hydrogel containing liposomes for the controlled delivery of paclitaxel: in vitro drug release, cell cytotoxicity, and uptake studies. *International Journal of Nanomedicine,* 6**,** 151-166.

Nielsen, L. S., Schubert, L. and Hansen, J. (1998) Bioadhesive drug delivery systems: I. Characterisation of mucoadhesive properties of systems based on glyceryl mono-oleate and glyceryl monolinoleate. *European Journal of Pharmaceutical Sciences,* 6 (3)**,** 231-239.

Nylander, T., Mattisson, C., Razumas, V., Miezis, Y. and Hakansson, B. (1996) A study of entrapped enzyme stability and substrate diffusion in a monoglyceride-based cubic liquid crystalline phase. *Colloids and Surfaces a-Physicochemical and Engineering Aspects,* 114**,** 311-320.

Paasch, S., Schambil, F. and Schwuger, M. J. (1989) RHEOLOGICAL PROPERTIES OF LAMELLAR LYOTROPIC LIQUID-CRYSTALS. *Langmuir,* 5 (6)**,** 1344-1346.

Pandit, N. K. and Kisaka, J. (1996) Loss of gelation ability of Pluronic® F127 in the presence of some salts. *International Journal of Pharmaceutics,* 145 (1–2)**,** 129-136.

Pisal, S. S., Paradkar, A. R., Mahadik, K. R. and Kadam, S. S. (2004) Pluronic gels for nasal delivery of Vitamin B12. Part I: Preformulation study. *International Journal of Pharmaceutics,* 270 (1-2)**,** 37-45.

Rosevear, F.B., 1954. The microscopy of the liquid crystalline neat and middle phases of soaps and synthetic detergents. J. Am. Oil Chem. Soc. 31, 628–639.

Rothen-Weinhold, A., Oudry, N., Schwach-Abdellaoui, K., Frutiger-Hughes, S., Hughes, G. J., Jeannerat, D., Burger, U., Besseghir, K. and Gurny, R. (2000) Formation of peptide impurities in polyester matrices during implant manufacturing. *European Journal of Pharmaceutics and Biopharmaceutics,* 49 (3)**,** 253-257.

Shah, J. C., Sadhale, Y. and Chilukuri, D. M. (2001) Cubic phase gels as drug delivery systems. *Advanced Drug Delivery Reviews,* 47 (2-3)**,** 229-250.

Shah, M. H., Biradar, S. V. and Paradkar, A. R. (2006) Spray dried glyceryl monooleate–magnesium trisilicate dry powder as cubic phase precursor. *International Journal of Pharmaceutics,* 323 (1-2)**,** 18-26.

Shah, M. H. and Paradkar, A. (2005) Cubic liquid crystalline glyceryl monooleate matrices for oral delivery of enzyme. *International Journal of Pharmaceutics,* 294 (1–2)**,** 161-171.

Spicer, P. T., Hayden, K. L., Lynch, M. L., Ofori-Boateng, A. and Burns, J. L. (2001) Novel process for producing cubic liquid crystalline nanoparticles (cubosomes). *Langmuir,* 17 (19)**,** 5748-5756.

Spicer, P. T., Small, W. B., Lynch, M. L. and Burns, J. L. (2002) Dry powder precursors of cubic liquid crystalline nanoparticles (cubosomes). *Journal of Nanoparticle Research,* 4 (4)**,** 297-311.

Spicer, P.T., 2003, Cubosomes: bicontinuous cubic liquid crystalline nanostructured particles, in Schwarz, J.A., Contescu, C., and Putyera K. (Eds). Marcel Dekker Encyclopedia of Nanoscience and Nanotechnology, 881 –892 (Marcel Dekker, New York, USA).

Steinleitner, A., Lambert, H., Kazensky, C. and Cantor, B. (1991) POLOXAMER 407 AS AN INTRAPERITONEAL BARRIER MATERIAL FOR THE PREVENTION OF POSTSURGICAL ADHESION FORMATION AND REFORMATION IN RODENT MODELS FOR REPRODUCTIVE SURGERY. *Obstetrics and Gynecology,* 77 (1)**,** 48-52.

Technology, H. F. P. o. *The Counter Rotating Screw Drive.* Available from: http://www.hb-fein.com/hbf/begriffserklaerung.html?L=1 (Accessed 21 November).

Vehring, R. (2008) Pharmaceutical particle engineering via spray drying. *Pharmaceutical Research,* 25 (5)**,** 999-1022.

Wang, H.-X., Zhang, G.-Y., Feng, S.-H. and Xie, X.-L. (2005) Rheology as a tool for detecting mesophase transitions for a model nonyl phenol ethoxylate surfactant. *Colloids and Surfaces A: Physicochemical and Engineering Aspects,* 256 (1)**,** 35-42.

Whelan T, Dunning D, The dynisco extrusion processors handbook. 1st ed. 1988, London: London School of polymer Technology.

Xu, C., Li, P. P., Cooke, R. G., Parikh, S. V., Wang, K., Kennedy, J. L. and Warsh, J. J. (2009) TRPM2 variants and bipolar disorder risk: confirmation in a family-based association study. *Bipolar Disorders,* 11 (1)**,** 1-10.